Prog. Solid St. Chem. Vol. 15, pp. 173–255, 1984
Printed in Great Britain.

0079–6786/84 $0.00 + .50

FROM BONDS TO BANDS AND MOLECULES TO SOLIDS

Jeremy K. Burdett*

Department of Chemistry, The University of Chicago, Chicago, Illinois 60637, U.S.A.

CONTENTS

*Camille and Henry Dreyfus Teacher-Scholar

I. INTRODUCTION

1.1. Scope

Solids, of course, are just infinite molecules. However, understanding concerning their geometrical and electronic structure has lagged considerably behind the dramatic progress made in the molecular area over the past twenty years. With the recent availability of fast and cheap computation and a gradual enlightenment by physicists and chemists alike concerning each other's viewpoint in this field, the time is surely ripe for progress to be made. Our major goal in this article will be to show the striking similarities between the electronic structure of molecules and solids and to suggest that there is profit to be gained by extending ideas developed for molecules to the realm of the solid state. We will rely very heavily on the linear combination of atomic orbitals approach of the chemist or the tight-binding approach of the solid-state physicist. These are two models identical in all but name. We will also make extensive use of symmetry arguments, in the form of group theoretical techniques and will use perturbation theory to access results of interest. For the reader who is unfamiliar with these methods reference to the books by Cotton[1] and by Heilbronner and Bock[2] is strongly suggested. The reader who feels comfortable with such concepts can jump to Section III. We will focus almost exclusively on very simple systems, for it is here that the workings of the theory is most transparent and the analogies between molecules and solids easiest to appreciate. We make no apologies for spending approximately a third of this article in developing orbital ideas for molecules. Many of the orbital tricks we will use in the rest of the article have their foundation here.

1.2. The Molecular Orbital Approach

The Schrödinger equation can be solved exactly for the case of one-electron atoms, e.g., H, He^+, Li^{2+}. For the case of many-electron atoms approximate (but in many cases very good) solutions may be obtained numerically. In many-electron molecules one way in which approximate solutions may be obtained is via the linear combination of atomic orbital (LCAO)—molecular orbital method. We will describe one version of this which will enable the generation of one-electron energy levels of molecules and (eventually) solids. We refer the reader elsewhere for more complete accounts concerning the generation of more sophisticated orbital models.[3,4]

Let us take the valence orbitals $\{\varphi_i\}$ of the atoms which make up the molecule and write a LCAO molecular orbital wavefunction which we hope will suffice to describe the energy levels of the molecule.

$$\psi = \sum_i c_i \varphi_i \tag{1}$$

Now ψ is an eigenstate of some one-electron Hamiltonian H, i.e.,

$$H\psi = E\psi . \tag{2}$$

This leads to an expression for the energy of the state described by this wavefunction:

$$E = \frac{\int \psi^* H \psi d\tau}{\int \psi^* \psi d\tau} = \frac{\langle \psi | H | \psi \rangle}{\langle \psi | \psi \rangle} , \tag{3}$$

where the integration occurs over all space. Substitution of equation (1) into equation (3) leads to

$$E = \frac{\sum\sum_{ij} c_i c_j \langle \varphi_i | H | \varphi_j \rangle}{\sum\sum_{ij} c_i c_j \langle \varphi_i | \varphi_j \rangle} . \tag{4}$$

This expression contains three terms of interest. $\langle \varphi_i | \varphi_j \rangle = S_{ij}$ is the overlap integral between atomic orbitals on different atoms. It is always ≤ 1. If our atomic basis set $\{\varphi_i\}$ is normalized then $\langle \varphi_i | \varphi_j \rangle = 1$ for the case $i = j$. $\langle \varphi_i | H | \varphi_i \rangle = H_{ii}$ represents the energy of an electron in orbital φ_i. It is called the Coulomb integral and is often approximated by the ionization energy of an electron from that orbital. $\langle \varphi_i | H | \varphi_j \rangle = H_{ij}$ is an integral which represents the interaction between orbitals φ_i and φ_j. It is called the resonance integral by molecular chemists and the hopping or transfer integral by physicists. It is often estimated using the Wolfsberg–Helmholz relationship

$$H_{ij} = \tfrac{1}{2} K S_{ij} (H_{ii} + H_{jj}) , \tag{5}$$

where K is a constant, usually set equal to 1.75. The energies of the molecular orbitals are obtained from equation (4) in the following way. The Variation Theorem states that all approximate wavefunctions of a system will give energies that are never lower than the true ground-state energy of the system. So minimization of equation (4) with respect to all the coefficients c_i, c_j will lead to the best estimate of the orbital energy using the expansion of equation (1). If there are n atomic orbitals in $\{\varphi_i\}$ then there will be n equations demanded by the minimization expressions $\partial E / \partial c_i = 0$. They have the particularly simple form of equations (6).

$$\begin{aligned}
&(H_{11} - E)c_1 + (H_{12} - S_{12}E)c_2 + \ldots + (H_{1n} - S_{1n}E)c_n = 0 \\
&(H_{21} - S_{21}E)c_1 + (H_{22} - E)c_2 + \ldots + (H_{2n} - S_{2n}E)c_n = 0 \\
&\quad\vdots \\
&(H_{n1} - S_{n1}E)c_1 \quad (H_{n2} - S_{n2}E)c_2 + \ldots + (H_{nn} - E)c_n = 0 \ .
\end{aligned} \tag{6}$$

These equations will be consistent only if the secular determinant of equation (7) is equal to zero.

$$\begin{vmatrix}
H_{11} - E & H_{12} - S_{12}E & \cdots\cdots & H_{1n} - S_{1n}E \\
H_{21} - S_{21}E & H_{22} - E & \cdots\cdots & H_{2n} - S_{2n}E \\
\vdots & \vdots & & \vdots \\
H_{n1} - S_{n1}E & H_{n2} - S_{n2}E & \cdots\cdots & H_{nn} - E
\end{vmatrix} = 0 \ . \tag{7}$$

Given the values of the H_{ii}, S_{ij} and H_{ij}, equation (7) may be solved to give n values of the energy — the energy levels of the molecule. Each value of E may in turn be used with the collection of equations (6) to give the values of the orbital coefficients, the c_i of equation (1).

An example will illustrate the approach. Assemble an H_2 molecule from two hydrogen atoms which carry singly occupied 1s valence orbitals. The secular determinant is

$$\begin{vmatrix}
H_{11} - E & H_{12} - S_{12}E \\
H_{12} - S_{12}E & H_{11} - E
\end{vmatrix} = 0 . \tag{8}$$

Since the two hydrogen 1s orbitals are equivalent we have put $H_{11} = H_{22}$. (Also $H_{12} = H_{21}$ by symmetry.) Solution of this determinant gives

$$(H_{11} - E) = \pm (H_{12} - S_{12}E) \tag{9}$$

$$E = \frac{H_{11} \pm H_{12}}{1 \pm S_{12}} \ . \tag{10}$$

The result is shown pictorially in 1. Notice that the higher energy orbital is destabilized

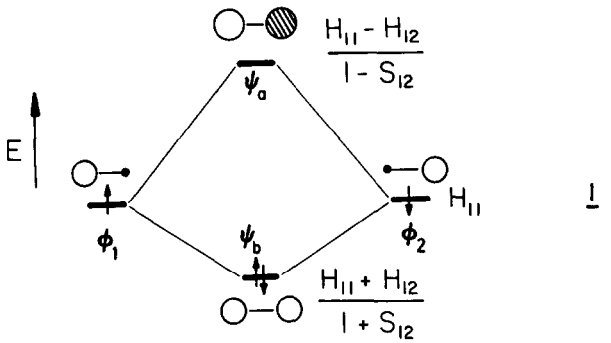

1

(relative to a free hydrogen AO) more than the lower orbital is stabilized. The bond (or binding) energy of H_2 on this model is simply

$$2\left[\frac{H_{11}+H_{12}}{1+S_{12}}-H_{11}\right]=\frac{2(H_{12}-S_{12}H_{11})}{1+S_{12}}\ . \tag{11}$$

With these values of the energies we can now go back to equation (6) and evaluate the coefficients. With a little bit of algebra it is easy to find for ψ_b that $c_1/c_2=1$ and for ψ_a that $c_1/c_2=-1$. The extra piece of information we need to fix the values of c_1 and c_2 is the normalization condition

$$\int\psi^*\psi d\tau=1\ . \tag{12}$$

This leads simply to

$$\begin{aligned}\psi_b&=\frac{1}{\sqrt{2(1+S_{12})}}(\varphi_1+\varphi_2)\\ \psi_a&=\frac{1}{\sqrt{2(1-S_{12})}}(\varphi_1-\varphi_2)\end{aligned} \tag{13}$$

In ψ_b the orbitals are mixed in phase – the bonding orbital, and in ψ_a they are mixed out of phase – the antibonding orbital. Notice that because of the sign before S_{12} in the denominators the coefficients are larger in ψ_a. 1 shows a useful pictorial representation of these functions where the sign of the mixing coefficient (c_i of equation (1)) is indicated by the presence or absence of shading. Note that the absolute signs have no meaning but the relative phases are important.

There is another useful way to generate the molecular orbitals of H_2, and indeed more complex systems, which we will use below, and that is by taking advantage of the symmetry of the problem. H_2 belongs to the $D_{\infty h}$ point group. Using standard techniques[1] we can show that the two 1s orbitals transform as $\sigma_g^+ + \sigma_u^+$. A useful group theoretical result enables us to construct symmetry adapted linear combinations of orbitals with these transformation properties. For a point group G with symmetry elements $g \in G$, and a basis set of orbitals $\{\varphi_i\}$, a wavefunction which transforms as the k^{th} irreducible representation is simply given by

$$\psi(k)=\sum_{g\in G}\chi_k(g)\,g\varphi_m\ . \tag{14}$$

Here $\chi_k(g)$ is the character of the k^{th} irreducible representation. φ_m is any member of the set $\{\varphi_i\}$. For the H_2 problem it is a simple matter to use equation (14) and a character table for the $D_{\infty h}$ group to give

$$\psi(\sigma_g^+) \propto \varphi_1 + \varphi_2$$
$$\psi(\sigma_g^+) \propto \varphi_1 - \varphi_2 \quad . \tag{15}$$

Normalization of these functions gives the same expressions as those in equation (13). The energies of ψ_a and ψ_b may then be obtained by substitution of these normalized functions back into equation (3). The reader should check to ensure that the expressions that result are identical to those of equation (10).

The hydrogen molecule of course is a very simple example but the numerical generation of the energy levels of complex molecules, by using ionization energies as estimates of the H_{ij} and evaluating the S_{ij} by integration of wavefunctions, has proven to be an extremely valuable way to study molecular electronic structure.[5]

2. ENERGY LEVELS OF MOLECULES

2.1 Linear π Systems

There is a simplification we can make to the approach in Section I.B which will be extremely useful to us in the generation of orbital diagrams of molecules and solids. In the Hückel approximation,[2,6] initially developed for the π levels of conjugated organic molecules, all H_{ii} values for the carbon pπ AO's are put equal to α, all H_{ij} put equal to β if the atoms are bonded together (zero otherwise) and all the S_{ij} $(i \neq j)$ in equations (6) and (7) put equal to zero. The two orbital problem of H_2 described above is then isomorphic

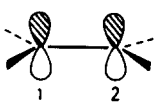

2

with the π orbital problem of ethylene 2. The secular determinant of equation (8) then becomes

$$\begin{vmatrix} \alpha - E & \beta \\ \beta & \alpha - E \end{vmatrix} = 0 \ , \tag{16}$$

which has roots 3 $E = \alpha \pm \beta$. Notice that in this model the bonding orbital is stabilized to

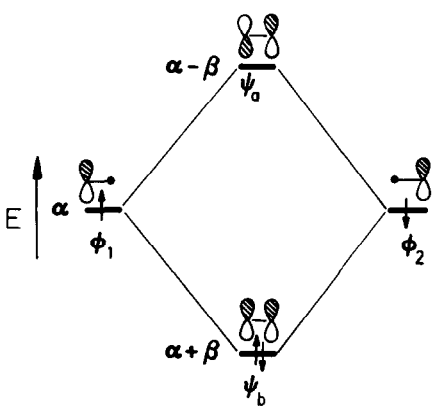

3

the same extent that the antibonding orbital is destabilized (β). The π bond energy of ethylene is then 2β. Since the overlap integrals have been dropped in the Hückel approximation

the wavefunctions for the bonding and antibonding combinations are particularly simple.

$$\psi_b = 2^{-\frac{1}{2}} (\varphi_1 + \varphi_2)$$
$$\psi_a = 2^{-\frac{1}{2}} (\varphi_1 - \varphi_2) \quad . \tag{17}$$

All conjugated organic systems are open to an analogous treatment. The secular determinant for allyl 4, the three orbital problem, is just

$$\begin{vmatrix} \alpha-E & \beta & 0 \\ \beta & \alpha-E & \beta \\ 0 & \beta & \alpha-E \end{vmatrix} = 0 \quad . \tag{18}$$

Notice that the H_{13} and H_{31} entries are equal to zero since atoms 1 and 3 are not bonded to each other. Solution of the secular determinant gives the results shown in 6. Once

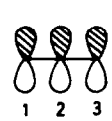

4

5

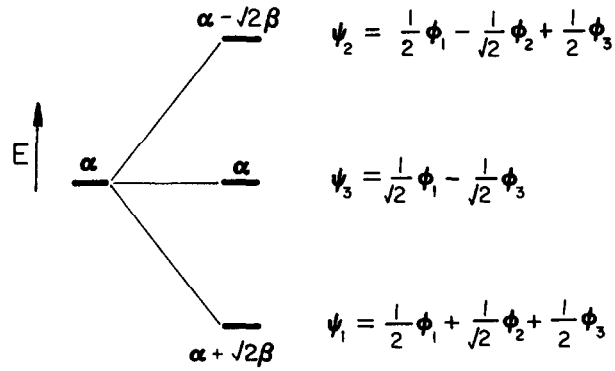

6

again symmetry arguments will enable the same result to be achieved in a neat fashion. We do not need in fact to make use of all the symmetry elements of the point groups to which the molecule belongs. (In 4 we drew the carbon skeleton as a straight line when in fact it is bent.) The important symmetry properties of the functions we need are those associated with the mirror plane of 5. All functions need either to be symmetric or antisymmetric with respect to reflexion in this plane. The character table for a point group which contains (in addition to the identity operation) this reflexion operation is given in Table 1.

Table 1

	E	σ
A	1	1
B	1	-1

Using atomic orbitals of 4 as a basis for a representation it is easy to show that they transform as 2A + B. Use of equation (14) with $\varphi_m = \varphi_1$ or φ_3, two symmetry equivalent orbitals, gives after normalization

$$\text{a species} \qquad \xi_1 = 2^{-\frac{1}{2}} (\varphi_1 + \varphi_3)$$
$$\text{b species} \qquad \xi_3 = 2^{-\frac{1}{2}} (\varphi_1 - \varphi_3) \, . \tag{19}$$

Use of equation (14) with $\varphi_m = \varphi_2$ gives the other a species function

$$\text{a species} \qquad \xi_2 = \varphi_2 \, . \tag{20}$$

We may now set up a secular determinant for this problem using not $\varphi_1 - \varphi_3$ as a basis but the functions $\xi_1 - \xi_3$ of equations (19) and (20)

$$\begin{vmatrix} H_{11}-E & H_{12} & H_{13} \\ H_{21} & H_{22}-E & H_{23} \\ H_{31} & H_{32} & H_{33}-E \end{vmatrix} = 0 . \tag{21}$$

The elements H_{ii} of equation (21) are easily evaluated using the explicit form of the ξ_i

$$\begin{aligned} H_{11} &= \left\langle 2^{-\frac{1}{2}}(\varphi_1+\varphi_3)\middle|H\middle|2^{-\frac{1}{2}}(\varphi_1+\varphi_3)\right\rangle = \alpha \\ H_{22} &= \left\langle 2^{-\frac{1}{2}}(\varphi_1-\varphi_3)\middle|H\middle|2^{-\frac{1}{2}}(\varphi_1-\varphi_3)\right\rangle = \alpha \\ H_{33} &= \left\langle \varphi_2\middle|H\middle|\varphi_2\right\rangle = \alpha \end{aligned} \tag{22}$$

One of the rules of group theory is that orbitals of different symmetry do not interact with each other, but orbitals of the same symmetry can. (Under some conditions the interaction energy may however be zero.) We can show this by evaluating

$$H_{13} = \left\langle 2^{-\frac{1}{2}}(\varphi_1+\varphi_3)\middle|H\middle|2^{-\frac{1}{2}}(\varphi_1-\varphi_3)\right\rangle = \tfrac{1}{2}(\alpha-\alpha) = 0 \tag{23}$$

and

$$H_{12} = \left\langle 2^{-\frac{1}{2}}(\varphi_1+\varphi_3)\middle|H\middle|\varphi_2\right\rangle = \sqrt{2}\beta . \tag{24}$$

The use of symmetry here has then reduced the 3×3 determinant of equation (21) to one (equation (25)) which contains a 2×2 block plus a 1×1 block along the diagonal. The

$$\begin{vmatrix} \alpha-E & \sqrt{2}\beta & 0 \\ \sqrt{2}\beta & \alpha-E & 0 \\ 0 & 0 & \alpha-E \end{vmatrix} = 0 , \tag{25}$$

simplification that this has produced is the reduction of a cubic equation in equation (21) to a quadratic in equation (25). Solution of the 'a block' of equation (25) gives

$$E = \alpha \pm \sqrt{2}\beta . \tag{26}$$

By analogy with the ethylene problem described above the lower energy level ψ_1 corresponds to the bonding, in phase combination of ξ_1 and ξ_3 7 and the higher energy level ψ_2 to the antibonding, out-of-phase combination 8. The third level ψ_3 corresponds to ξ_3. It

$$\psi_1 = \frac{1}{\sqrt{2}}(\xi_1+\xi_2) = \frac{1}{\sqrt{2}}\left(\frac{1}{\sqrt{2}}(\phi_1+\phi_3)+\phi_2\right)$$

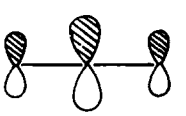

7

$$\psi_2 = \frac{1}{\sqrt{2}}(\xi_1-\xi_2) = \frac{1}{\sqrt{2}}\left(\frac{1}{\sqrt{2}}(\phi_1+\phi_3)-\phi_2\right)$$

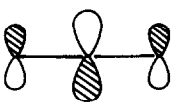

8

is of the wrong symmetry to interact with any other orbital. Since also $H_{ij} = 0$ between all nonbonded atoms, this orbital remains nonbonding. The use of symmetry considerations, while perhaps not obvious in this example actually results in general in a considerable economy of effort in many orbital problems as we will see below.

There is a simple expression[6] for the energy levels (equation (27)) and orbital coefficients (equation (28)) of a one-dimensional chain containing n π orbitals. For the j^{th} level

$$E_j = \alpha + 2\beta \cos \frac{j\pi}{n+1} \qquad j = 1,2,3, \ldots n \tag{27}$$

and for the coefficient on the r^{th} center.

$$c_{jr} = \frac{2}{n+1} \sin \frac{rj\pi}{n+1} \, . \tag{28}$$

The number of nodes in the wavefunction increases by one as the energy increases. This is shown pictorially in Fig. 1 where we show the level structure of the first few members in the series. Note that the orbital energies are symmetrically located about $E = \alpha$. This means that for odd membered chains there is a central, exactly nonbonding, orbital with this energy.

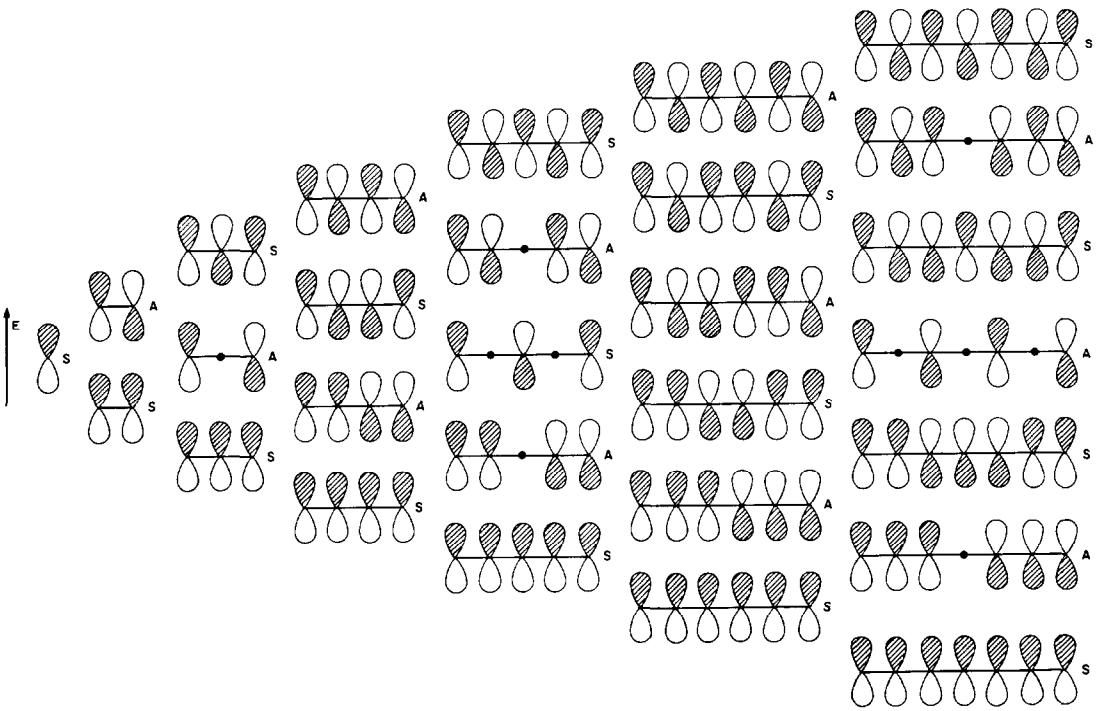

Fig. 1. Energy levels of the first few linear polyenes

One interesting point concerning the energy levels of allyl, is the charge distribution in molecules of this type as a function of the electronic configuration. Recall that the square of the wavefunction, $\psi^*\psi$, gives the probability distribution of electrons in that orbital. So for an arbitrary wavefunction ψ written in terms of an LCAO using two atomic orbitals χ_1 and χ_2 (equation (29)) the electronic charge

$$\psi = c_1 \chi_1 + c_2 \chi_2 \, , \tag{29}$$

in orbital χ_1 is Nc_2^2 where N is the number of electrons in this orbital. (This simple expression needs to be modified[4] if we go beyond the Hückel approximation and include over-

lap, but it will suffice for our purposes here). Correspondingly the electronic charge in χ_2 is Nc_2^2. The total number of electrons is obviously equal to $N(c_1^2+c_2^2)=N$ since the wavefunction is normalized. Applying this technique to the allyl problem of 6, with two electrons in ψ_1 (allyl$^+$) the charge distribution is shown in 9. Note that the central atom carries more negative charge than the 'ligands' or end atoms. For the allyl$^-$ ion itself with two more electrons (which enter ψ_2) the charge distribution is now different. Here the

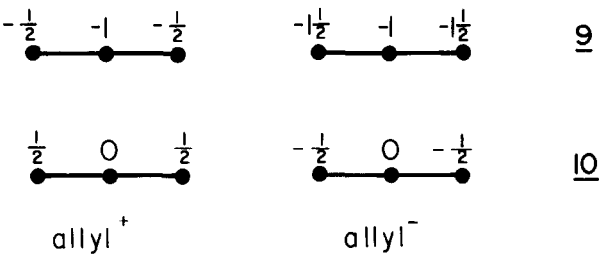

largest electron density is located on the terminal atoms. These results are more conventionally shown in a slightly different way by calculating the atomic charges on each center 10. All this entails is subtraction from the results of 9 the number of electrons assigned to each orbital before interaction. In our case this is just one electron per orbital.

It is instructive to take the details of the allyl orbitals and see how the situation is affected energetically by the replacement of an atom by one with a different electronegativity. We will simulate this by allowing this new atom to have a different α value from the old. There are several ways to obtain the orbital energies of this new species. One could, for example, solve the secular determinant of equation (18) which has been suitably modified. The route we will take employs the techniques of perturbation theory.[2,5,8] This allows us to take the energy levels of a symmetrical molecule (such as allyl) for which it is easy to obtain the orbital energies and wavefunctions, and derive the corresponding details for a related molecule which differs in some way. In the present case the perturbation which we apply is just a change in α on one of the atoms. Later, in the next section we will assemble the orbital diagrams of 'complex' molecules from those of simpler fragments. In this case the perturbation then consists of making the linkages between the two fragments; i.e., $H_{\mu\nu}$ between two atomic orbitals increases from 0 to the value it takes in the molecule.

The perturbed energy may be written in the following fashion for the i^{th} energy level

$$E_i = E_i^{(0)} + E_i^{(1)} + E_i^{(2)} + \ldots \quad (30)$$

Where $E_i^{(1)}$ and $E_i^{(2)}$ are the first and second order energy corrections to $E_i^{(0)}$ the unperturbed energy $(|E_i^{(1)}| > |E_i^{(2)}|)$. If the perturbation is the change in the values of some of the Coulomb and interaction integrals, $\delta H_{\mu\nu}$ then these energy corrections become

$$E_i^{(1)} = \delta\langle\psi_i|H|\psi_i\rangle \quad (31)$$

and

$$E_i^{(2)} = \sum_j \frac{|\delta\langle\psi_i|H|\psi_j\rangle|^2}{E_i^{(0)} - E_j^{(0)}} \quad (32)$$

where

$$\delta\langle\psi_i|H|\psi_j\rangle = \sum_{\mu\nu} c_{i\mu}\,\delta H_{\mu\nu}\,c_{j\nu}. \quad (33)$$

The sum in equation (32) is over all other energy levels, j, of the problem.

These expressions may readily be applied to the allyl problem and in fact the use of this example nicely illustrates the workings of the mathematics of equations (31) to (33). The first order correction is easy to see. The perturbation we consider here is just the changing of α on one orbital to $\alpha + \delta\alpha$. So $E_i^{(1)} = c_{i1}^2 \delta\alpha$ where c_{i1} is the coefficient in orbital i of the atomic orbital (say φ_1 of 4) where the perturbation occurs. In Fig. 2 we show the first order energy changes that result by applying this prescription for the two cases of terminal and central atom substitution, by using the values of the coefficients (the c_i) for 6.

The second order correction is a little more tricky. Consider first the basic case of two arbitrary orbitals χ_1 and χ_2. Then for $i = 1$

$$E_1^{(2)} = \frac{|\delta\langle\psi_1|H|\psi_2\rangle|^2}{E_1^{(0)} - E_2^{(0)}} \tag{34}$$

and for $i = 2$

$$E_2^{(2)} = \frac{|\delta\langle\psi_1|H|\psi_2\rangle|^2}{E_2^{(0)} - E_1^{(0)}} = -\frac{|\delta\langle\psi_1|\ |\psi_2\rangle|^2}{E_1^{(0)} - E_2^{(0)}} \,. \tag{34}$$

The result of such a perturbation is to push the lower energy orbital out of χ_1 and χ_2 to lower energy still, and the higher energy orbital to yet higher energy 11. In the present

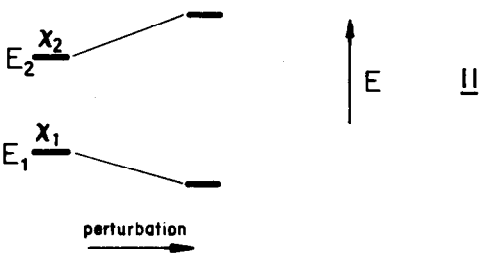

case the second energy correction for orbital i is

$$E_1^{(2)} = \frac{c_{i1}^2 c_{j1}^2 (\delta\alpha)^2}{E_i^{(0)} - E_j^{(0)}} \tag{35}$$

Using the values for the E_i and c_{i1} from 6 the second order energy shifts are shown in Fig. 2.

Table 2

Substitution position	Energy Change	
	two electron	four electron
central atom	$-\lvert\delta\alpha\rvert + (\delta\alpha)^2/4\sqrt{2}\beta$	$-\lvert\delta\alpha\rvert + (\delta\alpha)^2/4\sqrt{2}\beta$
terminal atom	$-\frac{1}{2}\lvert\delta\alpha\rvert + 5(\delta\alpha)^2/16\sqrt{2}\beta$	$-\frac{3}{2}\lvert\delta\alpha\rvert + 5(\delta\alpha)^2/16\sqrt{2}\beta$

The total energy shifts for the two electron (allyl$^+$) and four electron (allyl$^-$) cases are obtained by weighting the energy changes of Fig. 2 with the number of electrons in each orbital. The results are given in Table 2 above, and show that for substitution by a more

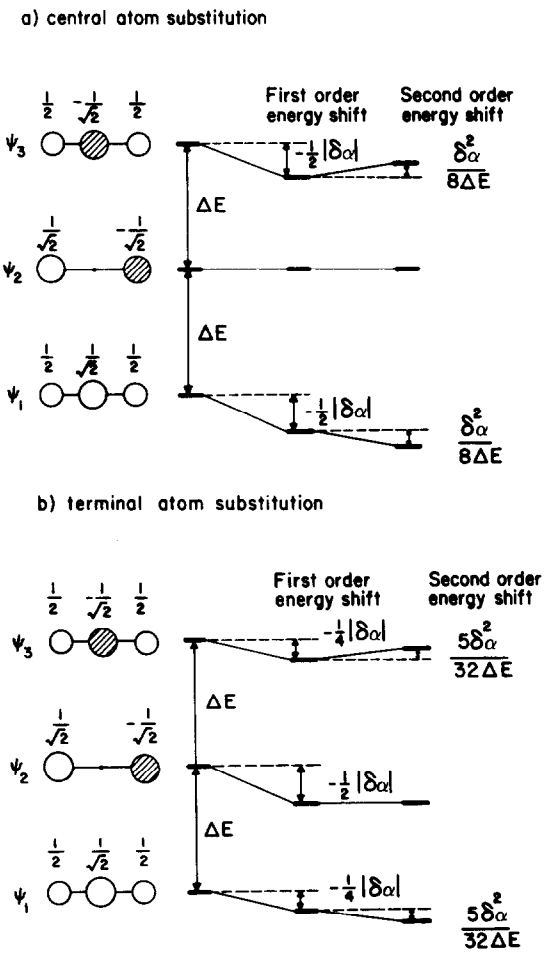

Fig. 2. Perturbation treatment of central versus terminal substitution in a linear three orbital problem. ($\Delta E = \sqrt{2}\beta < 0$).

electronegative atom (i.e., $\delta\alpha < 0$) the maximum stabilization for the two electron case is for central atom substitution. For the four electron case the maximum stabilization occurs for end atom substitution. Although the extension of this result to more complex orbital problems is not obvious, such substitution patterns are indeed actually observed in 'real' systems. 12 shows some examples. Here the twelve electron species Ga_2O, where the two perpendicular

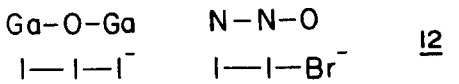

12

π orbitals corresponging to ψ_1 of 6 are full but those corresponding to ψ_3 are empty, shows central atom substitution. However the sixteen electron system N_2O, where both sets of π orbitals corresponding to ψ_1 and ψ_3 are full, shows terminal substitution by the electronegative atom. In the polyhalide ions, where the π manifold is full but the orbitals corresponding to ψ_1 and ψ_3 of the σ set are full, the more electronegative atom is always located in a terminal position.

The correlation of these results with the charge distribution of 10 is important. Notice that the more electronegative atom always occupies the site which carries the highest

negative charge in the unsubstituted parent.[9,10] This is a result which will be useful to us later on.

2.2 Cyclic Systems

Let us see how to generate the level structures of cyclic systems. We shall do this in three different ways, each of which will be illustrative in its own right. First we will assemble the cyclobutadiene levels from those of two ethylene molecules 13. 14 shows a mirror

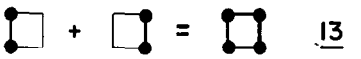

13

14

plane present in both sides of 13 which will be useful in dividing the problem into two symmetry blocks, one containing functions symmetric with respect to this plane and one containing functions antisymmetric with respect to this plane. The two symmetric functions are shown in 15. They are just the in-phase bonding orbitals of the ethylene molecule of 3 with energies

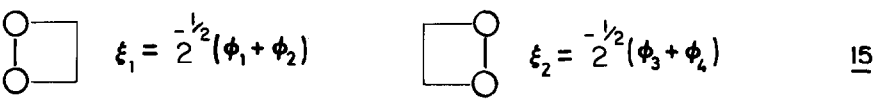

15

of $E = \alpha + \beta$. Now the interaction integral between ξ_1 and ξ_2 is

$$\begin{aligned}\langle \xi_1 | H | \xi_2 \rangle &= \langle 2^{-\frac{1}{2}}(\varphi_1 + \varphi_2) | H | 2^{-\frac{1}{2}}(\varphi_3 + \varphi_4) \rangle \\ &= \tfrac{1}{2}\langle \varphi_1 | H | \varphi_4 \rangle + \tfrac{1}{2}\langle \varphi_2 | H | \varphi_3 \rangle \\ &= \beta \ , \end{aligned} \tag{36}$$

and so the secular determinant for the symmetric block of orbitals is

$$\begin{vmatrix} H_{11} - E & H_{12} \\ H_{21} & H_{22} - E \end{vmatrix} = \begin{vmatrix} (\alpha+\beta) - E & \beta \\ \beta & (\alpha+\beta) - E \end{vmatrix} = 0 \tag{37}$$

This has roots $E = \alpha, \alpha + 2\beta$. The new wavefunctions are just

$$\psi_1 = 2^{-\frac{1}{2}}(\xi_1 + \xi_2) = \tfrac{1}{2}(\varphi_1 + \varphi_2 + \varphi_3 + \varphi_4) \quad \text{for} \quad E = \alpha + 2\beta$$

and

$$\psi_2 = 2^{-\frac{1}{2}}(\xi_1 - \xi_2) = \tfrac{1}{2}(\varphi_1 + \varphi_2 - \varphi_3 - \varphi_4) \quad \text{for} \quad E = \alpha ,$$

derived in an exactly analogous way to the ethylene problem of 3. The two antisymmetric functions are shown in 16. They are the antibonding ethylene combinations with $E = \alpha - \beta$. Solution of the secular determinant for these levels leads in a similar way to $E = \alpha - 2\beta$ and $E = \alpha$. Their respective wavefunctions are $\psi_3 = 2^{-\frac{1}{2}}(\xi_3 - \xi_4) = \frac{1}{2}(\varphi_1 - \varphi_2 - \varphi_3 + \varphi_4)$ and $\psi_4 = 2^{-\frac{1}{2}}(\xi_3 + \xi_4) = \frac{1}{2}(\varphi_1 - \varphi_2 + \varphi_3 - \varphi_4)$. The complete assembly process is shown in Fig. 3. One prominent feature of this diagram is the double orbital degeneracy in the middle of the level stack. It will figure in several discussions later on. Since these levels are degenerate we have a choice as to how their wavefunctions are written. Although the form of ψ_2 and ψ_3 of Fig. 3 is perfectly fine, so is a linear combination of them, 17. These descrip-

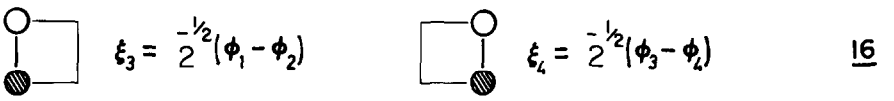

16

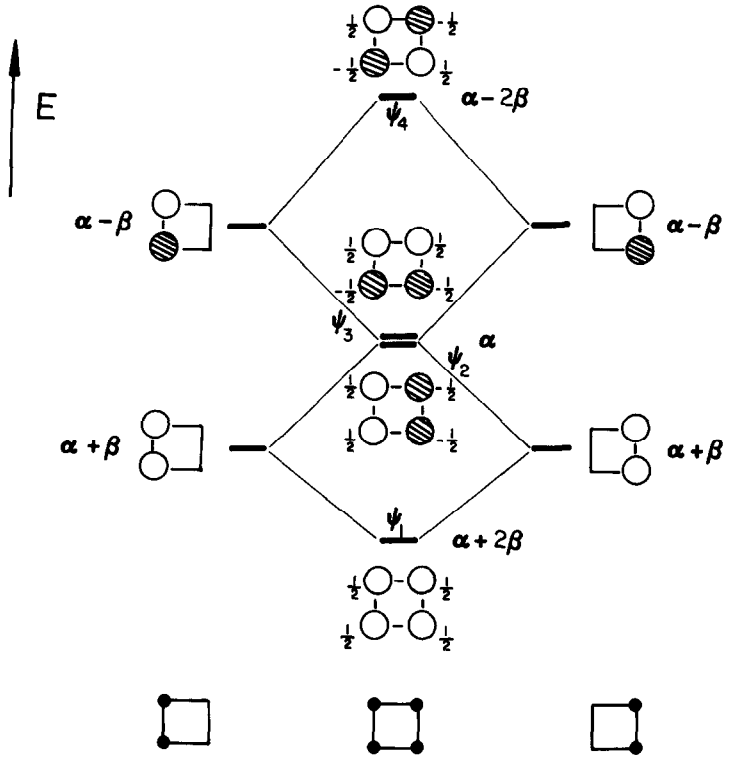

Fig. 3. Assembly of the pπ orbitals of cyclobutadiene

tions better emphasize perhaps the nonbonding nature of this pair located at $E = \alpha$, the energy of an isolated p orbital.

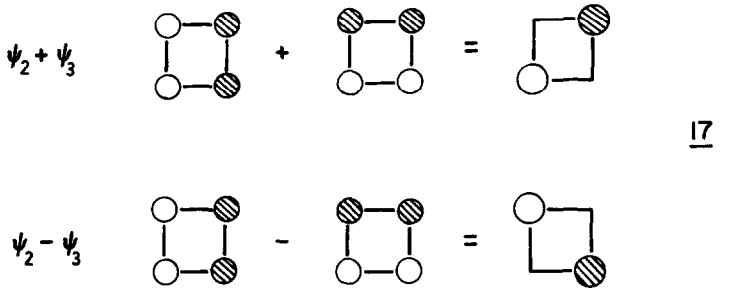

17

In a second route we will assemble the orbital diagram from four separate p orbitals, 18. The point group of the cyclobutadiene molecule is D_{4h} but for our purposes it is sufficient to use the group C_4, the cyclic group of order 4. Its character table is shown in Table 3. Using the four pπ orbitals as a basis for a representation it is easy to show that they transform as a+b+e, i.e., each irreducible representation of C_4 is contained just once in the reducible representation. This is a general result which has implications later in application of these ideas to solids. For a cyclic $(CH)_n$ molecule there will be nπ molecular orbitals, one belonging to each irreducible representation of the group C_n. Using the character table for C_4 and the projection operator of equation (14), it is easy to write down a normalized wavefunction of a symmetry

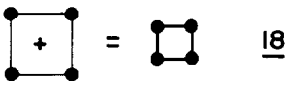

18

Table 3

C_4	E	C_4	C_2	C_4^3
A	1	1	1	1
B	1	−1	1	−1
E	1	i	−1	−i
	1	−i	−1	i

$$\psi(a) = \tfrac{1}{2}(\varphi_1 + \varphi_2 + \varphi_3 + \varphi_4)\,. \tag{38}$$

By substitution into equation (3) its energy is simply

$$\begin{aligned} E &= \tfrac{1}{4}\langle \varphi_1+\varphi_2+\varphi_3+\varphi_4 | H | \varphi_1+\varphi_2+\varphi_3+\varphi_4 \rangle \\ &= \tfrac{1}{4}(4\alpha + 8\beta) = \alpha + 2\beta\,. \end{aligned} \tag{39}$$

Similarly for the wavefunctions of e symmetry

$$\begin{aligned} \psi(e) &= \tfrac{1}{2}(\varphi_1 + i\varphi_2 + \varphi_3 + i\varphi_4) \\ \psi'(e) &= \tfrac{1}{2}(\varphi_1 + i\varphi_2 + \varphi_3 + i\varphi_4) \end{aligned} \tag{40}$$

where in the normalization procedure we have made sure to use $\int \psi^* \psi d\tau = 1$. (i.e., used the complex conjugate ψ^*). These two functions may be converted into two new (real) ones using the license allowed us for degenerate wavefunctions

$$\begin{aligned} \psi''(e) &= 2^{-\frac{1}{2}}(\psi(e) + \psi'(e)) = 2^{-\frac{1}{2}}(\varphi_1 - \varphi_3) \\ \psi'''(e) &= 2^{-\frac{1}{2}}(\psi(e) - \psi'(e)) = 2^{-\frac{1}{2}}(\varphi_2 - \varphi_4) \end{aligned} \tag{41}$$

$\psi''(e)$ and $\psi'''(e)$ are identical to those of 17. They are nonbonding orbitals and substitution into equation (3) gives $E = \alpha$. Use of the characters for the b representation of Table 3 leads to

$$\psi(b) = \tfrac{1}{2}(\varphi_1 - \varphi_2 + \varphi_3 - \varphi_4) \tag{42}$$

and an energy of $E = \alpha - 2\beta$ as found above.

The general result[6] for a cyclic system with n atoms is a very simple one. The energy of the j^{th} orbital is given by

$$E_j = \alpha + 2\beta \cos \frac{2j\pi}{n} \tag{43}$$

where j runs from 0, ±1, ±2 ... (±n/2 for n even) or ((n−1)/2 for n odd). The simple form of equation (43) leads to a useful mnemonic (a Frost circle) for remembering the energy levels of these molecules. Inscribe in a circle of radius 2β an n-vertex polygon such that one vertex lies at the bottom. The points at which the two figures touch define the Hückel

19

energy levels of the molecule as in 19. The coefficient of the p^{th} atomic orbital determines the form of the wavefunction as

$$\psi_j = \sum_{p=1}^{n} c_{jp}\varphi_p = n^{-\frac{1}{2}} \sum_{p=1}^{n} e^{\frac{2\pi i j(p-1)}{n}} \cdot \varphi_p \tag{44}$$

It is an expression which is very similar to that of equation (14). Indeed rewriting it as in equation (45) highlights the similarity.

$$\psi_j = n^{-\frac{1}{2}} \sum_{p=1}^{n} e^{\frac{2\pi i j(p-1)}{n}} \; C_n^{p-1} \; \varphi_1 \; . \tag{45}$$

The exponential is simply the character $\chi_j(C_n^{p-1})$ of the cyclic group of order n as the reader may readily check for the case of $n=4$ shown in Table 3. The prefactor of $n^{-\frac{1}{2}}$ is a (Hückel) normalization constant.

This complex form of the wavefunction is very useful and will be especially so in our discussions later on solids. A linear combination of the wavefunctions of a pair of degenerate orbitals produces two new orbitals which are equivalent in every respect. Using this fact the functions of equation (44) for the case of degenerate species may be rewritten in a somewhat nicer form by making use of the trigonometric identity $e^{ix} = \cos x + i \sin x$ (equation (46)) .

$$\begin{aligned} \psi'_j &= \tfrac{1}{2}(\psi_j + \psi_{-j}) = \tfrac{1}{2} n^{-\frac{1}{2}} \sum_{p=1}^{n} \cos \frac{2\pi j(p-1)}{n} \cdot \varphi_p \\ \psi''_j &= \tfrac{1}{2}(\psi_j - \psi_{-j}) = \tfrac{1}{2} n^{-\frac{1}{2}} \sum_{p=1}^{n} \sin \frac{2\pi j(p-1)}{n} \cdot \varphi_p \; . \end{aligned} \tag{46}$$

It is interesting to see how the wavefunction of equation (44) leads to the energies of equa-

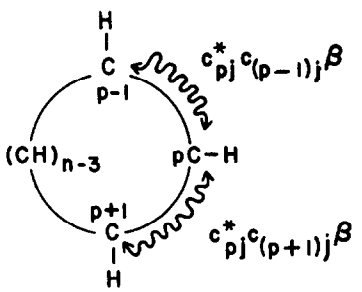

20

tion (43). Substitution of equation (44) into equation (3) gives an expression (equation (47)) for the energy. This represents the sum of all neighbor interactions (20)

$$E_j = \alpha + \beta \sum (c_{jp}c_{j(p-1)} + c_{jp}c_{j(p+1)}) \; , \tag{47}$$

$$E_j = \alpha+\beta \sum_p \left(n^{-\frac{1}{2}} e^{\frac{-2\pi i j(p-1)}{n}} \cdot n^{-\frac{1}{2}} e^{\frac{2\pi i j(p-1)}{n}} \right) \left[e^{\frac{2\pi i j}{n}} + e^{\frac{-2\pi i j}{n}} \right]$$

$$= \alpha + \beta \sum_{p} \frac{1}{n} \cdot 2\cos\left(\frac{2\pi j}{n}\right) \qquad (48)$$

$$= \alpha + 2\beta\cos\frac{2\pi j}{n} \ .$$

Figure 4 shows the energy levels of the first few cyclic molecules. Note how the number of nodes increases as the level stack is climbed.

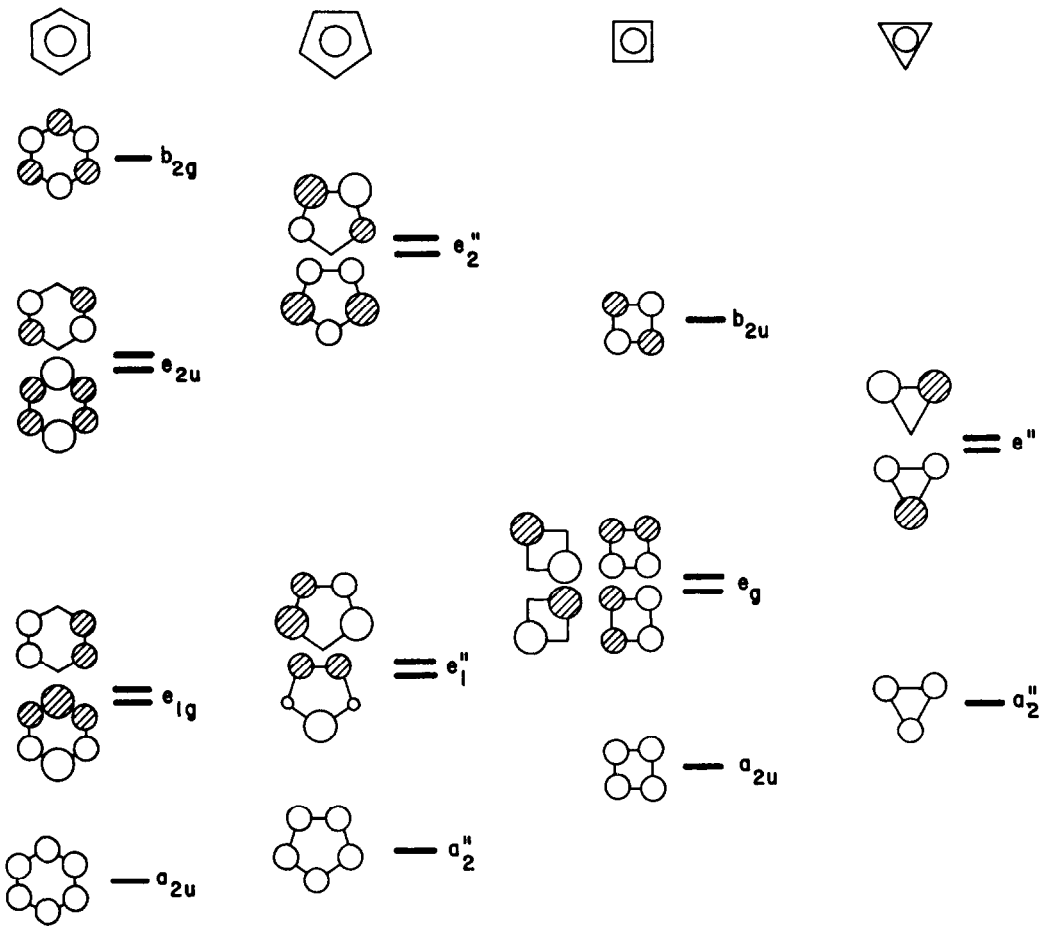

Fig. 4. Energy levels of the first few cyclic polyenes

As a third route to cyclobutadiene we will assemble the diagram in an approximate way from the levels of allyl plus an isolated atom 21 using perturbation theory. Again we will

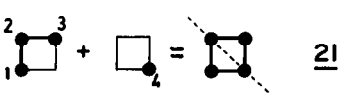

make use of symmetry arguments by classifying the levels as either symmetric or antisymmetric with respect to the mirror plane in 21, the same symmetry element we used before in generating the levels of allyl itself. 22 shows the interaction diagram where we show symmetry (S) or antisymmetry (A) with respect to the mirror plane of 21. The middle level of allyl (ψ_3) finds no symmetry match with an orbital of the single atom, and so remains unchanged in energy and unchanged in character. As we described earlier the interaction energy between two orbi-

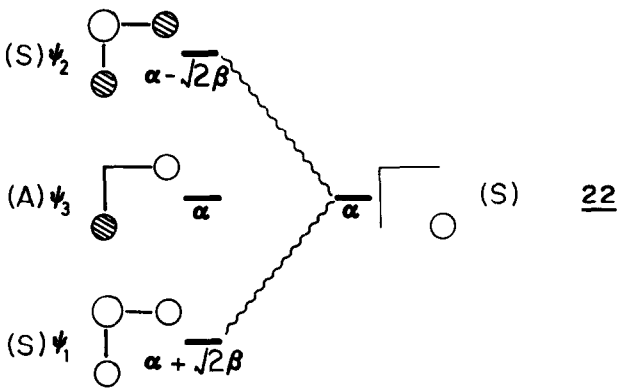

tals χ_1 and χ_2 with energies E_1 and E_2 respectively is simply given by second order perturbation theory as

$$\Delta E_{12} = \frac{|\delta \langle \chi_1 | H | \chi_2 \rangle|^2}{E_1^{(0)} - E_2^{(0)}} \quad . \tag{49}$$

With reference to 22 ψ_1 is depressed in energy by

$$\frac{|\delta \langle \psi_1 | H | \varphi_4 \rangle|^2}{(\alpha + \sqrt{2}\beta) - (\alpha))} \tag{50}$$

the numerator can be evaluated as

$$\delta \langle \psi_1 | H | \varphi_2 \rangle = \langle \tfrac{1}{2}\varphi_1 + \frac{1}{\sqrt{2}}\varphi_2 + \tfrac{1}{2}\varphi_3 | H | \varphi_4 \rangle = \beta \tag{51}$$

which means that

$$\Delta E^{(2)} = \frac{\beta}{\sqrt{2}\beta} = 0.707\ \beta$$

and the perturbed energy of ψ_1 is $\alpha + 2.12\,\beta$. φ_4 is destabilized by the same amount, $0.707\,\beta$. Now ψ_2 and ψ_4 may couple in exactly the same way. It is a simple matter to show that the second order energy numerator is the same as before which means φ_4 is depressed in energy by $0.707\,\beta$ and ψ_2 raised in energy by 0.707β. The overall result is that φ_4 remains unchanged in energy but ψ_1 ends up at $\alpha + 2.12\,\beta$, 23. Perturbation theory also tells us about the new

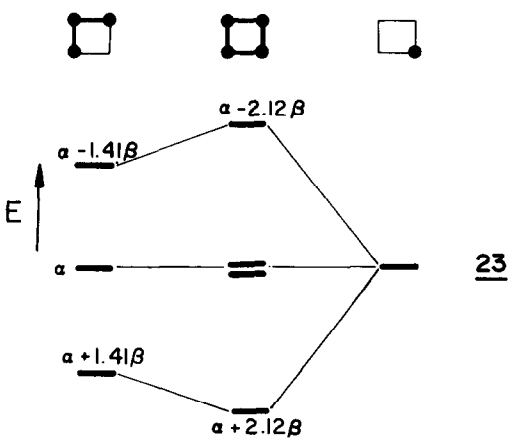

wavefunctions. With respect to a generalized pair of orbitals χ_1 and χ_2, χ_2 mixes into χ_1 in a bonding way

$$\chi_1' = \chi_1 + \frac{\delta\langle\chi_1|H|\chi_2\rangle}{E_1^{(0)} - E_2^{(0)}}\,\chi_2 \tag{52}$$

and χ_1 mixes into χ_2 in an antibonding way

$$\chi_2' = \chi_2 - \frac{\delta\langle\chi_1|H|\chi_2\rangle}{E_1^{(0)} - E_2^{(0)}}\,\chi_1 \,. \tag{53}$$

So the new wavefunctions become

$$\begin{aligned}
\psi_1' &= \tfrac{1}{2}\varphi_1 + \frac{1}{\sqrt{2}}\varphi_2 + \tfrac{1}{2}\varphi_3 + \frac{1}{\sqrt{2}}\varphi_4 = 0.5\,\varphi_1 + 0.7071\,\varphi_2 + 0.5\,\varphi_3 + 0.7071\,\varphi_4 \\
\psi_2' &= \tfrac{1}{2}\varphi_1 - \frac{1}{\sqrt{2}}\varphi_2 + \tfrac{1}{2}\varphi_3 - \frac{1}{\sqrt{2}}\varphi_4 = 0.5\,\varphi_1 - 0.7071\,\varphi_2 + 0.5\,\varphi_3 - 0.7071\,\varphi_4 \\
\psi_3' &= \varphi_4 - \frac{1}{\sqrt{2}}\left(\tfrac{1}{2}\varphi_1 + \frac{1}{\sqrt{2}}\varphi_2 + \tfrac{1}{2}\varphi_3\right) + \frac{1}{\sqrt{2}}\left(\tfrac{1}{2}\varphi_1 - \tfrac{1}{2}\varphi_2 + \tfrac{1}{2}\varphi_3\right) \\
&= \varphi_4 - \varphi_2 \\
\psi_3' &= \psi_3 = \frac{1}{\sqrt{2}}\varphi_1 - \frac{1}{\sqrt{2}}\varphi_3 \,.
\end{aligned} \tag{54}$$

The new wavefunctions describing the level at $E = \alpha$ have just the forms we found before by other routes. This is not the case for the new wavefunctions ψ_1' and ψ_2'. A part of the problem lies in a mixing, which we have ignored, between two orbitals on the same fragment (orthogonal before the perturbation) under the influence of the perturbation. If χ_1 and χ_3 are two levels on the same fragment they mix as a result of interaction with χ_2 of another fragment in the following way

$$\chi_1' = \chi_1 + \frac{\delta\langle\chi_1|H|\chi_2\rangle\,\delta\langle\chi_2|H|\chi_3\rangle}{\left(E_1^{(0)} - E_3^{(0)}\right)\left(E_1^{(0)} - E_2^{(0)}\right)} \,. \tag{55}$$

So ψ_1' looks like

$$\begin{aligned}
\psi_1' &= \tfrac{1}{2}\varphi_1 + \frac{1}{\sqrt{2}}\varphi_2 + \tfrac{1}{2}\varphi_3 + \frac{1}{\sqrt{2}}\varphi_4 + \frac{\beta\cdot\beta}{(-2\sqrt{2}\beta)(-\sqrt{2}\beta)}\left(\tfrac{1}{2}\varphi_1 - \frac{1}{\sqrt{2}}\varphi_2 + \tfrac{1}{2}\varphi_3\right) \\
&= 0.625\,\varphi_1 + 0.582\,\varphi_2 + 0.625\,\varphi_3 + 0.582\,\varphi_4
\end{aligned} \tag{56}$$

and

$$\psi_3' = 0.625\,\varphi_1 - 0.582\,\varphi_2 + 0.625\,\varphi_3 - 0.582\,\varphi_4 \,. \tag{57}$$

These new functions, though improved, are still not exactly what we found by exact solution of this problem above, and indeed they should not be. Perturbation theory did not give exact values for the energies of the top and bottom orbitals of cyclobutadiene, and correspondingly the wavefunctions will be approximate too. We could have performed the necessary numerology by solving two secular determinants, one for the symmetric levels and one for the antisymmetric ones. The results are of course those of Fig. 3, $E = \alpha$ (antisymmetric block) and $E = \alpha$, $\alpha + \beta$, $\alpha - \beta$ (symmetric block). However the perturbation treatment is a very useful approach for understanding where these levels have come from. In Fig. 5 we show a similar result for the assembly 24 of the levels of pentalene, from those of cyclopentadiene and allyl, two building blocks whose orbitals we have derived already. Again the agreement with the 'exact' result is not perfect.

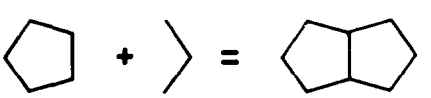

24

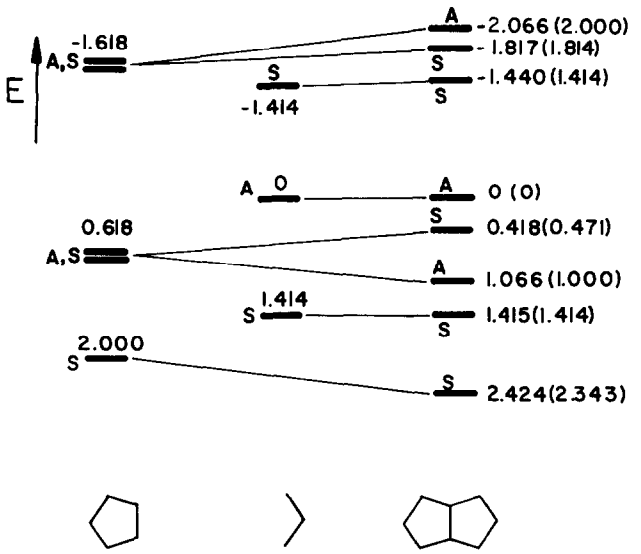

Fig. 5. Perturbation treatment for the assembly of the pπ levels of pentalene. Exact values shown in parentheses. (The energies are in units of β relative to α = 0.) The labels A and S refer to the parity of the wavefunction with respect to the mirror symmetry of the problem

The atomic charges in cyclopentadienyl will of course all be equal from the symmetry of the molecule, but pentalene has three symmetry inequivalent sites. Either by working out the form of the wavefunctions of the molecule by using the ideas of perturbation theory, or more realistically, looking up the coefficients in the compendium of Streitweiser, Brauman and Coulson[7] we may calculate the π-charge distribution in pentalene and pentalene$^-$. They are shown in 25. Notice that on formation of the negative ion the extra electron density has appeared only on the atoms at the 1 position. Making use of our observation above concerning the site preferences in substituted molecules, 24 leads to the prediction of electropositive atoms in the 1 position and the electronegative atoms elsewhere. This is just what is found in the molecule $B_4N_4H_6$ 26.

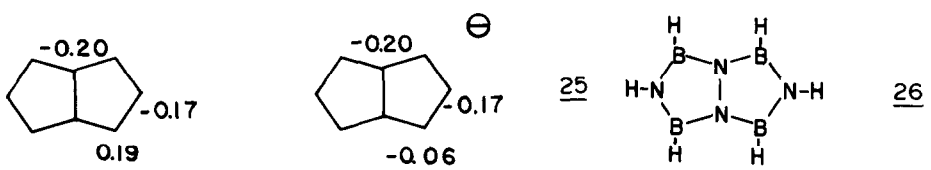

There are several results which have their basis in graph theory which are worth mentioning here. The reader may have noticed that the level structures of almost all of the systems we have studied (with the exception of cyclopentadiene and pentalene) contain a mirror symmetry about $E = \alpha$. i.e., all the levels occur in pairs at $E = \alpha \pm x\beta$. If there are an odd number of atoms then there is at least one level at $E = \alpha$. (The level structure of pentalene (Fig. 5) shows no such symmetry.) This is a general feature of orbital situations which, when all centers are labeled either with a star or left unstarred, no two starred or no two unstarred centers are adjacent. Such molecules are described as alternant hydrocarbons[6] or, in the jargon of graph theory, as bipartite systems. 27 and 28 show some examples of alternant systems. For molecules of this type the levels are always symmetrically placed about $E = \alpha$. 29 shows some nonalternant hydrocarbons where two starred atoms are adjacent. This

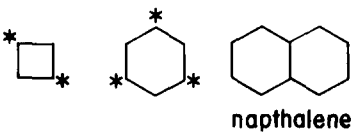

napthalene 27

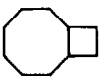

28

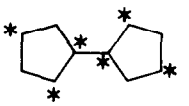

azulene 29

will always be the case for molecules containing odd membered rings. For these systems there is no such symmetry. Of particular interest to us is the variation in the energy difference between structures as a function of the number of $p\pi$ electrons ($N_{p\pi}$). 30 shows the energy difference between napthalene and the molecules in 28 and 29. Notice that the curve representing the energy difference between the two alternant systems is, like their individual orbital structures, symmetrical about the half-way point, but the energy difference between an alternant and nonalternant molecule shows no such symmetry at all. (Of course for real systems the only points of 30 which have any chemical meaning is the region around 10 elec-

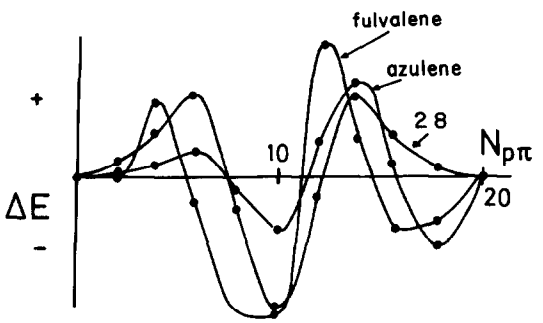

30

trons (five pairs) where each carbon atom contributes just one $p\pi$ electron. At this point napthalene, with two six membered rings is more stable than any of the other molecules.

Another result, coming from graph theory,[11] is that equation (58) holds for regular graphs, i.e., those systems where the coordination number (v) is the same for all atoms:

$$M = \frac{1}{n} \sum_j \chi_j^2 = v\beta^2 \tag{58}$$

From equation (48) therefore for all annulenes where each atom is two coordinate

$$M = \frac{1}{n} \sum_j 4\beta^2 \cos^2 \frac{2\pi j}{n} = 2\beta^2 \ . \tag{59}$$

This is a well known trigonometric identity. Equation (59) applies to all systems, irrespective of their alternant or nonalternant character.

A further observation of Guttman and Trinajstic[12] is that for neutral carbon compounds, where each carbon atom contributes one $p\pi$ electron, loops of length $(4m+2)$ stabilize the structure but loops of length $4m$ destabilize the structure ($m = 1, 2 \ldots$). That this is the

case is quite clear from 30 where the structure with two six rings (napthalene) is most stable for five π electron pairs. The molecule 28 is unstable, compared to naphtalene around this half-filled point.

2.3 Jahn-Teller Instabilities

An extremely useful theorem of Jahn and Teller[4,13] allows us to predict some of the conditions under which a symmetric structure will lie at a local energy maximum with respect to particular distortions away from that structure. We will not discuss the operational details[14] here but the basic philosophy is easy to follow. If there is an asymmetric occupation of a degenerate set of levels at a particular geometry then the energy will be lowered by a distortion which removes the degeneracy as shown in 31 for the case where the two

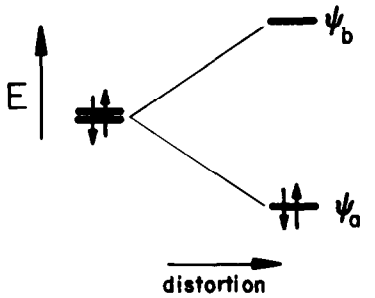

31

electrons have their spins paired. For the triplet situation where the electron spins are parallel and the Pauli principle demands that the two electrons lie in separate orbitals, then on distortion one electron goes up in energy while the other goes down and there is no resulting stabilization. The cyclobutadiene molecule is an interesting example of this situation. With four pπ electrons the electronic configuration is $(a)^2$ $(e)^2$ and singlet and triplet states are possible. The former being Jahn-Teller unstable, and the latter Jahn-Teller stable at the square geometry. Although the Jahn-Teller approach does not tell us in detail how the molecule will distort, 32 shows how the energy levels will change on 'dimerization'. This

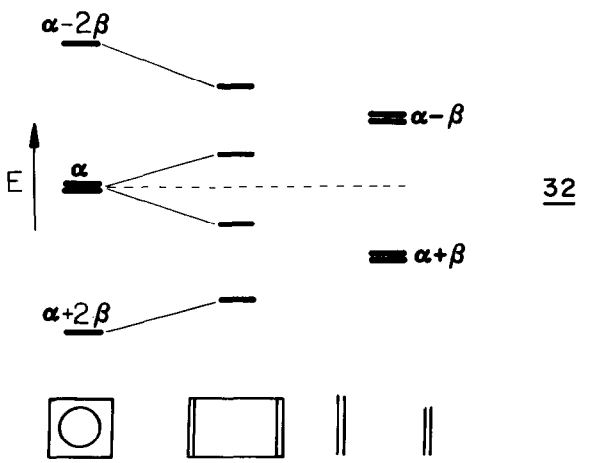

32

dimer structure lies somewhere along the pathway to fragmentation into two double bonded units (also shown in 32) and is just the reverse of the assembly process we used above to derive the cyclobutadiene levels in the first place. Numerically of course the π energy is equal

to $4(\alpha+2\beta)$ at both the left- and right-hand sides (where two bonds are completely broken) of 27. In viewing the distortion however we can assume that two of the linkages shorten ($|\beta_1| > |\beta|$) while the other two lengthen ($|\beta_2| < |\beta|$). The reader can readily verify using the first order perturbation expression of equation (31) along with the wavefunction of Fig. 3 that the new π energies are those given in 33. If $\beta_1 + \beta_2 \simeq 2\beta$ then the π stabilization on

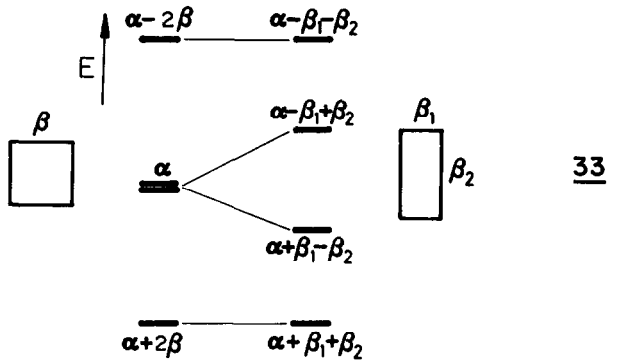

33

distortion is just $2(\beta_1-\beta_2)$. The experimental evidence for singlet butadiene points to a nonsquare planar molecule, but whether it is a rectangle or rhombus is still open to question.[15]

We can ask how to stabilize a singlet cyclobutadiene molecule against such a distortion by mimicking in some way the opening up of the energy gap between HOMO and LUMO which occurs on geometrical distortion. One way this can be done[16] is by substitution of the hydrogen atoms by electron withdrawing and electron donating groups. These will respectively increase and decrease the value of $|\alpha|$ of the atom to which they are attached. Two disubstituted possibilities arise, 34 and 35. Let us use perturbation theory to see which one will

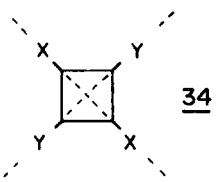

34

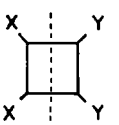

35

be best. All we need to do is to calculate the energy shifts of the four orbitals of Fig. 3 as a result of increasing α (by $\delta\alpha$) on two atoms and decreasing α (by $\delta\alpha$) on the other two. The problem is no more complex than that of the substituted allyl system of Fig. 2 but we can use symmetry considerations to help us out. We will choose the form of the e species wavefunctions to match the point symmetry of the substituted systems; the orbitals of 17 for 34 and those of Fig. 3 for 35, respectively.

First let us look at the alternating substitution pattern of 34. The resulting first and second order changes are shown in 36. Notice there is no first order shift for ψ_1 or ψ_4 since

$$E_1^{(1)} = [(\tfrac{1}{2})^2 + (\tfrac{1}{2})^2]\delta\alpha + [(\tfrac{1}{2})^2 + (\tfrac{1}{2})^2](-\delta\alpha) = 0 . \qquad (60)$$

Also note that the splitting between ψ_2 and ψ_3 is exactly $2\delta\alpha$. Both ψ_1 and ψ_4 are symmetric with respect to reflection in the two mirror planes 34 one of which passes through the two X atoms and the other through the two Y atoms. ψ_2 and ψ_3 are antisymmetric with

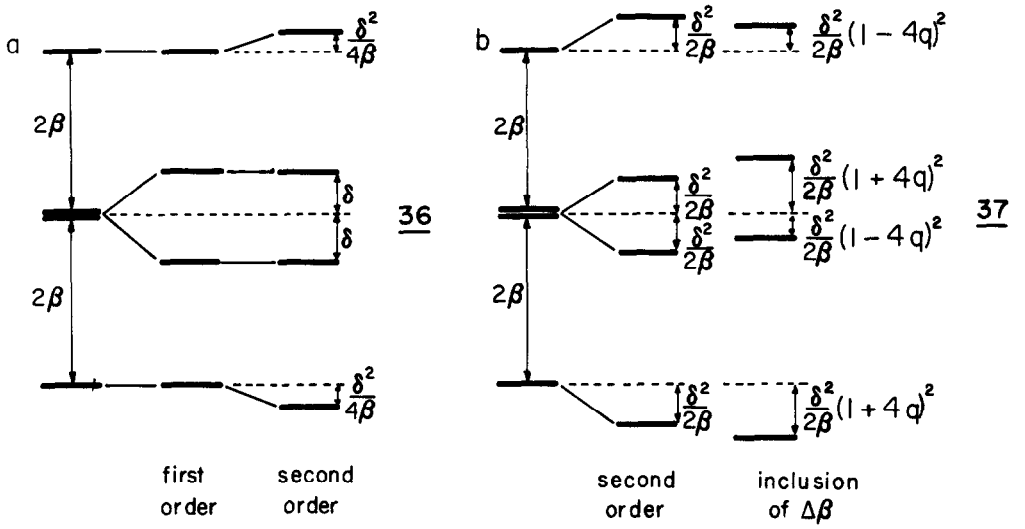

respect to one of these operations. So ψ_1 and ψ_4 interact energetically in second order but ψ_2 and ψ_3 remain unchanged. The interaction energy is

$$\frac{[(\frac{1}{4}+\frac{1}{4})\delta\alpha+(-\frac{1}{4}-\frac{1}{4})(-\delta\alpha)]^2}{(\alpha+2\beta)-(\alpha-2\beta)} = \frac{(\delta\alpha)^2}{4\beta} \quad . \tag{61}$$

Second, for the pattern of 35 all the first order energy corrections are identically zero, since they are all of the form of equation (60). $\psi_1 - \psi_4$ of Fig. 3 may be classified according to their parity under the mirror plane of 35. In second order the symmetric functions ψ_1 and ψ_3 will interact with each other. Similarly the antisymmetric functions ψ_2 and ψ_4 will interact with each other. In both cases the interaction energy is

$$\frac{[(\frac{1}{4}+\frac{1}{4})\delta\alpha+(-\frac{1}{4}-\frac{1}{4})(-\delta\alpha)]^2}{(\alpha+2\beta)-\alpha} = \frac{(\delta\alpha)^2}{2\beta} \quad . \tag{62}$$

The overall result is shown in 37. With a total of four π electrons, the stabilization energy of 34 is $2\delta\alpha + (\delta\alpha)^2/2\beta$ and that of 35 is $2(\delta\alpha)^2/\beta$. Assuming that $|E^{(1)}| > |E^{(2)}|$, then for this electronic configuration the pattern 34 is preferred. Indeed all 'push-pull' cyclobutadienes that have been made are of this type 38.[17] The molecule $B_2N_2R_4$, where R is a substituent, has this pattern too.

For the hypothetical case of two π electrons or of six π electrons then the results of 36 and 37 suggest that the XXYY pattern of 35 should be preferred. 39 shows schematically an energy difference plot as a function of the number of π electron pairs (P_π).

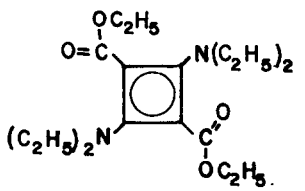

38

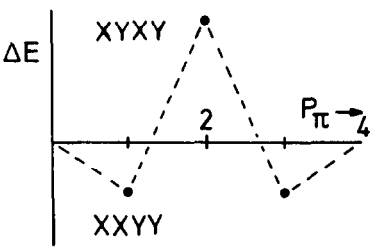

39

The picture here is a simplified one. According to the Wolfsberg-Helmholz formula (equation (5)), changing the value of $H_{ii}(\alpha)$ also leads to a change in $H_{ij}(\beta)$. This consideration will not affect the energies for the substitution pattern 34 since all the linkages involve unlike atoms and here the change in β is given by

$$\delta\beta = (\delta\alpha - \delta\alpha) = 0 \ . \tag{63}$$

For the two linkages in 30 which involve like atoms then $\delta\beta \propto \delta\alpha$ and $\delta\beta \propto -\delta\alpha$ respectively. Using a proportionality constant of q in these last two expressions leads to the changes indicated at the right-hand side of 37. The only changes occur in contributions to the second order energy. The result is a change in the form of the plot of 39. If these second order corrections are small then an asymmetry 40 develops. If these effects are large then there is a reversal of the form 41 of the more stable isomer for three pairs of π electrons.

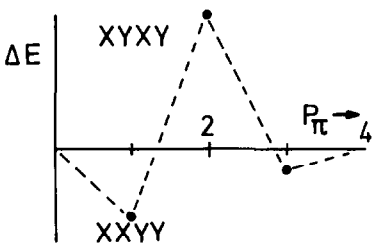

40

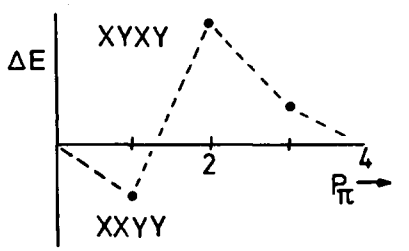

41

The molecule S_2N_2, with this electronic configuration is an example of this situation. It has the pattern 34. We shall see a similar series of plots in the solid state later.

Another way to stabilize the square geometry is to add two more electrons to cyclobutadiene. The molecules S_4^{+2}, Se_4^{+2} and Te_4^{+2} have this electronic configuration, and indeed they have a square geometry.[18]

3. ELECTRONIC STRUCTURES OF SIMPLE SOLIDS

3.1 Energy Bands

In this section we tackle the orbital problem for the case of that infinite molecule, the extended solid state array. First we look at the one-dimensional system with its obvious simplicity, and consider the situation presented by an infinite chain of carbon atoms each carrying one pπ orbital, i.e., polyacetylene, $(CH)_n$. (As we will see, very similar results apply to other systems with one 'frontier' orbital per atom or structural unit). In all our deliberations in this article we will consider only the case of crystalline materials, i.e., those with a regularly repeating motif. The unit cell of the infinite chain is of length a 42. From the results described in Section 2.A we know qualitatively what the orbitals of

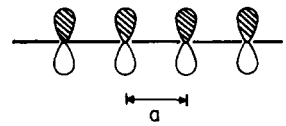

42

this infinite system looks like. Equation (27) tells us immediately there is an infinite set of orbitals, the lowest energy of which is at $E = \alpha + 2\beta$ and is bonding between all adjacent pairs of atoms. The highest energy orbital is at $E = \alpha - 2\beta$ and is antibonding between all adjacent atom pairs. Between them lies a continuum of orbitals 43 which we call an energy

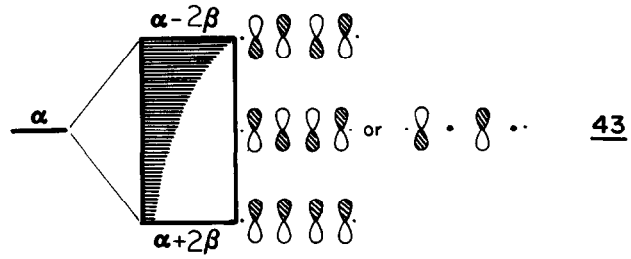

43

band with a width of $4|\beta|$. Just as in the finite linear molecule case of Fig. 1, the number of nodes increases as the energy increases. Right in the middle of the stack at $E=\alpha$ there is a nonbonding orbital.

One easy way to describe the energy levels of such an infinite system is to impose Born-von Karman boundary conditions on the problem. In practice this entails imperceptibly bending the one-dimensional chain of atoms into a loop, as shown schematically in 44. Of

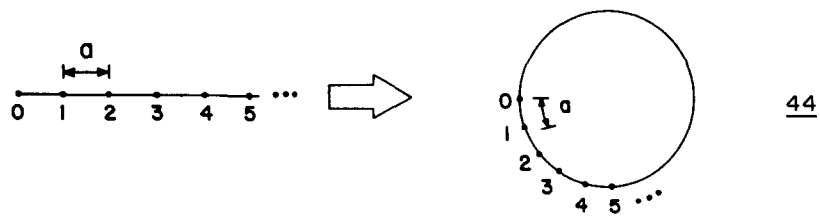

44

course the number, N, of atoms (orbitals) in this loop is huge. So the bending of the chain is 'imperceptible' only as far as the atoms of the chain are concerned. Equation (43) then tells us that there will be N energy levels whose energies are given by equation (64)

$$E_j = \alpha + 2\beta \cos(2j\pi/N) \tag{64}$$

where j takes all integral values from 0, ±1, ±2 ... ±N/2. This is a very unwieldy expression since N/2 is extremely large but it may be rewritten in a much neater fashion by defining a new index k such that

$$E(k) = \alpha + 2\beta \cos ka. \tag{65}$$

Here a is the unit cell length of 42 and $k = 2j\pi/Na$, called the wavevector takes values from 0 continuously to $\pm\pi/a$. Figure 6 shows the transition[19] from the finite to the infinite case. Recall that for an n membered ring j in equation (43) took values from 0, ±1, ±2 through $(n-1)/2$ for an odd-membered ring. So for the five-membered ring the extremal value of $|j|$ is $j_{max} = 2$. For the fifteen-membered ring the corresponding value of j_{max} is 7

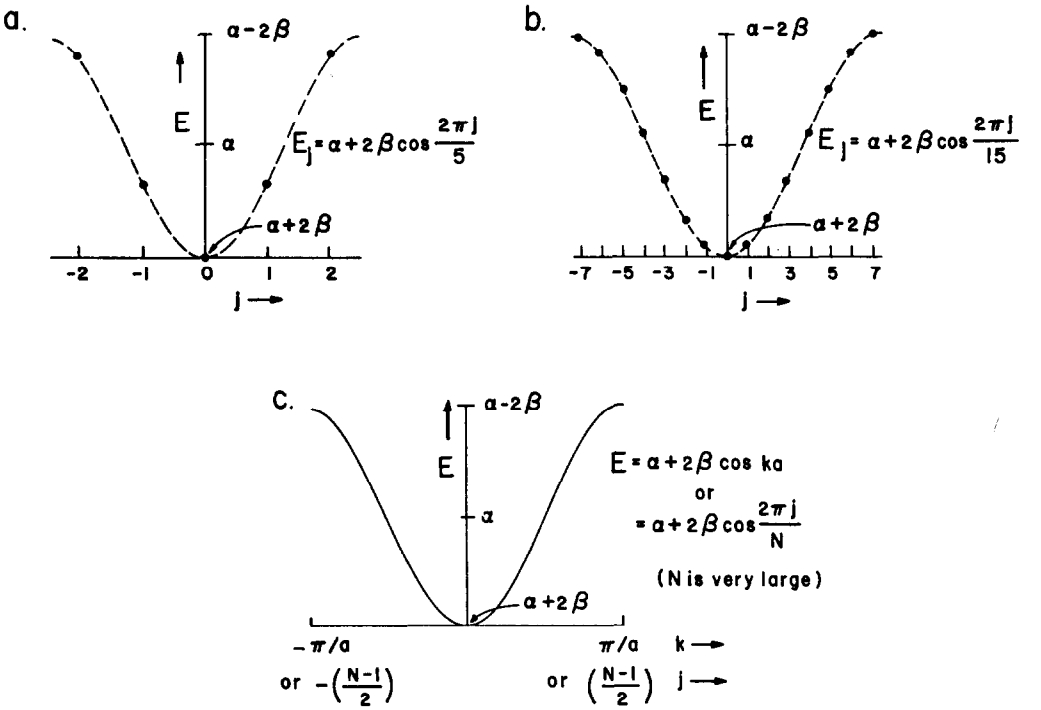

Fig. 6. The transition from the finite to infinite case pπ energy levels of (a) cyclopentadiene, (b) 15-annulene, and (c) an infinite loop or one-dimensional solid as a function of the j or k index.

What happens if values of $|j|$ larger than j_{max} are used? The reader may readily show that the energy levels already derived with $j < j_{max}$ are generated: i.e., use of $j > j_{max}$ gives redundant information. Similarly in equation (65), use of values of $|k| > \pi/a$ also leads to no new information. In the crystalline state the levels lying between $-\pi/a < a < \pi/a$ are called the (first) Brillouin zone. $k = 0$ is the zone center, $k = \pm\pi/a$ is the zone edge and the variation of the energy with k is the dispersion of the band. Figure 6c is just then a 'smoothed out' version of Fig. 6b with a continuum of levels (in the limit $N \to \infty$) rather than a discrete set.

The wavefunctions of this infinite unit are also easily written down by the substitution of $k = 2j\pi/Na$ in equation (45) as

$$\psi_j = N^{-\frac{1}{2}} \sum_{p=1}^{n} e^{\frac{2\pi i j(p-1)}{n}} c_n^{p-1} \varphi_1$$

$$\psi(k) = N^{-\frac{1}{2}} \sum_{p=1}^{N} e^{ik(p-1)a} \varphi_p \quad . \tag{66}$$

Group theory allows us to write down a similar expression for the orbitals of this infinite, periodically repeating chain. An expression analogous to equation (14) for the molecular case is given in equation (67) for the translation group T. This is an infinite group made up of all translations $t \in T$. There are correspondingly an infinite number of k values

$$\psi(\underline{k}) = \sum_{t \in T} \chi_k(t)\, t\varphi_1 \tag{67}$$

$$= \sum_{t \in T} e^{ikR_t} \varphi_t(\underline{r} - \underline{R}_t), \tag{68}$$

but the characters take on a simple exponential form. Here R_t is the distance along the chain which the translation operation t moves φ_1 and $\varphi_t(\underline{r}-\underline{R}_t)$ is an orbital translationally equivalent to φ_1, i.e., $t\varphi_1(\underline{r}) = \varphi_t(\underline{r}-\underline{R}_t)$. If we write $R_t = (p-1)a$ then it is obvious that equations (66) and (68) are identical except for a normalization constant. This was to be expected since via the construction of 44 the infinite translation group and the cyclic group of infinite order are isomorphous. In other words k, the wavevector, in equations (66) and (68) are the same. In three dimensional systems the vector nature of k becomes apparent and, as we will see later, we need to replace the exponential in this equation with a vector dot product $\exp(i\underline{k}\cdot\underline{R}_t)$ where $\underline{R}_t = \sum_i (p_i-1)\underline{a}_i$, a sum over the primitive lattice vectors $\underline{a}_i$. Just as the vector $\underline{R}_t$ (with dimensions of length) maps out a direct space (x,y,z coordinates) so $\underline{k}$ (with dimensions of $(\text{length})^{-1}$) maps out a reciprocal space. The symmetry adapted functions $\psi(\underline{k})$ are called Bloch functions, $\psi(\underline{k}) = \sum_p c_{kp}\varphi_p$. As in the case of the cyclic system, all the levels turn up in pairs (positive and negative k values). To understand the orbital structure of the (one-dimensional) solid we only need one set of values; we choose the positive set, the right-hand side of Fig. 6c.

The energy levels themselves can also be derived by using an approach identical to the one in Section 2.2 and shown in 20. The energy of the level of the infinite chain described by a given value of k is given by multiplying by N, the number of orbitals in the chain, the energy contribution from the interaction of a single orbital with its neighbors

$$\begin{aligned} E(k) &= Nx\left[\left\langle N^{-\frac{1}{2}}\exp(-ikpa)\varphi_p\,|H|\,N^{-\frac{1}{2}}(\exp(-ik(p-1)a)\varphi_{p-1} + \right.\right. \\ &\qquad \left.\left. \exp(ikpa)\varphi_p + \exp(ik(p+1)a)\varphi_{p+1}\right\rangle\right] \\ &= Nx[\alpha+\beta(\exp(ika)+\exp(-ika))] \\ &= \alpha+2\beta\cos ka\ . \end{aligned} \tag{69}$$

The top of the band occurs at $k=\pi/a$ where $\cos ka = -1$ and $E=\alpha-2\beta$. The bottom of the band is found at $k=0$ where $\cos ka = 1$ and $E=\alpha+2\beta$. The middle of the band occurs at $k=\pi/2a$ where $\cos ka = 0$ and $E=\alpha$. At $k=0$ the phase factor linking an orbital with its neighbor is, from equation (68), equal to +1 and so the Bloch function looks like 45. This is bonding between all adjacent atom pairs. At $k=\pi/a$ the phase factor is −1 and the Bloch function looks like 46. The number of states with a given energy n(E) is usefully shown in a density of states plot (Fig. 7b). n(E) turns out to be proportional to $(\partial E/\partial k)^{-1}$ for the


45


46

solid state continuum of levels,[20] a function which the reader will see has the shape shown. We will describe below how the density of states is constructed in general. For comparison the density of states plot for the discrete molecular benzene case is shown in 47. Filling up the levels of the energy band with with electrons each will give a total of 2N electrons for the N atom chain (N is large!). Normally when describing band occupancy we refer to the number of electrons per unit cell, and so this π band for the infinite chain may contain a maximum of 2 electrons.

The collection of $p\pi$ orbitals we have just studied would describe the electronic π band of polyacetylene 48 in a geometry where all the C—C distances are equal. Since there is one electron contributed per carbon $p\pi$ orbital the π band is exactly half full. We show this by the crosshatching of the occupied states in Fig. 7b. Throughout this article we will use the simple representation of this situation shown in 49. Note that such a system

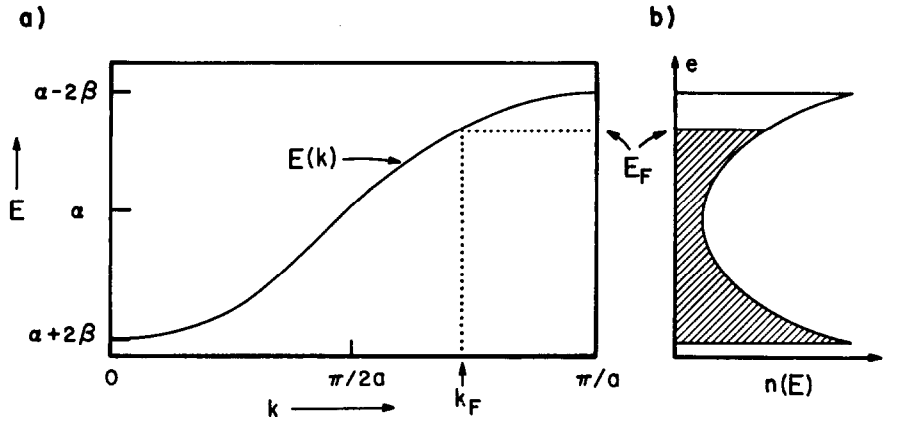

Fig. 7. (a) E versus k (dispersion) curve for a one-dimensionsl chain of pπ orbitals; (b) density of states plot, n(E). The energy levels are filled up (indicated by shading) to the Fermi level E_F, corresponding to k_F. For polyacetylene the band would be half full.

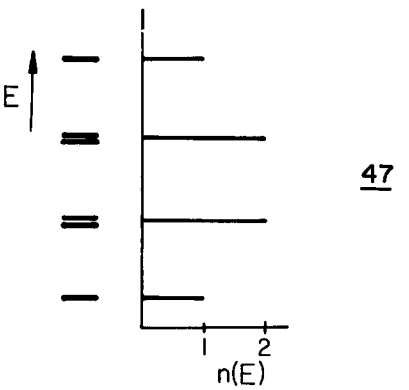

47

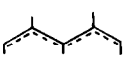

48

49

50

is metallic. In 50 we show another electronic possibility where all the levels are filled with unpaired electrons. A solid with this electronic arrangement would be a magnetic insulator. The interplay between the stabilities of these two distributions will be discussed later The top of the occupied stack of levels is called the Fermi level with an energy E_F. The corresponding $\underline{k}$ point (Fig. 7a) is labelled $\underline{k}_F$.

This LCAO type of approach applied to solids is called the tight-binding model by solid state physicists. It will be clear that it is really no different to the LCAO scheme for molecules. In Section 1.2 we showed that the levels of a molecule were accessible by solution of the determinantal equation

$$\left|H_{ij} - S_{ij}E\right| = 0 \,. \tag{70}$$

Here the H_{ij} and S_{IJ} were the interaction and overlap integrals between a basis set of

atomic orbitals $\{\varphi_i\}$. In the solid state the analogous equation is

$$\left| H_{ij}(\underline{k}) - S_{ij}(\underline{k})\, E \right| = 0 , \tag{71}$$

where now the H_{ij} and S_{ij} integrals are those between the Bloch functions (equation (68)) constructed for each atomic orbital contained in the unit cell. Whereas for the molecule equation (70) is solved just once to generate the energy levels, equation (71) needs to be solved (in principle) at an infinite number of $\underline{k}$ points. Sometimes we are lucky and are able to write down an analytic expression (as in equation (69) for example) for E(k) but more usually we need to solve equation (71) numerically for a mesh of $\underline{k}$ points which will represent the behaviour of the whole energy band when averaged. We will use the method later on to estimate the energies of structural alternatives. This 'special points' method[21,22] is in general a very useful way of replacing a complex integration over $\underline{k}$ space with a set of individual calculations. For a solid state system in general the density of states may be obtained by using the technique in Fig. 8. Solution of equation (71) at a large number of $\underline{k}$ points will generate an even larger number of energy levels which may be arranged in order of increasing energy. The number of such levels contained within a small energy increment can be evaluated and used to produce a histogram for n(E). A little cosmetic smoothing produces the desired result. Generation of a dispersion diagram (behavior of E with respect to k) proceeds in the same manner. Smooth curves are drawn between the sets of points representing the energies at different k values.

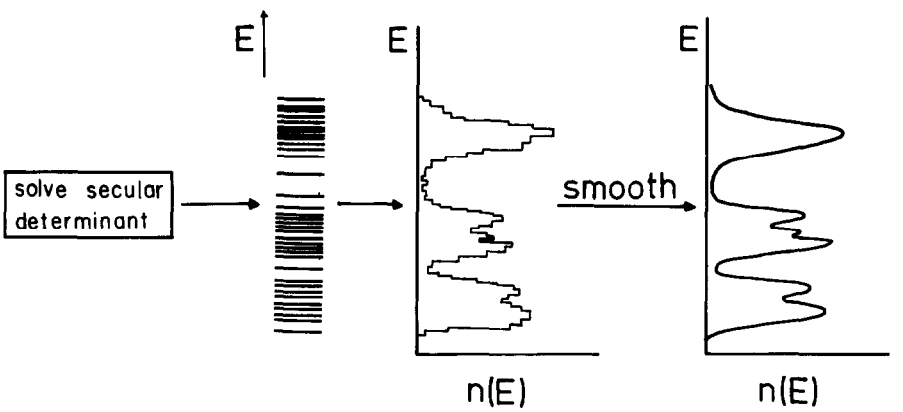

Fig. 8. Schematic showing the method of generating the energy density of states n(E)

In section 2 we extensively used the Hückel approximation by putting $S_{ij} = \delta_{ij}$ in equation (7). In much of this section too we will do the same by writing $S_{ij}(\underline{k}) = \delta_{ij}$ since it will allow algebraic access to several results of interest. Later we will relax this restriction when we look at more complex systems.

3.2. The Peierls Instability[23]

In the previous section we chose a repeat unit for the calculation which contained a single orbital. If we choose a two-atom repeat unit as in 51 how do the results change?

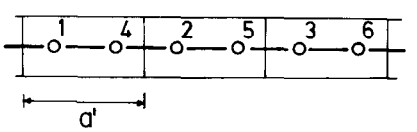

51

Any observable will have the same calculated value, of course, but the E(k) diagram will be different since there are now two $p\pi$ orbitals per cell. We need to solve equation (71) (with $S_{ij}(k) = \delta_{ij}$ in the Hückel approximation) where the Bloch basis orbitals are given by equation (66). With reference to 51 we may write the Bloch function as

$$\psi_1(k) = n^{-\frac{1}{2}} (\ldots \varphi_1 e^{-ika'} + \varphi_2 + \varphi_3 e^{ika'} \ldots) \tag{72}$$

$$\psi_2(k) = n^{-\frac{1}{2}} (\ldots \varphi_4 e^{-ika'/2} + \varphi_5 e^{ika'/2} + \varphi_6 e^{3ika'/2}) \tag{73}$$

Now to set up the 2×2 secular determinant we need to calculate the H_{ij}

$$H_{11} = \langle \psi_1(k) | H | \psi_1(k) \rangle = n^{-\frac{1}{2}} \cdot n^{-\frac{1}{2}} \cdot (n\alpha) = \alpha \tag{74}$$

and

$$H_{22} = \langle \psi_2(k) | H | \psi_2(k) \rangle = n^{-\frac{1}{2}} \cdot n^{-\frac{1}{2}} \cdot (n\alpha) = \alpha \, . \tag{75}$$

Both of these elements are independent of k since there is no interaction (in the Hückel approximation) between (for example) φ_1 in one cell and φ_2 or φ_3 in adjacent cells. H_{12}, however does contain β and is dependent on k.

$$H_{12} = \langle \psi_1(k) | H | \psi_2(k) \rangle = n^{-\frac{1}{2}} \cdot n^{-\frac{1}{2}} n (e^{ika'/2} + e^{-ika'/1}) \beta$$

$$= 2\beta \cos ka'/2 \, . \tag{76}$$

The secular determinant is then

$$\begin{vmatrix} \alpha - E & 2\beta \cos ka'/2 \\ 2\beta \cos ka'/2 & \alpha - E \end{vmatrix} = 0 \, , \tag{77}$$

with roots $E = \alpha \pm 2\beta \cos ka'/2$, a result shown in 52. Remembering that a in 39 is half the a' of 51 the relationship between Fig. 7 and 52 is clear to see. The E(k) diagram of the

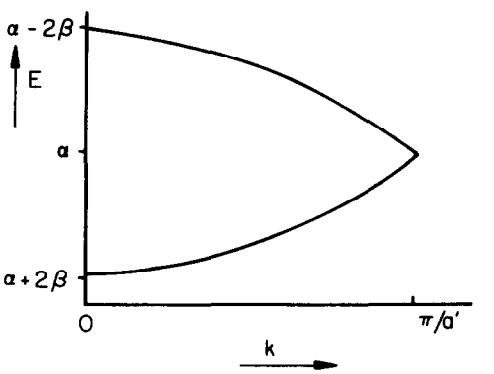

52

two orbital cell is just that of the one orbital cell with the levels folded back along $k = \pi/2a$ 53. Now there are two orbitals for each value of k.

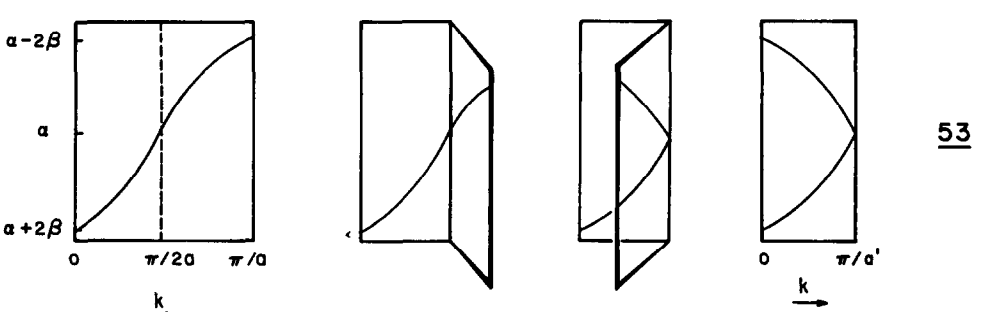

53

Another way to derive this result is to take as a basis the π and π^* levels of the diatomic unit in the unit cell, (ψ_1 and ψ_2 respectively) and to set up a secular determinant

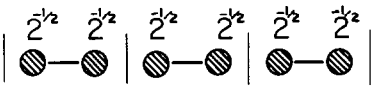

54

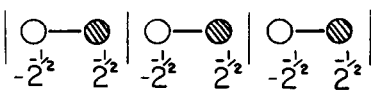

55

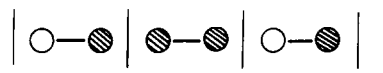

56

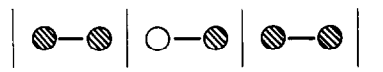

57

as before. From 54 it is easy to see that $H_{11} = (\alpha+\beta) + 2^{\frac{1}{2}} \cdot 2^{\frac{1}{2}} \beta (e^{ika'} + e^{-ika'}) = (\alpha+\beta) + \beta \cos ka'$, and from 55 that $H_{22} = (\alpha-\beta) + 2^{-\frac{1}{2}}(-2^{-\frac{1}{2}})\beta(e^{ika'} + e^{-ika'}) = (\alpha-\beta) - \beta \cos ka'$. H_{12} from 56 is $2^{-\frac{1}{2}} \cdot (-2^{-\frac{1}{2}})\beta e^{ika'} + 2^{-\frac{1}{2}}(+2^{-\frac{1}{2}})\beta e^{ika'} = -i\beta \sin ka'$. H_{21} from 57 is $(2^{-\frac{1}{2}})(2^{-\frac{1}{2}})\beta e^{ika'} + (2^{-\frac{1}{2}})(-2^{-\frac{1}{2}})\beta e^{-ika'} = i\beta \sin ka'$. The secular determinant becomes

$$\begin{vmatrix} (\alpha+\beta) + \beta \cos ka' - E & -i\beta \sin ka' \\ i\beta \sin ka' & (\alpha-\beta) - \beta \cos ka' - E \end{vmatrix} = 0 . \tag{78}$$

Note that this is Hermitian, i.e., $H_{12} = H_{21}^*$. Equation (78) has roots

$$\begin{aligned} E &= \alpha \pm \sqrt{\beta^2(2 + 2\cos ka')} \\ &= \alpha \pm 2\beta \cos ka'/2 \end{aligned} \tag{79}$$

which is the same result as before. Notice that both at the zone edge and the zone center $H_{12} = 0$. So the form of the wavefunctions are easily written down 58. They are just simple

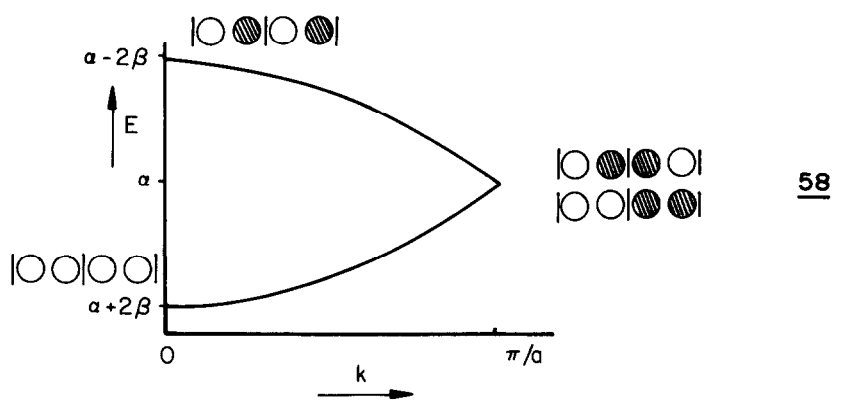

58

combinations of the π or π^* functions, in phase at $k = 0$ and out of phase at $k = \pi/a'$. We could then regard the one-dimensional energy band of 52 as being made up of π and π^* bands as in 59 which touch at one point in the Brillouin zone 59. There is a qualification concerning such a simple viewpoint. Because of the zero off-diagonal entry at $k = 0, \pi/a'$ in equation (78) there is no mixing between the π and π^* functions at these points. However

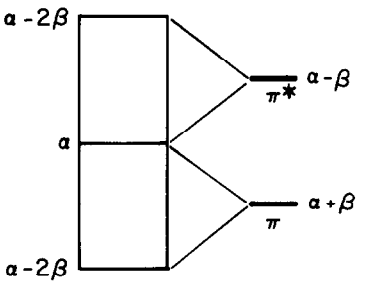

59

the two functions can and will mix together at other k points so that a description in terms of two separate bands (one π, the other π^*) is not a rigorous one.

At $k = \pi/a'$ there is an orbital degeneracy. 60 shows one way of writing the wavefunctions at this point, which we have just employed in 58. However a linear combination of them, as in 61 is just as good and emphasizes their nonbonding character. Recall, we had a similar choice for cyclobutadiene.

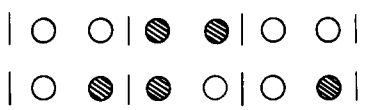

60

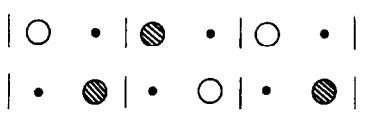

61

Polyacetylene itself however does not have the regular structure shown in 48 but is a semiconductor[24] and exhibits the bond alternation shown in 62. The energy bands for this arrangement are readily derived with reference to 63. Now, in addition to different values

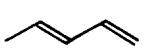

62

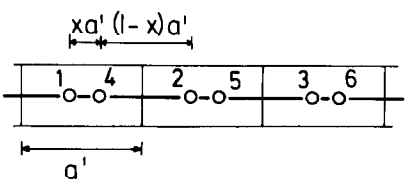

63

of R_t in equation (68) there are two different interaction integrals, β_1 and β_2 to be included. The secular determinant is easily derived by suitable modification of H_{12} (equation (76)) and becomes

$$\begin{vmatrix} \alpha - E & \beta_1 e^{ikxa'} + \beta_2 e^{-ik(1-x)a'} \\ \beta_1 e^{-ikxa'} + \beta_2 e^{ik(1-x)a'} & \alpha - e \end{vmatrix} = 0 . \qquad (80)$$

Solution of this determinant leads to

$$E = \alpha \pm (\beta_1^2 + \beta_2^2 + 2\beta_1 \beta_2 \cos ka')^{\frac{1}{2}} . \qquad (81)$$

Note that explicit dependence on x has disappeared. (β_1 and β_2 will, of course, be x dependent). At $k = 0$, $E = \alpha \pm (\beta_1 + \beta_2)$ and at $k = \pi/a'$ $E = \alpha \pm (\beta_1 - \beta_2)$. The E(k) diagram

which results now looks like 64. For the case where $|\beta_1| > |\beta_2|$ the corresponding density of states is also shown in 65. Let us estimate the energy of the distorted structure of 62 compared to that of 48. We should integrate the function E(k) to get the best answer but

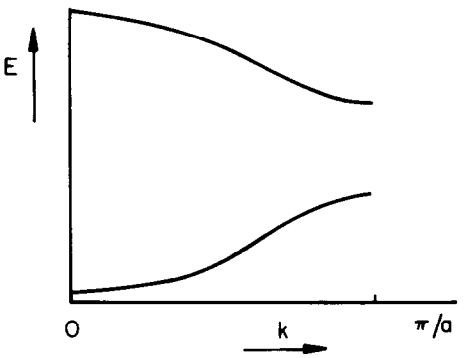

64

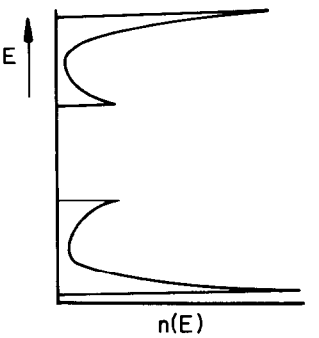

65

for our purposes it will be sufficient to represent the energy as being the average of that at the zone edge and that at the zone center. For the symmetric structure 48

$$E = 2 \cdot \tfrac{1}{2}\left[(\alpha + 2\beta) + (\alpha)\right] = 2(\alpha + \beta) \ . \tag{82}$$

For the distorted structure 62

$$\begin{aligned} E &= 2 \cdot \tfrac{1}{2}\left[(\alpha + \beta_1 + \beta_2) + (\alpha + \beta_1 - \beta_2)\right] \\ &= 2(\alpha + \beta_1) \ . \end{aligned} \tag{83}$$

If we assume that $2\beta = \beta_1 + \beta_2$ then the stabilization energy on distortion is $\beta_1 - \beta_2$ for a unit cell containing two atoms ($|\beta_1| > |\beta_2|$). This result is an extremely important one. With one electron per orbital the $p\pi$ band of 58 is half full, there is no HOMO—LUMO gap and there is a degeneracy at the zone edge. On distortion 48 → 62, which results in a lowering of the orbital energy, a HOMO—LUMO gap (a band gap, E_g in the language of the solid state) is opened up, and the degeneracy is removed. The situation is strongly reminiscent of that of singlet cyclobutadiene of Section 2.3. There the symmetrical structure distorted to a dimer structure. Here the atoms of the chain have dimerized in a similar way. This distortion is then the solid state analog of the Jahn-Teller distortion. It is called a Peierls distortion. As we will see throughout this article there are many similarities between the two. The distortion energy in both the molecular and solid state analogs is the same, $(\beta_1 - \beta_2)/2$ per atom. (In some ways this result is artificial since we have averaged the zone-center and zone-edge energies, when integration of equation (81) should have been performed. This approximation will, however, serve our purpose.) 66 shows the analogy in

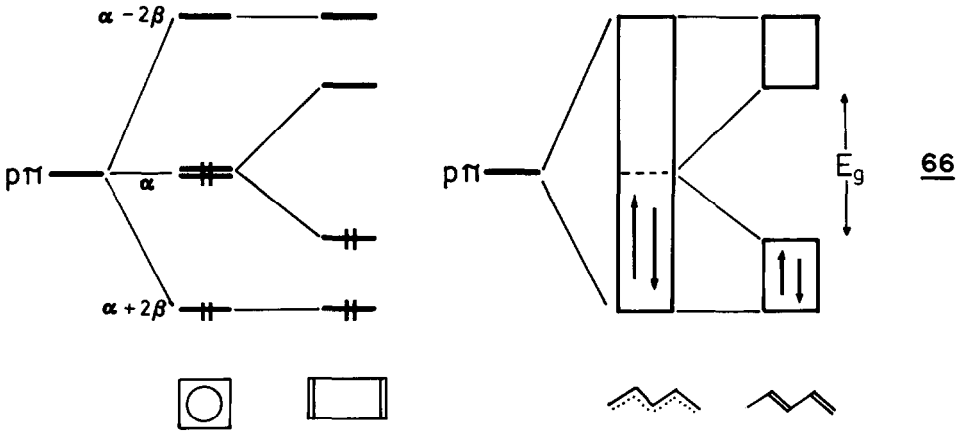

a pictorial fashion where the energy levels, and the energetic locations of the energy bands are those we have derived here and in Section 2.2. Table 4 shows some examples of Peierls distorted systems some of which are described in more detail later in this article. Notice that the system does not always distort to convert the metallic half-filled band into an insulator. Also increasing the temperature (e.g., in the VO_2 example) is often a way to reverse the effect. Application of pressure is also effective in this regard. How can we stabilize a system such as that of Fig. 7 against the Peierls distortion? In the case of cyclobutadiene two extra electrons per four atom unit remove the Jahn-Teller instability. In the present case we need to fill the entire band with electrons. The result is the structure of fibrous sulfur and of elemental selenium and tellurium, where there are chains of atoms with equal distances between them.[18] The chain however, is now nonplanar, and a spiral structure is found.

Table 4. Peierls Distortion in Linear Chains

1) Polyacetylene (bond alternation)	Doped Polyacetylene (no alternation?)
2) NbI_4 chain pairing up of metal atoms	NbI_4 under pressure metal atoms equidistant
3) VO_2 chain (rutile structure) pairing up of metal atoms	VO_2 at higher temperatures metal atoms equidistant
4) Elemental hydrogen H—H dimers	High pressure-metallic behavior Presumably... H—H—H—H... chains
5) $BaVS_3$ [VS_3 chain] metallic at room temperature	Metal-insulator transition on cooling, but a magnetic insulator 50 rather than diamagnetic 49
6) (TTF) Br $(TTF)_2^{+2}$ dimers	(TTF) $Br_{0.7}$ metallic conduction in chain (cf. polyacetylene)

Another route, suggested by the observation of the $B_2N_2R_4$ molecule and the discussion concerning the relative stabilities of the substitution patterns 34 and 35 of cyclobutadiene is via substitution of the chain atoms in a similar way. To generate the levels of the ...XY... solid we need to take those of the two atom cell and apply a perturbation. We will increase the α value of X by $\delta\alpha$ and decrease that of Y by $\delta\alpha$. The resulting energy level

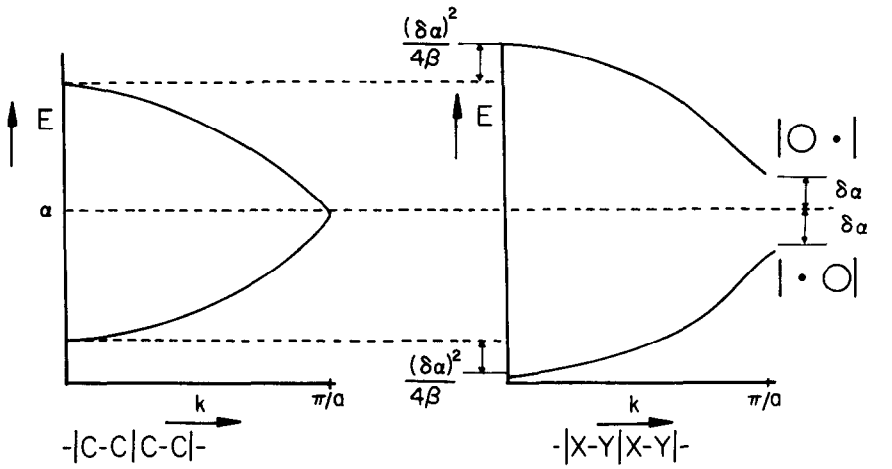

67

shifts are shown in 67. At the zone edge the energy correction is in first order and is $n \cdot n^{-\frac{1}{2}}\,\delta\alpha = \delta\alpha$ for the X located level and $n \cdot n^{-\frac{1}{2}} \cdot n^{-\frac{1}{2}}(-\delta\alpha) = -\delta\alpha$ for the Y located level At the zone center the energy correction occurs in second order and is $(\delta\alpha)^2/4\beta$. The wavefunctions at the zone edge remain unchanged as a result of the perturbation but at the zone center they mix together. From equation (52) the new wavefunction for the energy level at $E \sim \alpha + 2\beta + (\delta\alpha)^2/4\beta$ is given by 68 and describes a function weighted more heavily on the more electronegative (Y) atom. Similarly the higher energy orbital at $k = 0$ becomes 69 and is predominantly X located. Perhaps the most important result is the opening up of a band

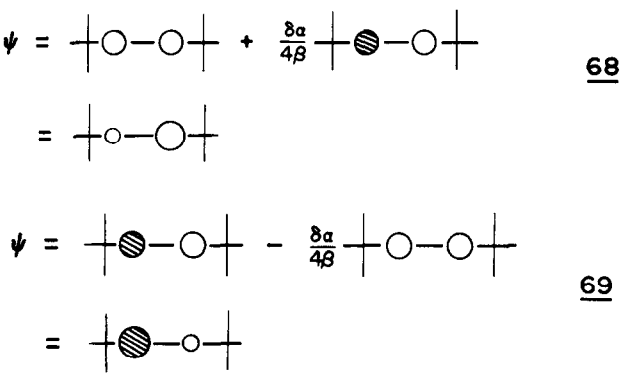

68

69

gap at the zone edge. Substituted polyacetylenes or their analogs 70 however are either unknown or poorly characterized but we see no reason why the molecular reasoning should not prevail here too.

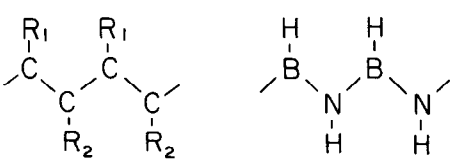

70

Having shown how ...XY... substitution opens up a band gap we need also to examine, as we did in the molecular case, the relative merits of ...XYXY... and ...XXYY... substitution. To probe this we need to generate the energy levels of a four orbital cell since we shall be interested in comparing ...XXYY... and ...XYXY... alternatives. By making use of the folding back trick of 53 this is quite simple to do and is shown in 71. Just as the

levels of the two atom cell could simply be obtained by using the π and π^* orbitals of ethylene as a basis, so the nodal properties of the levels of the four atom cell can be obtained from those of butadiene (of Fig. 1). Half of the perturbation problem has been done for us already since the form of the functions of cyclobutadiene are identical to the levels of 71 at $k = 0$. The energy shifts at this point for the ...XXYY... and ...XYXY... substitutions are then given by 36 and 37 respectively. In fact the energy shifts at $k = 0$ for the ...XYXY... pattern are just the sum of those shown in 67 for the simple two atom

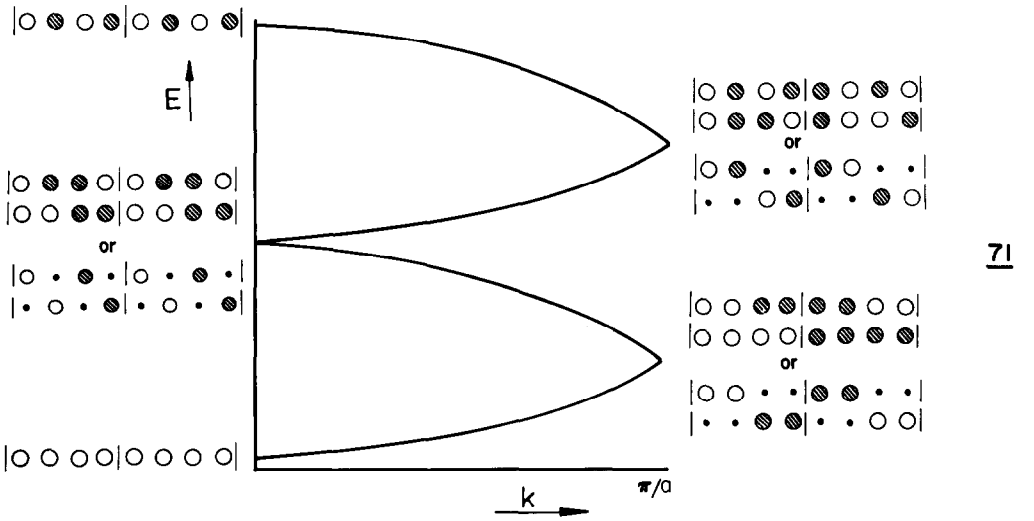

71

cell at $k = 0$ plus that at $k = \pi/a$. This comes about because the diagram for ...XYXY... is simply that of ...XY... folded back along $k = \pi/2a$. This leaves the energy shifts at the zone edge for the four atom cell of 71. For the ...XYXY... pattern we will make the approximation that the mean of the shifts at $k = 0$ and $k = \pi/a$ of the ...XY... problem of 67 will suffice. For the ...XXYY... pattern it is easy to see that the levels split apart in first order by $2\delta\alpha$ and that there is no second order correction. The energy shifts for the two substitution patterns are shown in 72. Approximating the band energy as before by

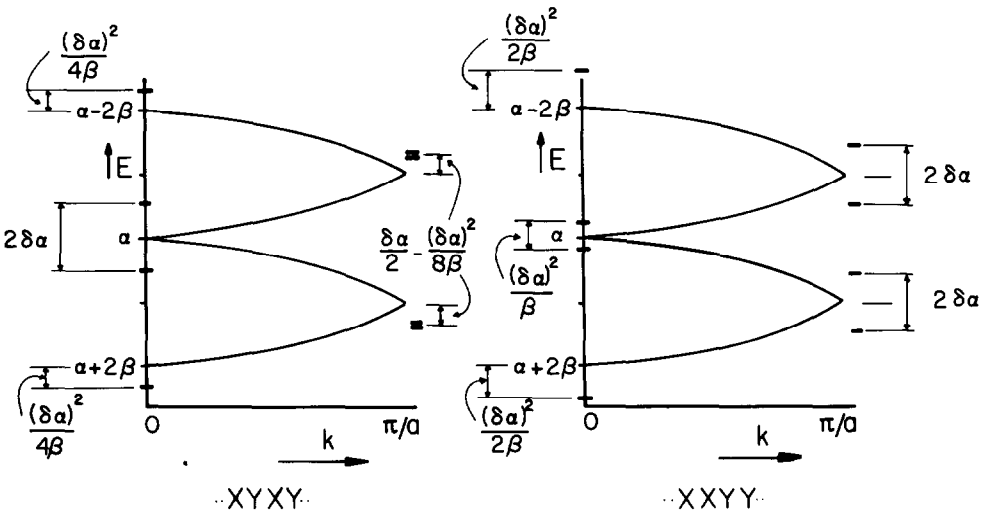

72

averaging the zone-center and zone edge values of a filled level the stabilization energies of the two alternatives as a function of band filling are given in Table 5 where the more stable structure is indicated with an arrow. Notice the symmetry associated with this Table, the entries for the quarter filled and quarter empty bands are identical.

Table 5. Stabilization Energies of Structural Alternatives

Band filling	...XYXY...	...XXYY...
0	0	0
1/4	$(\delta\alpha)/2 + (\delta\alpha)^2/8\beta$	$\delta\alpha + (\delta\alpha)^2/2\beta$ ←
1/2	2 ←	$(\delta\alpha)^2/\beta$
3/4	$(\delta\alpha)/2 + (\delta\alpha)^2/8\beta$	$\delta\alpha + (\delta\alpha)^2/2\beta$ ←
1	0	0

The relative stabilities of the two possibilities then vary with band filling as in 73 where we show the results obtained by numerical solution of the problem but understandable using our discussion. At the 1/4 and 3/4 filled band the ...XXYY... structure is more stable but at the 1/2 filled band the ...XYXY... structure is more stable in exact analogy with the case of the substituted cyclobutadienes 39 of Section 2.3. Again our treatment here has been virtually the simplest possible. The problem can be reworked by including the variations induced in the interaction integrals (β) by the changes in α, in an appropriately similar way to the cyclobutadiene problem of 37. The result is very similar.[25] The antibonding part of the band receives an extra destabilization for the ...XXYY... substitution in an analogous way to that shown at the right-hand side of 37 for the molecular case.

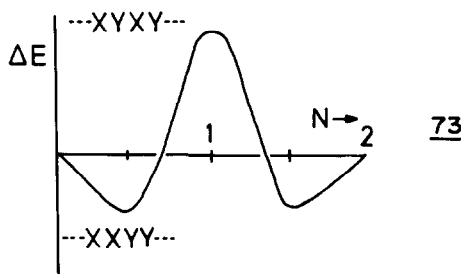

73

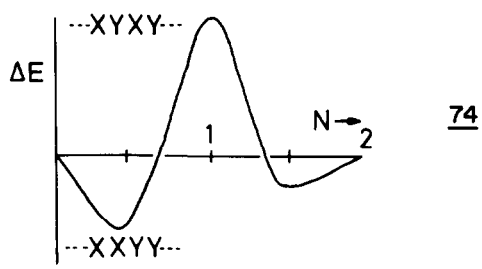

74

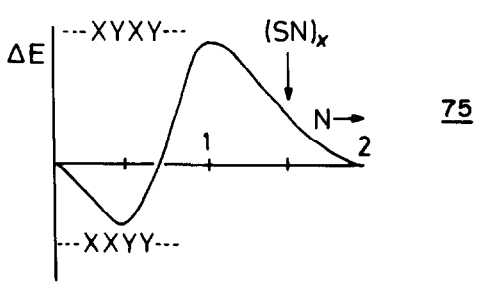

75

Taking this into account leads to the two possibilities related to the molecular pictures of 40, 41 shown in 74 and 75 depending upon the size of the effect. We shall see an example of 74 later but the case of 75 is found for $(SN)_x$ polymer. This material has three π electrons per π band and is found as the —S—N—S—N— isomer and not as —S—S—N—N— . A band structure calculation[25] using the observed geometry of the polymer confirms the state of affairs in 75. Recall that the molecule S_2N_2 has the alternating arrangement too. Most organic donor-acceptor complexes, based on the stacking up of planar molecules crystallize in the ...XYXY... arrangement.[26] Although we do not discuss these systems in any detail here, the basic electronic arrangement is one which at its simplest involves the interaction of a doubly occupied donor level with an empty acceptor level on the adjacent molecule. This corresponds to a one electron pair per two orbitals problem, and the alternating arrangement of donor and acceptor is understandable from our discussion above. However, the system $NBP{\cdot}TCNQF_4$ and $Ni(tfd)_2{\cdot}PTZ$ crystallize in the ...XXYY... structure. Both of these species correspond electronically to one electron pair per four orbitals.[25] The observation of this isomer for these two cases is in nice agreement with the theory. A sample of some of the structures found for various band fillings is given in Table 6.

Table 6. ...XXYY... versus ...XYXY...

Electronic Situation	Band Filling		
	1/4	1/2	3/4
73, 40	$NBP{\cdot}TCNQF_4$	CsCl[a] examples in 3D, BN in 2D, most organic donor acceptor complexes in 1D	CuTi[a] examples in 3D
	and		
75, 41	$Ni(tfd)_2{\cdot}PTZ$		S_2N_2, $(SN)_x$

[a] These examples are discussed in Section 4.2.

3.3 Building up more Complex Systems

The results achieved for the linear chain may be readily extended to produce the energy bands of more complex systems. Many of the systems we shall discuss are as yet unknown in the laboratory. The structure of the ladder, 76 is easily generated by linking two chains

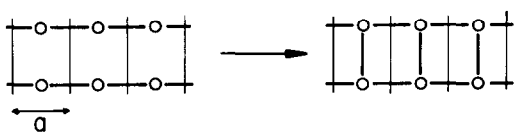

76

together. The secular determinant is a trivial one. If the Bloch orbitals on the two chains are ψ_1 and ψ_2 then

$$\begin{vmatrix} \alpha + 2\beta\cos ka - E & \beta \\ \beta & \alpha + 2\beta\cos ka - E \end{vmatrix} = 0 \qquad (84)$$

with roots $E = \alpha \pm \beta + 2\beta\cos ka$. The result is shown in 77. Another way to generate this result is to use as a basis the π and π^* levels of the ladder unit cell 78 in which case the secular determinant is

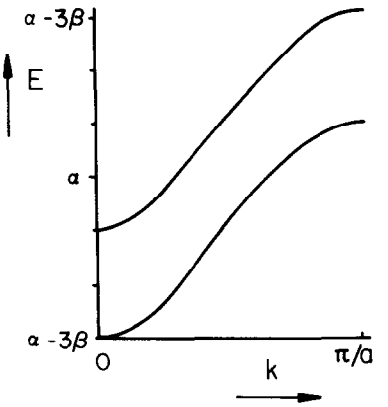

77

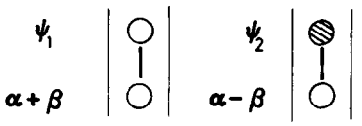

78

$$\begin{vmatrix} (\alpha+\beta)+2\beta\cos ka & 0 \\ 0 & (\alpha-\beta)+2\beta\cos ka \end{vmatrix} = 0 \qquad (85)$$

with the same roots as before. Note that in this new formulation there is no mixing between ψ_1 and ψ_2 of 78 since they have different parity with respect to reflection in the mirror plane which bisects the chain. The two bands of 77 may then be regarded as π and π^* bands of the ladder.

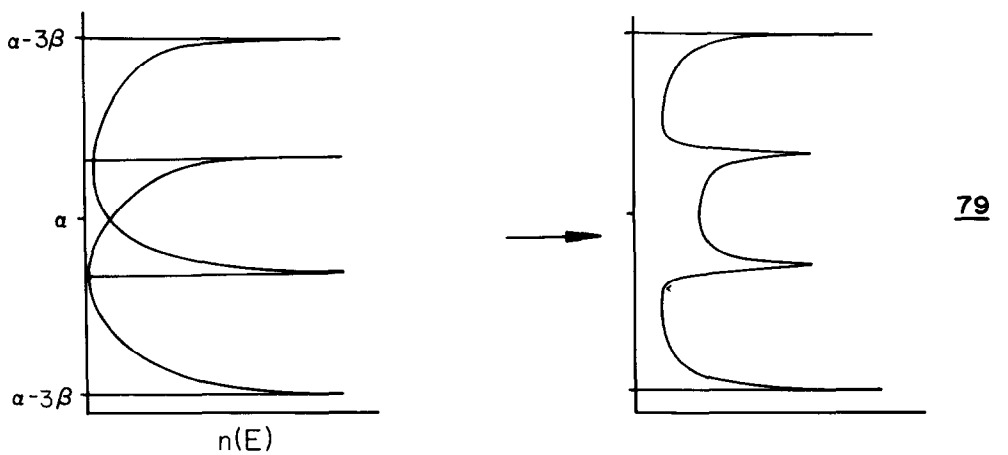

79

We can use the form of the density of states of Fig. 7b to construct the density of states for the ladder orbitals as in 79. A third way of generating these energy levels is to 'polymerize' cyclobutadiene 80. Here the symmetry of the basis orbitals with respect to

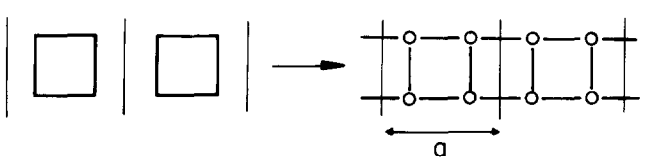

80

reflection in the mirror plane bisecting the ladder is very useful in simplifying the problem. 81 shows the wavefunctions of Fig. 3 which are symmetric with respect to reflection, and 82

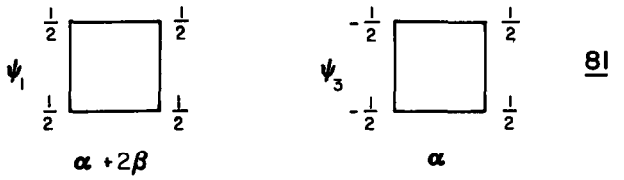

81

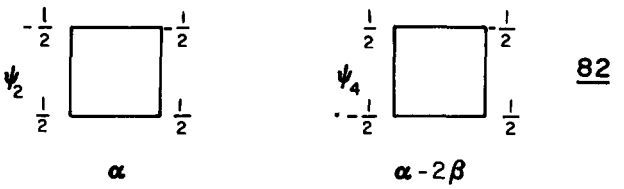

82

shows the functions which are antisymmetric. For the symmetric block we need to solve the secular determinant

$$\begin{vmatrix} H_{11}(k)-E & H_{13}(k) \\ H_{31}(k) & H_{33}(k)-E \end{vmatrix} = 0 \qquad (86)$$

Now

$$H_{11}(k) = (\alpha+2\beta) + 2\beta(\tfrac{1}{2}\cdot\tfrac{1}{2})e^{ika} + 2\beta(\tfrac{1}{2}\cdot\tfrac{1}{2})e^{-ika} = (\alpha+2\beta)+\beta\cos ka \qquad (87)$$

and in general

$$H_{11}(k) = (\alpha+n\beta) + 2\gamma\cos ka \qquad (88)$$

where γ is the interaction integral between one basis orbital and its neighbor in the next cell evaluated in terms of β and the products of orbital coefficients, and n gives the energy of the orbital of the isolated unit. Equation (86) then becomes

$$\begin{vmatrix} (\alpha+2\beta)+\cos ka-E & i\beta\sin ka \\ -i\beta\sin ka & (\alpha)-\beta\cos ka-E \end{vmatrix} = 0 \qquad (89)$$

with roots $E=(\alpha-\beta)\pm 2\beta\cos^2(ka/2)$. The antisymmetric block can be similarly constructed and the roots are found to be $E=(\alpha+\beta)\pm 2\beta\cos^2(ka/2)$. The energy bands then look like 83.

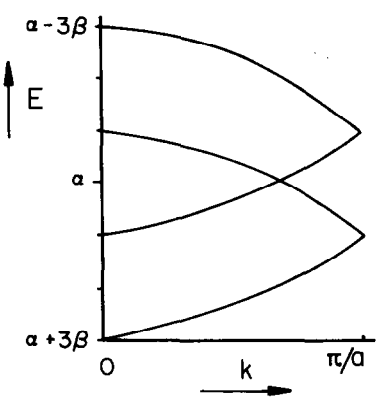

83

These are just like those of 77 but folded at $k=\pi/2a$. The $\cos^2(ka/2)$ dependence on k has arisen in exactly the same fashion as that for the single stranded chain when the repeat unit was doubled in 52.

A similar variety of approaches allows construction of the level pattern of polyacene where only half of the linkages are made between the two chains 84. We will generate the band structure of this system first by 'polymerizing' butadiene as shown in 85. The energy

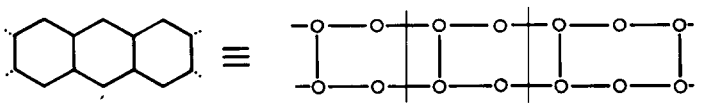

84

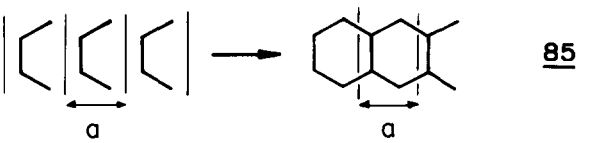

85

levels of the four orbital chain are shown in Fig. 1. To simplify our problem we shall divide them into functions symmetric 86 and antisymmetric 87 with respect to the mirror plane

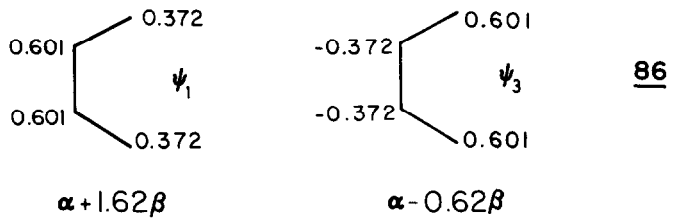

86

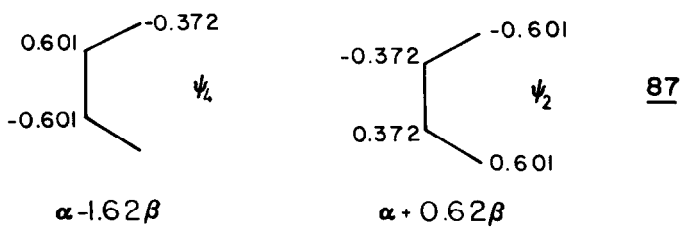

87

lying perpendicular to the plane of the polymer. For the symmetric block the secular determinant entries are

$$H_{11} = (\alpha+1.62\beta) + (2\times 2\times 0.372\times 0.601)\,\beta\cos ka$$
$$H_{33} = (\alpha-0.62\beta) - (2\times 2\times 0.373\times 0.601)\,\beta\cos ka \qquad (90)$$
$$H_{13} = [-2\times(0.372)^2]e^{ika} + [2\times(0.601)^2]e^{-ika}$$

which leads to the messy expression for the energies of

$$E = \frac{(2\alpha+\beta) \pm \beta\sqrt{(2.24+1.76\cos ka)^2 + 4(0.6-0.4\cos 2ka)}}{2} . \qquad (91)$$

At $k=0$, $E=\alpha+2.55\beta$, $\alpha-1.55\beta$ and at $k=\pi/a$, $E=\alpha, \alpha+\beta$. For the antisymmetric block the arithmetic is similar and we find at $k=0$, $E=\alpha-2.55\beta$, $\alpha+1.55\beta$ and at $k=\pi/a$, $E=\alpha$, $\alpha-\beta$. Qualitatively the band structure looks like 88 with a degeneracy at the zone edge at $E=\alpha$. Using these bands we may construct a density of states for the π levels shown in 89. Figure

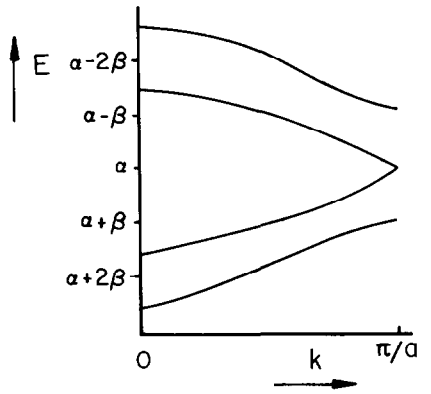

88

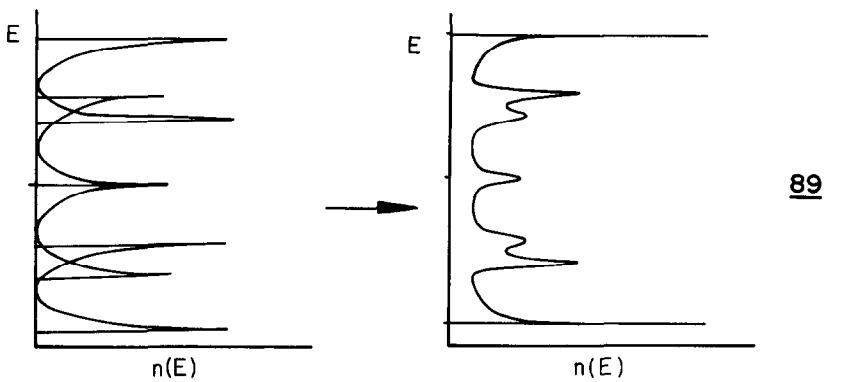

89

9 shows a band structure for polyacene using the extended Hückel approach. The broad features of the π bands we have generated here are retained but the degeneracy at the zone edge has been converted into a crossing at smaller k. This occurs as a result of the inclusion of overlap across the rings, ignored in our treatment. How this occurs is difficult to see using our approach here. It becomes quite transparent however if the band structure is assembled via the process in 90. This we will do in a qualitative fashion. The left-hand side of 90 has a band structure which is simply two superimposed diagrams 58. This is shown

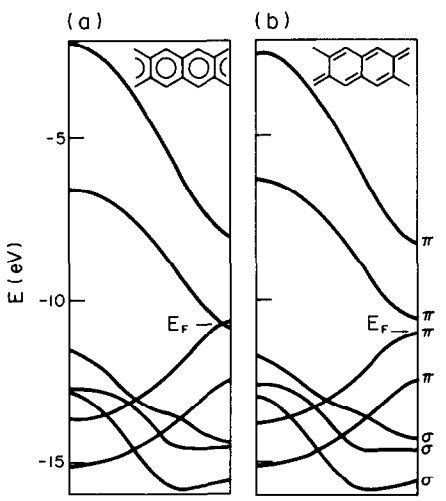

Fig. 9. (a) Band structure for polyacene using the Extended Hückel approach. (b) Band structure for a distorted polyacene using the Extended Hückel method. (Adapted from Ref. 28.)

90

by the dashed lines of 91. As a first approximation at $k = 0$ we will just construct bonding and antibonding pairs from the levels at the bottom and top of the band. (These will not be the final energies of the bands since the orbitals we have generated are not orthogonal and there will be a second order energy correction.) At $k = \pi/a$, making similar combinations of

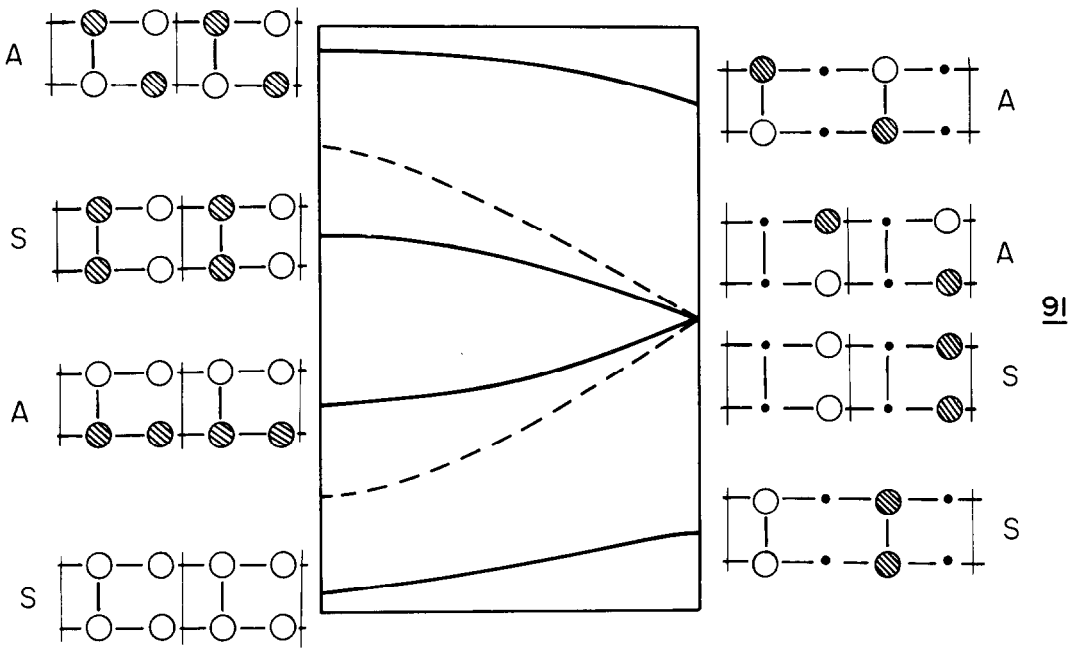

91

the orbitals of 58 leads to one bonding, one antibonding and two nonbonding orbitals. The two nonbonding orbitals are degenerate in 91 only because overlap across the six-membered ring is neglected. If this is included then they will split apart in energy as in Fig. 9. The bonding partner (symmetric (S) with respect to the mirror plane lying parallel to, and bisecting the chain) obviously then drops to lower energy. Since this must correlate with a symmetric function at the left-hand side of 91 it therefore goes up in energy with decreasing k and so crosses the other orbital with $E \geqslant \alpha$ at a little less than $k = \pi/a$. Figure 9b shows the result of a calculation for polyacene where each of the carbon chains has undergone a pairing distortion. As in the polyacetylene example itself, a band gap opens up at the zone edge. We will discuss later the problem of Peierls type distortions in polyacene and related systems containing more polyacetylene chains.

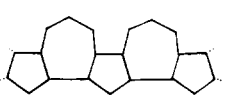

92

The energy bands of these chains have been easy to derive since we have gained a considerable simplification by making use of the mirror symmetry of the problem. A much more difficult problem arises in the generation of the bands of the unknown species polyazulene 92 where there is no such symmetry. The level structure can be generated as in 93 by using perturbation theory in a way analogous to the derivation of the pentalene levels of Fig. 5.

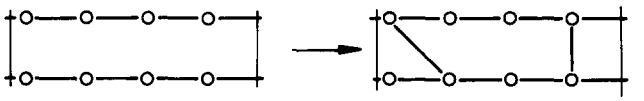

93

Although instructive, this is extremely tedious. 94 shows the π bands generated by numerical solution of the 8 X 8 secular determinant. Note that in contrast to the polyacene problem, the levels do not lie symmetrically about $E = \alpha$, a direct result of the presence of odd membered rings. The polyazulene net is not bipartite and so its level structure at all k lacks such symmetry.

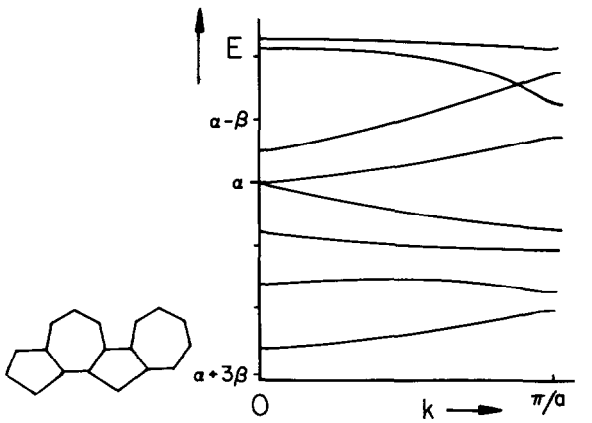

94

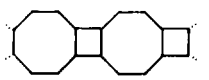

95

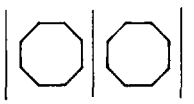

96

The level structure of poly-[8]-annulene, 95, (for lack of a better label) may be derived in a way analogous to that of the ladder above, by starting off with the orbitals of the eight-atom ring, 96, as a basis. This exercise is left to the reader. The energy bands are shown in 97.

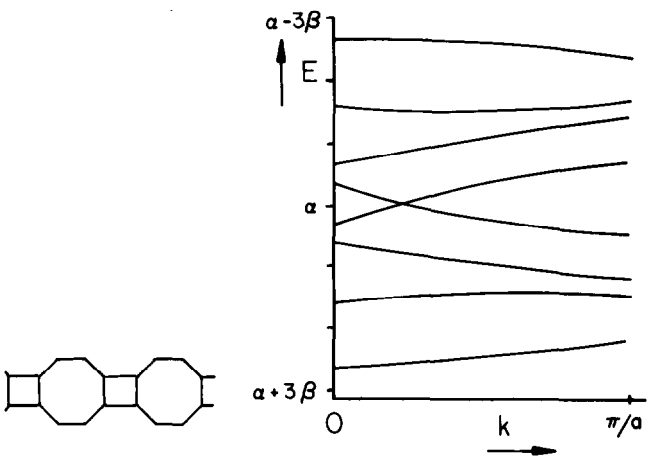

97

Of particular interest is the energy difference between these three structures as a function of band filling. This is shown in 98. $N_{p\pi}$ is the number of $p\pi$ electrons per atom. Notice that the energy difference curve for poly-[8]-annulene is symmetric with respect to reflection about this point ($N_{p\pi} = 1$) as demanded by the bipartite nature of both networks.

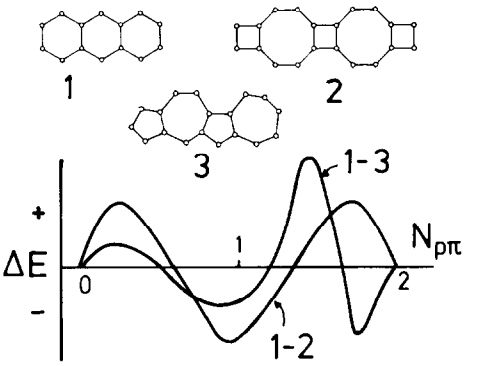

98

The curve for polyazulene on the other hand lacks such symmetry. It has its maximum stability just after the half-filled point at the band filling of about 0.7. As known for years by physical organic chemists and implied by the result[12] of Gutmann and Trinajstić for molecules discussed earlier, the most stable structure at the half-filled point is the one with six rings. Notice too that the poly-[8]-annulene structure (with 8-rings and 4-rings) is the least stable alternative at the half-filled point, a result analogous to that found in 30 for the 8-4 molecular case. Also the stability of polyazulene (5-rings and 7-rings) relative to polyacene reaches a maximum in approximately the same place in 98 as does the 5-7 relative to 6-6 molecular structures in 98.

Not all of the systems we shall describe are one-dimensional ones. Most 'real' systems are three dimensional in extent. For the latter case we may write the translation group as a simple product group involving translations along the three lattice vectors, $\underline{a}_i$ of Section 2.1. In this case the exponential in the Bloch sum of equation (68) becomes

$$e^{i(k_1 \underline{b}_1 \cdot \ell_1 \underline{a}_1)} e^{i(k_2 \underline{b}_2 \cdot \ell_2 \underline{a}_2)} e^{i(k_3 \underline{b}_3 \cdot \ell_3 \underline{a}_3)} = e^{i(\underline{k} \cdot \underline{r})} \tag{92}$$

where $\underline{b}_i \cdot \underline{a}_j = 2\pi\delta_{ij}$ and the reciprocal lattice vectors $\underline{b}_i$ are defined by

$$\begin{aligned} \underline{b}_1 &= 2\pi \frac{\underline{a}_2 \wedge \underline{a}_3}{\underline{a}_1 \cdot (\underline{a}_2 \wedge \underline{a}_3)} \\ \underline{b}_2 &= 2\pi \frac{\underline{a}_3 \wedge \underline{a}_1}{\underline{a}_1 \cdot (\underline{a}_2 \wedge \underline{a}_3)} \\ \underline{b}_3 &= 2\pi \frac{\underline{a}_1 \wedge \underline{a}_2}{\underline{a}_1 \cdot (\underline{a}_2 \wedge \underline{a}_3)} \end{aligned} \tag{93}$$

Just as the direct lattice vectors define this lattice, so these reciprocal lattice vectors define a reciprocal lattice. A simple example will illustrate its construction. In 99 we show a primitive orthorhombic lattice. The direct lattice vectors $\underline{a}_i$ are given by

$$\underline{a}_1 = a\hat{\underline{x}}\,; \qquad \underline{a}_2 = b\hat{\underline{y}}\,; \qquad \underline{a}_3 = c\hat{\underline{z}}\,, \tag{94}$$

where $\hat{\underline{x}}$, $\hat{\underline{y}}$ and $\hat{\underline{z}}$ represent unit vectors along x, y and z directions. The $\underline{b}_i$ are then simply

$$\underline{b}_1 = (2\pi/a)\,\hat{\underline{x}}\,; \qquad \underline{b}_2 = (2\pi/a)\,\hat{\underline{y}}\,; \qquad \underline{b}_3 = (2\pi/a)\,\hat{\underline{z}}\,, \tag{95}$$

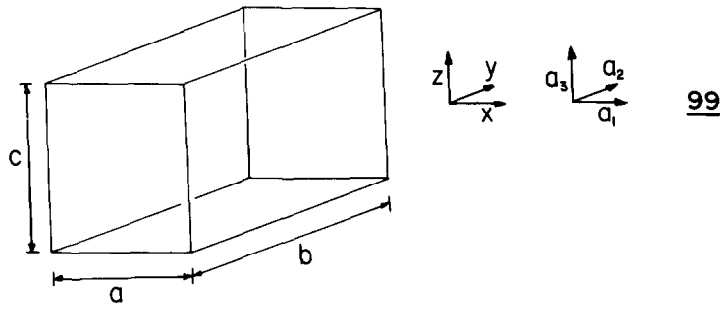

99

and the reciprocal lattice as in 100. Now the first Brillouin zone is defined as the volume enclosed by the set of planes which bisect perpendicularly all the lines drawn from one lattice point to all others in the reciprocal lattice. In practice only a small number of close points are needed. 101 shows the construction for the reciprocal lattice of 100.

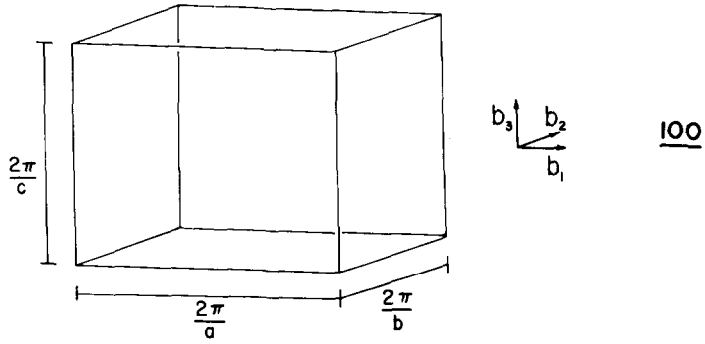

100

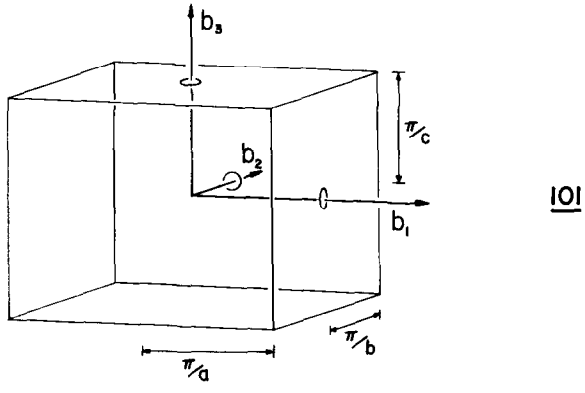

101

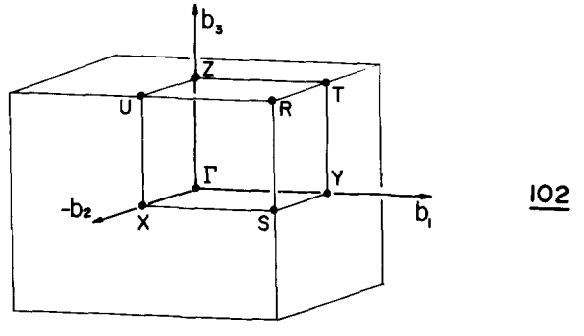

102

Various points which lie on the faces, edges or vertices of the Brillouin zone are usually given symmetry labels. 102 shows the conventional choice for our example. In units of $2\pi/a$ the values of k_1, k_2 and k_3 are

$$\begin{array}{lll} \Gamma;0,0,0 & X;0,\tfrac{1}{2}, & Z;0,0,\tfrac{1}{2} \\ Y;-\tfrac{1}{2},0,0 & T;-\tfrac{1}{2},0,\tfrac{1}{2} & U;0,\tfrac{1}{2},\tfrac{1}{2} \\ S;-\tfrac{1}{2},\tfrac{1}{2},0 & R;-\tfrac{1}{2},\tfrac{1}{2},\tfrac{1}{2} & \end{array} \qquad (96)$$

Notice that the one-dimensional example which we have exclusively described until now is the special case of 101, with $\underline{b}_2 = \underline{b}_3 = 0$. We have chosen for our example, a particularly simple zone. Other lattices give rise to zones which correspond to more complex polyhedra.[20,29]

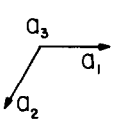

103

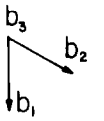

104

For the primitive hexagonal lattice, which we will use shortly, the situation is a little more complex. If the primitive direct lattice vectors are as in 103 then the reciprocal lattice vectors, by the construction of equations (93) become those of 104. The first Brillouin zone, also has hexagonal symmetry and is shown in 105. Notice that the point M is just $(\tfrac{1}{2},0,0)2\pi/a$ but K is $(\tfrac{1}{3},\tfrac{1}{3},0)2\pi/a$ by simple geometry.

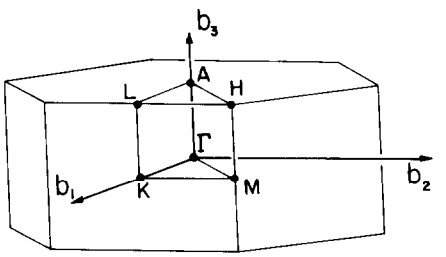

105

First we tackle the problem of the square net, 106 which has a set of primitive lattice vectors $a\hat{\underline{x}}$, $b\hat{\underline{y}}$ and $c\hat{\underline{z}}$ where we may visualize c as being very large and a = b (of 100). The two-dimensional zone we need to consider is therefore the one given in 107.

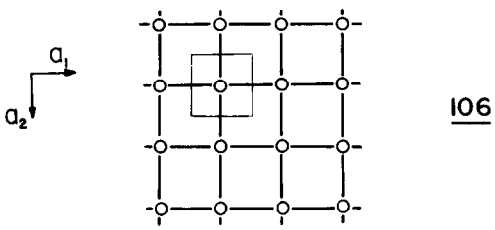

106

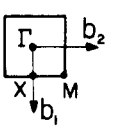

107

The energy band of the square net is easy to derive since it is a one-orbital problem. By analogy with the one-dimensional chain of Section 3.1 the $E(\underline{k})$ dependence is written as

$$E(\underline{k}) = \alpha + 2\beta\cos(\underline{k}\cdot\underline{a}_1) + 2\beta\cos(\underline{k}\cdot\underline{a}_2) \tag{97}$$

which therefore has a maximum energy of $\alpha-4\beta$ and a minimum energy of $\alpha+4\beta$. There is a pictorial problem is showing the dispersion of the energy in two dimensions but what we can do is trace the energetic behavior along lines joining symmetry points of the Brillouin zone.

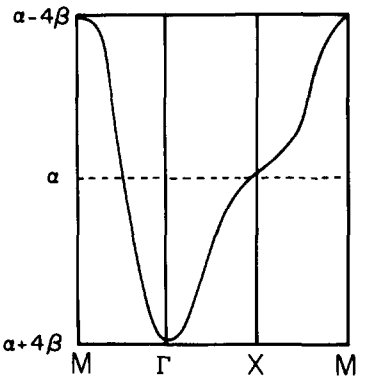

108

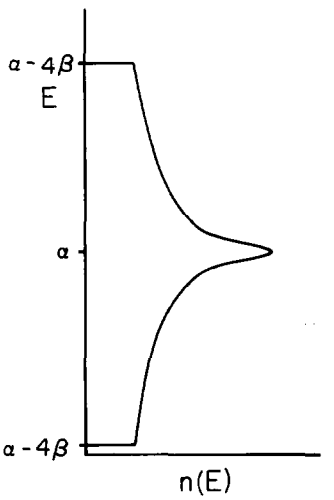

109

Using this technique the energetic dispersion is shown in 108. Its density of states is shown in 109 and indicates a maximum at the half-filled band. The band structure of this net may also be generated by linking together one-dimensional chains. The first step in this process is shown in 76, 77, where we constructed the energy bands of the ladder. Clearly the energy bands of a connected set of n chains will have an energy dependence of

$$E_j(k) = \alpha + 2\beta\cos(j\pi/n+1) + 2\beta\cos ka \ , \tag{98}$$

by using equation (27) ($j = 0,1,2,3 \ldots n$). Equations (97) and (98) become identical for an infinite collection of chains. Notice that the density of states of the ladder already has some of the features of that of the square net.

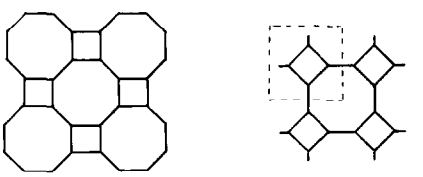

110

It is not much more difficult given these results to generate the π bands of the 48^2 net of 110, especially if it is redrawn to emphasize its construction as a square net with cyclobutadiene at each node. There are now four energy bands, each with a $\underline{k}$ dependence given by an equation (99) of exactly the same form as that of equation (97) but

$$E(\underline{k}) = (\alpha+n\beta) + 2\gamma_1\cos(\underline{k}\cdot\underline{a}_1) + 2\gamma_2\cos(\underline{k}\cdot\underline{a}_2) \qquad (99)$$

where γ_i $(i=1,2)$ now represents the interaction integral along the a_i directions between unit cells associated with the cyclobutadiene orbitals 111–114. It is easy to see that

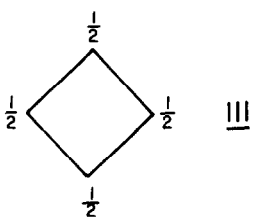

111

$\alpha+2\beta$

n=2

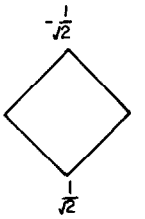

112

α

n=0

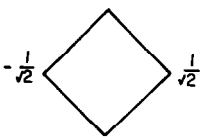

113

α

n=0

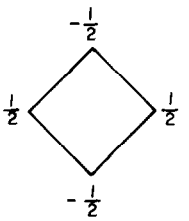

114

$\alpha-2\beta$

n=-2

$\gamma_i = \beta/4$ for 111 and 114. $\gamma_1 = \beta/2$ and $\gamma_2 = 0$ for 113 while $\gamma_1 = 0$, and $\gamma_2 = \beta/2$ for 112. The resulting band structure looks like 115. Notice that at $(\frac{1}{4},\frac{1}{4})2\pi/a$, the level pattern

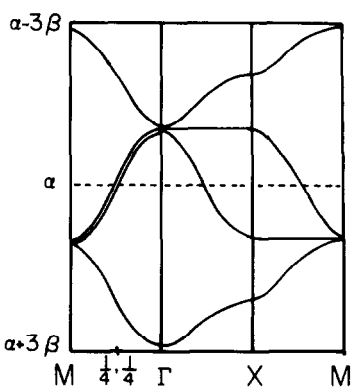

115

is identical with that of the isolated cyclobutadiene system since from equation (99) at this point $\cos(\underline{k}\cdot\underline{a}_i) = 0$. It is difficult to understand the density of states plots for two- and three-dimensional systems in the same way we used for one-dimensional ones. The plot for 110 however, is shown in 116 and, if we restrict ourselves to looking at that section of the zone between Γ and M, we might expect something resembling 117 which is not too different.

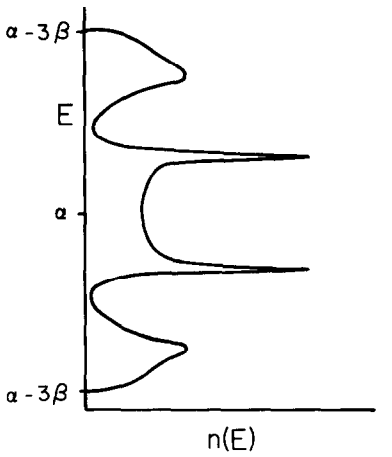

116

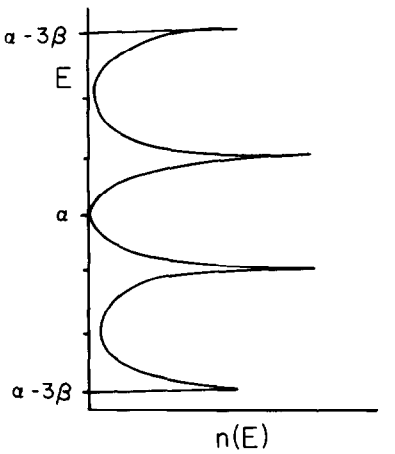

117

If we were to estimate the energy of this system by choosing the $\underline{k}$ point in the middle of a quadrant of the Brillouin zone 107 at $(\frac{1}{4},\frac{1}{4})2\pi/a$ then the level structure is identical to that of cyclobutadiene. It is therefore very interesting to find that the only known examples of isolated nets of this sort with a half filled π band are for $M^{II}B_2C_2$ where the squares contain alternating boron and carbon atoms[30] just as in the molecular case, and for exactly the same reasons we have described exhaustively before.

A slightly more adventurous derivation is of the π band of graphite. The unit cell we will use is shown in 118 with the primitive lattice vectors needed in equations (92),(93)

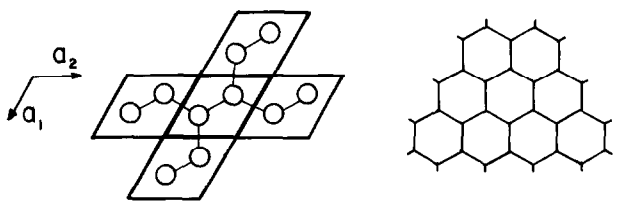

118

shown. Here we will need to take into account the vector nature of $\underline{k}$ and evaluate Bloch functions using the phase factor $\exp(i\underline{k}\cdot\underline{R}_t)$ a little more carefully, since $\underline{a}_1$ and $\underline{a}_2$ are not orthogonal. Using as a basis the two $p\pi$ orbitals of the cell in 118 the secular determinant becomes

$$\begin{vmatrix} \alpha - E & \beta\left(e^{i\underline{k}\cdot(\frac{2}{3}\underline{a}_1+\frac{1}{3}\underline{a}_2)} + e^{i\underline{k}\cdot(\frac{1}{3}\underline{a}_1-\frac{2}{3}\underline{a}_2)} + e^{i\underline{k}\cdot(\frac{1}{3}a_1+\frac{1}{3}a_2)}\right) \\ H_{12}^{*} & \alpha - E \end{vmatrix} = 0 \qquad (100)$$

with roots $E = \alpha \pm A^{\frac{1}{2}}\beta$ where

$$A = [3 + 2\cos(\underline{a}_1 + \underline{a}_2)\cdot\underline{k} + 2\cos\ \underline{a}_2\cdot\underline{k}\ + 2\cos\ \underline{a}_1\cdot\underline{k})]\,. \qquad (101)$$

Clearly again we cannot show the $E(\underline{k})$ dependence in two dimensions in an analogous way to the one-dimensional case but we will depict the energy changes along line in the Brillouin zone 102. At the three symmetry points Γ, M and K the energy is given by

$$\Gamma \quad E = \alpha \pm 3\beta\,; \qquad M \quad E = \alpha \pm \beta\,; \qquad K \quad E = \alpha \pm 0\beta\,. \qquad (102)$$

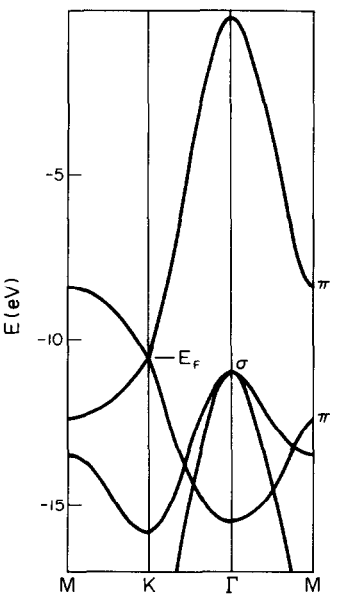

Fig. 10. Band structure for graphite using the Extended Hückel approach. (Adapted from Ref. 28.)

119 shows the graphite π band structure using these results. Figure 10 shows a band structure for graphite using an extended Hückel method which includes the σ bands too. Notice

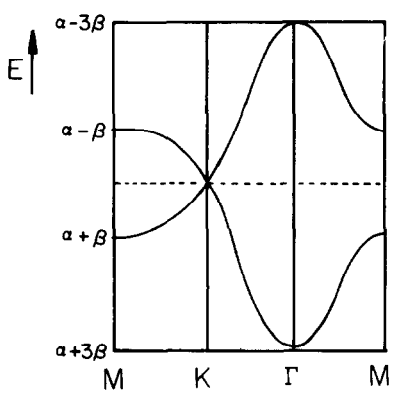

119

that the levels at $E > \alpha$ are destabilized more than the levels for which E are stabilized. This has an explanation identical to that discussed in Section 1.2. Inclusion of overlap destroys the symmetry associated with the orbitals or bands about the $E = \alpha$ level. Notice

however that the degeneracy at $E=\alpha$ at the point K is maintained even when overlap is included. With one electron per $p\pi$ orbital in graphite, this band is half filled and $\underline{k}_F$ lies at the point K. Graphite is thus a zero-gap semiconductor, one where valence and conduction bands just touch.

120

Exactly the same results are found if, instead of using the individual $p\pi$ orbitals as a basis, we use the π and π^* functions of the two orbital cell 120. The secular determinant is then

$$\begin{vmatrix} (\alpha+\beta)+\beta\cos\underline{k}\cdot\underline{a}_2+\beta\cos\underline{k}\cdot\underline{a}_1-E & i\beta(\sin\underline{k}\cdot\underline{a}_1+\sin\underline{k}\cdot\underline{a}_2) \\ -i\beta(\sin\underline{k}\cdot\underline{a}_1+\sin\underline{k}\cdot\underline{a}_2) & (\alpha-\beta)-\beta\cos\underline{k}\cdot\underline{a}_2-\beta\cos\underline{k}\cdot\underline{a}_1-E \end{vmatrix} = 0 \qquad (103)$$

with roots $E = \alpha \pm A^{\frac{1}{2}}\beta$ as before (equation (101)).

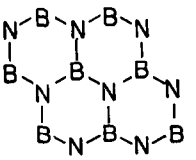

121

The secular determinant of equation (100) may easily be rewritten for the case of BN 121 by using two different values, α_N and α_B. The energy levels may be evaluated by expansion of the secular determinant in the usual way, as

$$E = \tfrac{1}{2}(\alpha_B+\alpha_N) \pm \tfrac{1}{2}\sqrt{(\alpha_B-\alpha_N)^2+4A^2} \ . \qquad (104)$$

The most striking result of this substitution is the removal of the degeneracy at the point K. Here the energies become $E=\alpha_N$ and $E=\alpha_B$. 122 shows schematically the result predicted.

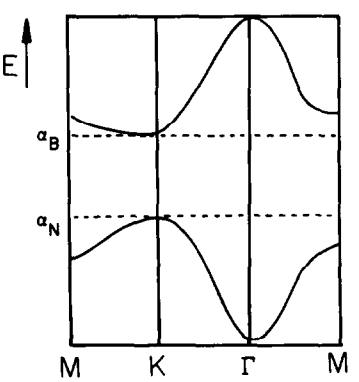

122

With two π electrons per pair only the lower band is filled. BN is thus an insulator and, in contrast to the metallic sheen of graphite, BN is a plain white solid. An extended Hückel band structure is shown in Fig. 11. Graphite and BN have half filled $p\pi$ bands and it is interesting to see that the observed structure of BN is one where the boron and nitrogen atoms alternate in two dimensions. Recall that for one-dimensional chains, with a half-filled

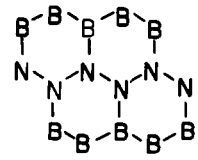

123

band the structure ...XYXY... was favored over the alternative ...XXYY... . Analogous arguments for the BN system favor 121 over, for example, 123.

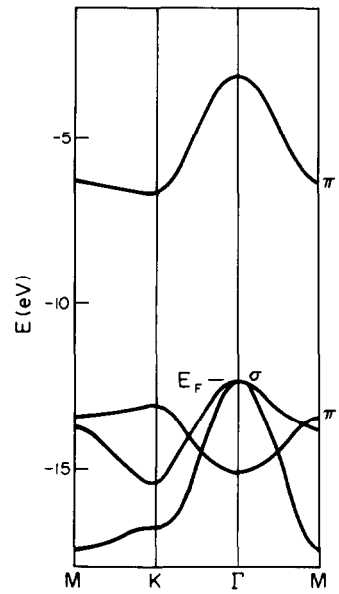

Fig. 11. Band structure for boron nitride (in the graphite structure) using the Extended Hückel approach. (Adapted from Ref. 28.)

The energy levels in graphite are filled up to the nonbonding level at $E=\alpha$. Occupation of deeper lying levels contributes to carbon-carbon bonding. Occupation of higher lying levels has a destabilizing effect and should give rise to an increase in the carbon-carbon distances. Figure 12 shows how this distance increases with the concentration of intercalated

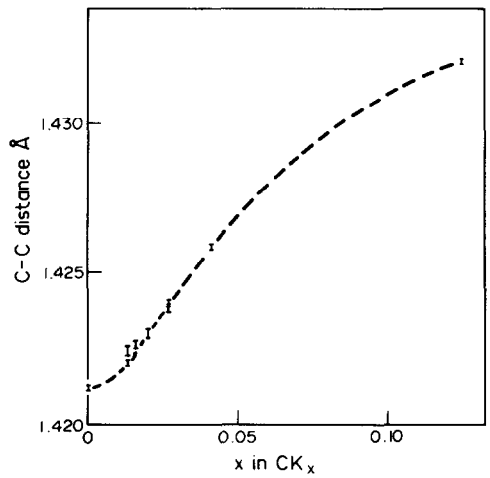

Fig. 12. Experimental values of the C—C intraplanar distance as a function of the extent of intercalation of potassium. (Adapted from ref. 52.)

donor atom, in nice agreement with this prediction. (But see Ref. 31 for a further analysis of this problem.)

A tough problem to tackle using the quantitative method we have adopted above, is the generation of the band structure of the net shown in 124 which contains 5 and 7 rings. It is not bipartite and lacks a lot of the symmetry we have found useful before. Its bands need to be generated numerically. The net is actually found for the nonmetal sheets of ScB_2C_2 where

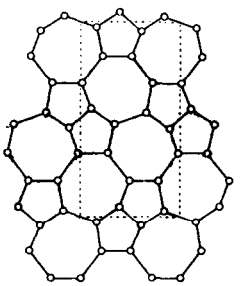

124

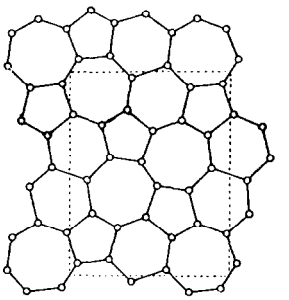

125

the metal ions lie between such nets. If the scandium atoms are considered to contribute their three valence electrons to the sheets then the unit $(B_2C_2)^{3-}$ has an average of 5/4 electrons per atom, i.e., the π band is 5/8 full. 125 shows another related net, that of the boron atoms in Y_2LnB_6. 126 shows the energy difference between the graphite, 48^2 and ScB_2C_2 nets as a function of band filling. ($N_{p\pi}$ is the number of $p\pi$ electrons per atom).

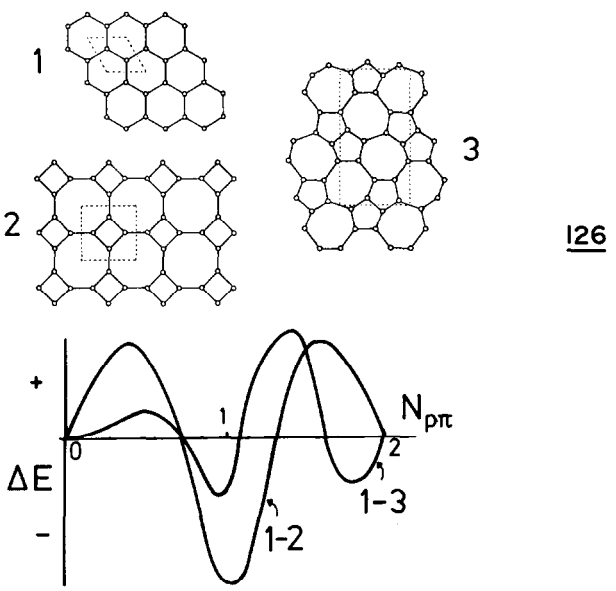

126

As in the case of the one-dimensional examples of 98 (and indeed in the molecular species of 30) the six-ring net is the most stable at the half-filled point, (i.e., as observed for graphite) the net containing 5 and 7 rings is most stable just after this point (i.e., as observed for ScB_2C_2) [32] and the 48^2 net is stable at the very beginning and very end of the filling curve. Notice that the nonbipartite nature of the net 124 shows up in the asymmetry of its energy difference curve with the bipartite graphite net. Beyond the scope of this article is discussion concerning the underlying physics of the plots of 98 and 126. In brief however we can show[33] that the energy differences between two structures of the type

energetically depicted in 126 (where each atom has the same coordinate number) is simply given by equation (105)

$$E(x) = \sum_r [N_r(1) - N_r(2)]\, f(r,x)\,, \tag{105}$$

where $N_r(1)$ and $N_r(2)$ are the numbers of r-rings in each of the two structures and $x(0 \to 1)$ is the extent of band filling. The functions $f(r,x)$ are universal expressions which describe the energetic contributions from an r-ring. Equation (105) also holds approximately for the one-dimensional cases of 98 (here not all the centers are three coordinate) and also more approximately in the molecular case of 30. The result of Gutman and Trinajstić[12] noted earlier is simply the special molecular case of $x = 0.5$, and emphasizes the stability of 6-rings and instability of 4- and 8-rings at the half-filled point.

In the ScB_2C_2 net of 124 there is clearly a preference for the carbon and boron atoms to occupy specific sites in the net. A calculation on an all carbon net with the geometry of 124 shows indeed that the carbon atoms in ScB_2C_2 occupy sites of higher negative charge in the unsubstituted parent. Band structure calculations[25] which include both σ and π bonding manifolds of orbitals show a stabilization of about 20 kcal/mole for the observed structure compared to the one where the boron and carbon atoms have been exchanged.

In Section 2.2 we discussed at some length the Peierls distortion on one-dimensional polyacetylene and showed how the distortion energy was $\frac{1}{2}(\beta_1 - \beta_2)/2$ per atom. It is of some considerable interest to calculate the distortion energy in polyacene 84 and graphite 118 since both of these systems have a degenerate pair of orbitals at the Fermi level. For polyacene we consider the distortion in 127 which retains the mirror symmetry bisecting the

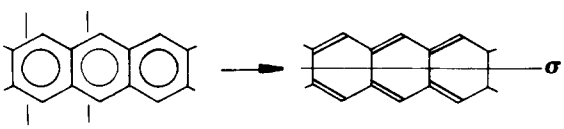

127

polymer. So the labels S and A used in 91 to describe the parity of the bands with respect to this plane are still good labels to use during and after the distortion. Immediately a striking difference between the distortion in polyacene and polyacetylene is apparent. In polyacene on distortion, the energy changes associated with the levels will occur via a mixing of the two antisymmetric bands, and via a mixing of the two symmetric bands, i.e., the energy change will occur in second order. In polyacetylene the splitting apart of the levels at the zone edge occurred in first order. We may readily calculate the energy shifts for the S and A pairs of 91 by solving the relevant secular determinant. The off-diagonal element linking either the two S bands or the two A bands at the zone edge is just $(\beta_1 - \beta_2)/2$ and so for the antisymmetric block

$$\begin{vmatrix} (\alpha-\beta)-E & \frac{1}{2}(\beta_1-\beta_2) \\ \frac{1}{2}(\beta_1-\beta_2) & \alpha-E \end{vmatrix} = 0 \tag{106}$$

which has roots $E = (\alpha - \beta/2) \pm (\beta^2 + (\beta_1 - \beta_2)^2)^{\frac{1}{2}}/2$. Expanding this in terms of $(\beta_1 - \beta_2)/\beta$ leads to the two new antisymmetric levels at the zone edge

$$E = \alpha + \frac{(\beta_1-\beta_2)^2}{4\beta}\,; \qquad E = \alpha - \beta - \frac{(\beta_1-\beta_2)^2}{4\beta}\,. \tag{107}$$

Similar expressions apply to the symmetric block and lead 128 to a band gap of $(\beta_1 - \beta_2)^2/2\beta$ for the polyacene distortion 127. Compare this with a value for polyacetylene of $(\beta_1 - \beta_2)/2$.

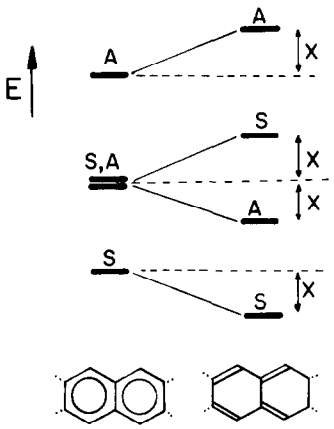

$$X = \frac{(\beta_1 - \beta_2)^2}{4\beta} \qquad 128$$

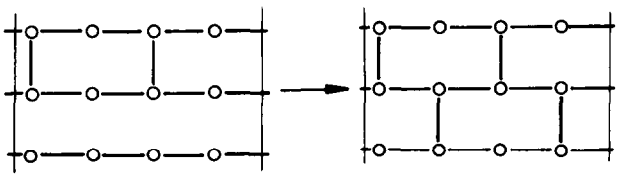

129

Let us build up the levels of a three stranded polymer to see how it will distort. We will just derive the level structure at the zone edge via the process 129 for the undistorted species. This is easy to do and is shown schematically in 130. We will leave it to the

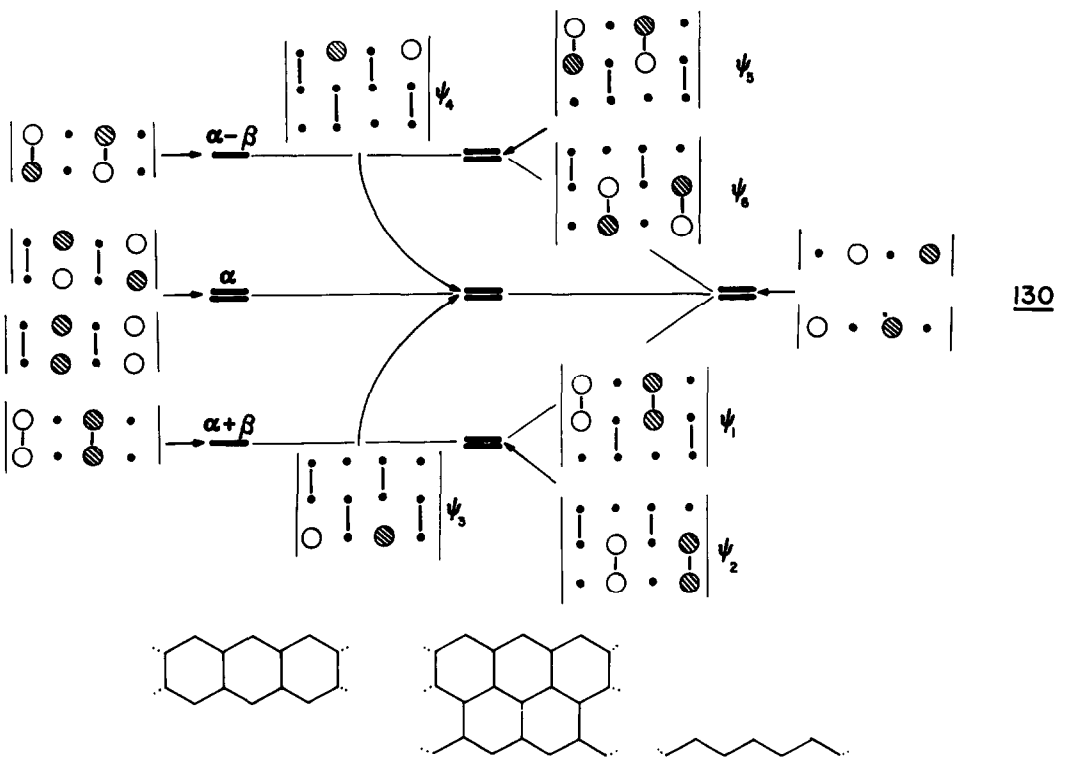

130

reader to show that during the distortion 131 ψ_5 pushes ψ_4 down in energy by exactly the same amount as ψ_1 pushes ψ_4 up in energy. ψ_4 therefore remains unchanged in energy on distortion up to second order. Analogously ψ_3 remains unchanged in energy too in second order. It can be shown that the splitting apart at the zone edge of ψ_3 and ψ_4 occurs in

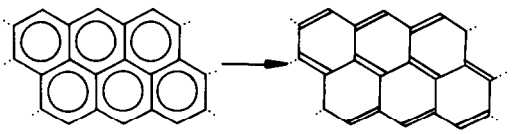

131

third order in the energy and that the band gap is $(\beta_1-\beta_2)^3/4\beta^2$. In general[34] for polymers of this type the energy gap goes as $(\beta_1-\beta_2)\delta^{n-1}$ where n is the number of strands and $\delta = (\beta_1-\beta_2)/\beta \ll 1$. So as n increases the stabilization energy drops off sharply. 132 shows the results of some numerical extended Hückel calculations[25] on systems of this type. The

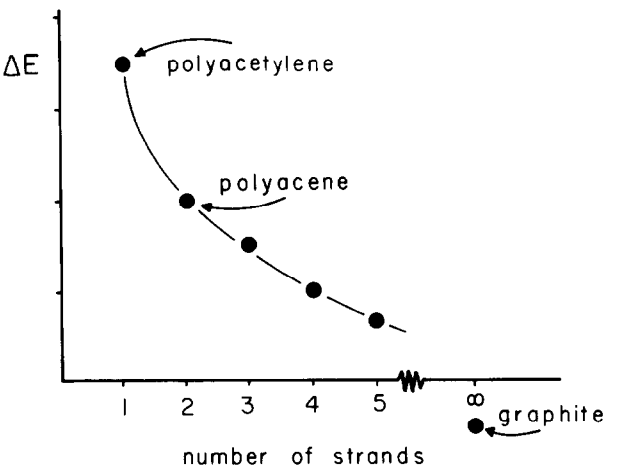

132

ordinate represents the relative energy differences between the undistorted parent and a slightly distorted version. (The numerical scale of the ordinate will depend on the size of the distortion.) The rapid decrease in stabilization energy on distortion as n increases is apparent. Opposing such a stabilization associated with the π levels is a small destabilization on distortion for the σ levels (the so-called elastic forces of the solid state physicist) which eventually outweighs the π distortion energy. For graphite the distortion is energetically unfavorable.

4. MORE ORBITALS AND MORE DIMENSIONS

4.1 Variations on the One-Dimensional Problem

Our discussion so far has centered on the band structures of systems built up from single atomic pπ levels. The results are transferable in many cases to several other systems. Algebraically the one-dimensional results apply to a chain of atoms bearing s or d_z^2 orbitals as in 133 and 134. Both of these problems are characterized by an interaction

133

134

integral β of the same type as that in 42. The simplest problem corresponding to 133 is a linear chain of hydrogen atoms 135. This should undergo a Peierls distortion since it has but one electron per orbital, in an exactly analogous fashion to polyacetylene. The resulting dimers 136 would be in accord with traditional ideas which we have concerning bonding in this molecule. On application of high pressure (~2Mbar) the process can be reversed and 136 → 135. The physical properties of 135 (or rather its three-dimensional analog) are interesting. 49 shows that such a structure should be metallic and indeed at these high

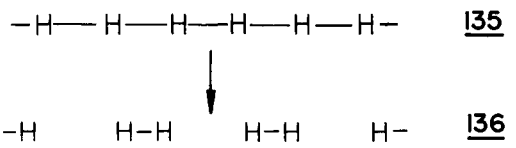

pressures metallic conduction has been observed.[35] This particular result is of interest to geophysicists, since the 'atmospheres' of several planets have been suggested to be made from such material.

An example of 134 is found in the salts of the ion $Pt(CN)_4^{2-}$. This species is square planar and, in the solid state, the planes stack,[36] one above the next as in 137. The valence orbitals of such a molecular unit are shown in 138 along with the orbital occupancy

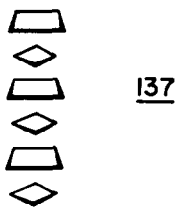

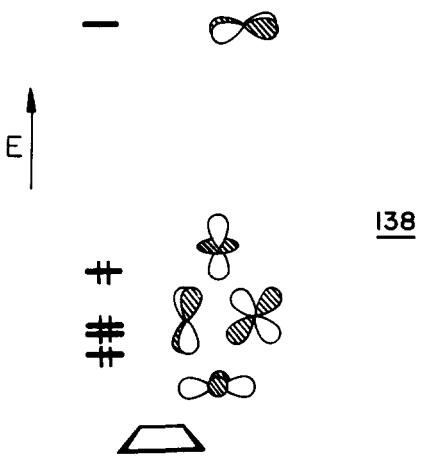

expected for a low spin d^8 (Pt(II)) configuration. The z^2 orbitals of each unit interact with the next in the fashion shown in 134 and a band, filled with two electrons, results 139.

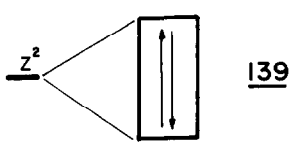

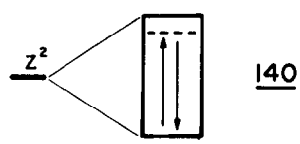

$K_2[Pt(CN)_4]$ is a white solid and an insulator ($5 \times 10^{-7}\,\Omega^{-1}\,cm^{-1}$) with equal Pt—Pt distances of 3.48 Å. The salt can be cocrystallized with elemental bromine which results in oxidation of the chain to give nonstoichiometric material $K_2(Pt(CN)_4)Br_\delta \cdot 3H_2O$. The chain ion is now formulated as $Pt(CN)_4^{\delta-2}$ and, as a result electron density is removed from the z^2 band 140. This material is metallic and, since the electron density has been removed from the very top of the band where (43) maximum antibonding interactions are found, it has a significantly shorter Pt—Pt distance (2.88 Å for $\delta = 0.3$).

There are many other materials which are built up using exactly the same principles. For example, the d^8 complexes of the glyoximate and dioximate ligands 141 and Ni, Pd and Pt also lead to stacks of planar units.[37] On cocrystallization with halogen, conducting

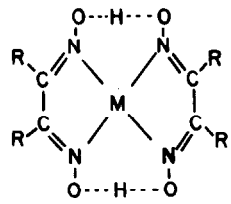

$M(gly)_2$ R=H
$M(dpg)_2$ R=Ph

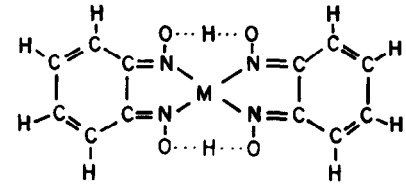

141

Mpc

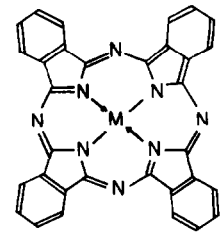

142

materials are produced. Similar features are found in phthalocyaninnes MPc 142 and porphyrins. Often the crystal structure of the doped, conducting material shows regularly stacked 143 and that of the pure material, slipped stacks of planar units 144.

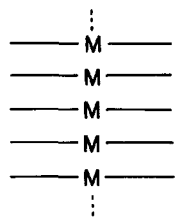

143

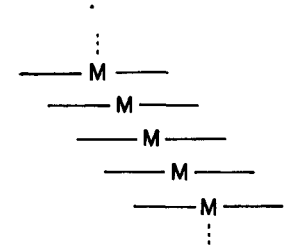

144

Conceptually very similar to these $Pt(CN)_4$ (often abbreviated as TCP) systems are a whole series of 'organic metals' which contain no metal atoms at all. Such species again are typified by the stacking up of planar molecules such as those in 145.[38] In the absence of

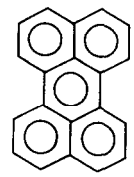

perylene

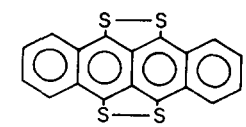

tetrathiotetracene
TTT

145

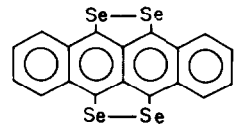

tetraselenotetracene
TSeT

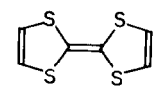

tetrathiofulvalene
TTF

dopants the crystals are not conductors of electricity. However just as in the TCP case, cocrystallization with halogen leads to conducting materials. Some examples are

$(\text{perylene})^{0.4}\ (I_3^- \cdot 2I_2)_{0.4}$	$5-50\ (\Omega\,\text{cm})^{-1}$
$(TTF)\,Br_{0.7}$	$300-500$
$(TTT)_2\,I_3^-$	2700
$(TSeT)Cl_{0.5}$	2100 .

A particularly interesting series is shown in 146. The parent material is an insulator but

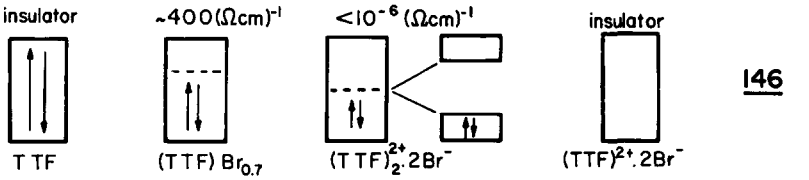

146

the nonstoichiometrically doped material $((TTF)Br_{0.7})$ is a metal. With a half filled band as in $(TTF)_2 2Br^-$ a Peierls distortion leads to dimerization and the observation of $(TTF)_2^{2+}$ pairs in the crystal. Finally, if the band is emptied completely, individual ions $(TTF)^{2+}$ are found. Not all of the structures of these species end up as neatly stacked planar molecules. In $(TTT)_2\,I_3^-$ for example the stacks are slipped somewhat as in 144.

There is an obvious difference between the energy bands derived from 42, 133 and 134 and that associated with a single pσ orbital at each center 147. Here since the positive

147

lobe of one orbital overlaps with the negative lobe of the p_z orbital carried by an adjacent atom in the chain, the interaction integral between them is positive rather than being negative. The only difference this makes to our discussion above is that maximum bonding between the atoms of the chain is now found at the zone edge, and maximum antibonding at the zone center, 148.

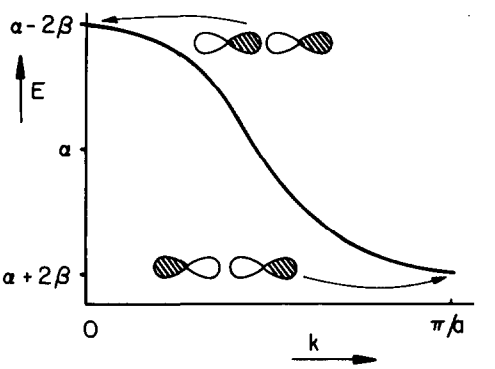

148

We are now in a position to qualitatively outline the σ band structure of a linear atomic chain containing s and p orbitals on each atom. We need to solve the relevant secular determinant which will include three different values of β, one for pσ–pσ, one for s–s and one for pσ–s interactions. This is

$$\begin{vmatrix} \alpha_s + 2\beta_{ss}\cos ka - E & 2i\beta_{sp}\sin ka \\ -2i\beta_{sp}\sin ka & \alpha_p - 2\beta_{pp}\cos ka - E \end{vmatrix} = 0\,. \qquad (108)$$

We will not write down the (messy) expression for the energy levels but just note that at $k = 0$ and $k = \pi/a$ the off-diagonal element is identically zero, i.e., there is no s—p mixing at either of these points. H_{sp} is at a maximum in fact for $k = \pi/2a$. 149 shows a qualitative diagram for such a system constructed by making use of this result and the fact that $|\alpha_s| > |\alpha_p|$. The dashed lines show the dispersion in the absence of sp mixing. Here we have

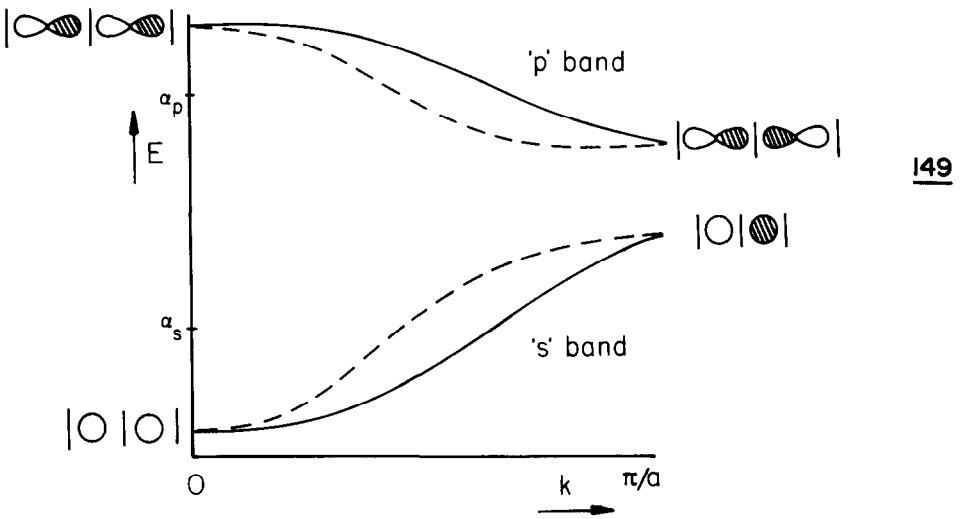

149

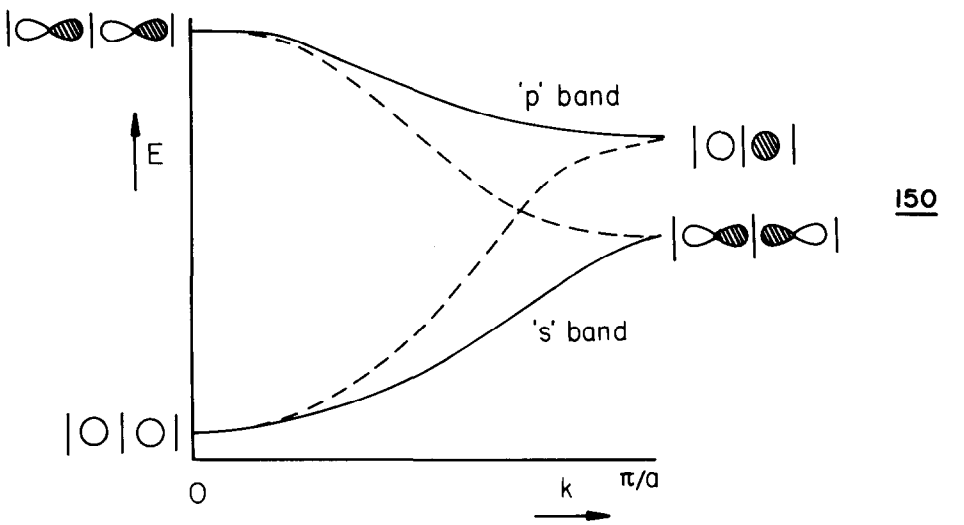

150

assumed that the s—p separation is large compared to the values of β for the s and p bands 150 shows a more realistic case where the unmixed s and p bands (dashed lines) cross in energy. As β_{sp} increases then the mixing in the middle of the zone gives rise to the energy dependence shown by the solid lines. Note that because of the different k-dependence of the p and s orbital energies the 's' band, while purely s—s bonding at the zone center, is purely p—p bonding at the zone edge. In addition to the presence of $p\sigma$ orbitals on the chain atoms there will be two $p\pi$ orbitals (p_x and p_y). These will be degenerate at all k (i.e., the π label is still a good one for the chain) and their behavior will be just like that found for polyacetylene. There is no overlap between these orbitals and any of the orbitals of σ type. A composite picture for a one-dimensional chain of atoms is shown in 151.

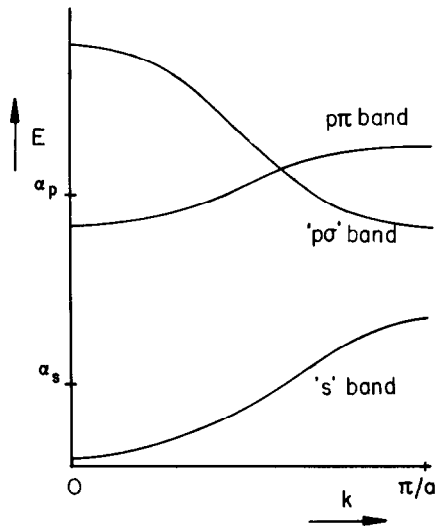

151

Let us now ask the following question. We known that the molecule ferrocene $(C_5H_5)_2Fe$ and bicyclobutadiene nickel $(C_4H_4)_2Ni$ are stable molecules with geometries shown in 152. With

152

these electron configurations, the eighteen electron rule is satisfied and there is a significant energy gap between HOMO and LUMO. For what metal will a similar energy gap be produced in the infinite species of 153 and 154? Starting with the case of 154 we need to

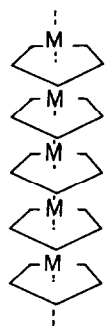

153

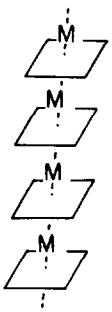

154

consider the five metal d orbitals 155 and the four cyclobutadiene orbitals of Fig. 3. We have used 156 the alternative form of the degenerate pair of orbitals ψ_2 and ψ_3 shown in 17. Symmetry arguments are useful here in simplifying this problem. Just as in the chain of sp atoms noted above, we could separately treat the orbitals of σ and π type, so here we can classify both the metal d and cyclobutadiene orbitals in terms of their σ, π and δ symmetry. Let us start off with the orbitals of σ symmetry. The secular determinant is

$$\begin{vmatrix} \alpha_d - E & 2i\beta \sin ka/2 \\ -2i\beta \sin ka/2 & \alpha_1 - E \end{vmatrix} = 0 . \qquad (109)$$

Here α_1 is the energy of the cyclobutadiene orbital ψ_1 ($=\alpha+2\beta$ in the notation of Sections II and III), and α_d is the d orbital Coulomb energy. Note that neither diagonal entry contains any k dependence since we have ignored M—M and cyclobutadiene-cyclobutadiene inter-

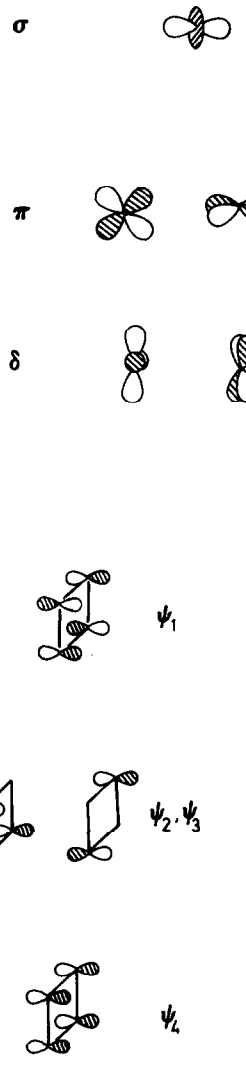

actions. β in equation (108) is the interaction integral between ψ_1 and z^2. It is probably quite small since the geometry is such that the cyclobutadiene orbitals lie close to the

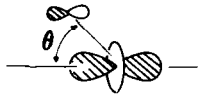

157

conical node in z^2 157 which occurs at $\theta = 54.73°$. The σ band structure then has a small dispersion and probably looks like 158. The secular determinant for the δ block will be

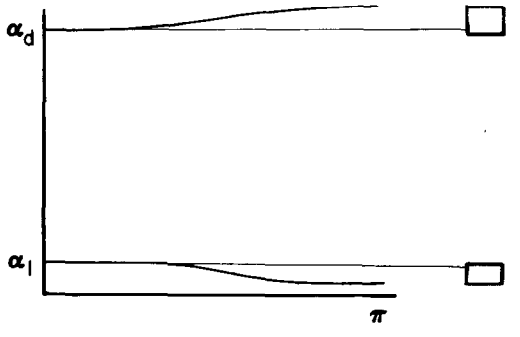

158

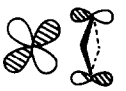

159

very similar to equation (108) and β will again be small since the overlap between ψ_4 and one of the δ components is not very favorable. Only in the case of the π type interaction is the interaction integral significant 159. The secular determinant is given by

$$\begin{vmatrix} \alpha_d - E & 2\beta\cos ka/2 \\ 2\beta\cos ka/2 & \alpha_2 - E \end{vmatrix} = 0 . \qquad (110)$$

In section 3.2 we looked at a problem of this type using perturbation theory. There are two bands. The bottom of the upper one lies at α_d and the top of the lower one lies at α_2. (See 67 and the associated discussion.) The band structure is then simply derived from these results and is shown in 160.

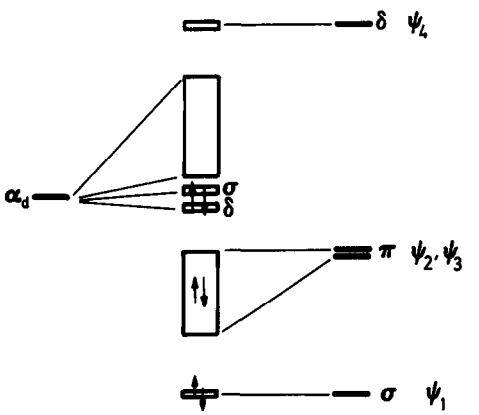

160

metal atom — bands of 153 — □

To fill all the bonding and nonbonding levels we need a total of twelve electrons per unit, a metal atom from the iron group is required. Such a system however, would have a zero band gap because of the touching of the (xz, yz) band and the z^2 and (x^2-y^2, xy) bands. In fact a numerical calculation, which models the cyclobutadienyl ring properly (the carbon atoms do carry s orbitals) results in a pushing up of the (xy, yz) band at the zone edge and an opening up of a band gap of about 1.5 eV. The polymetalcyclopentadienyl system 153 presents a similar case. Analogous arguments lead to the prediction of a manganese group metal for this polymer.

Another problem which may be tackled along similar lines is the generation of the band structure of the hypothetical MH_4 system shown in 161. The chain is composed of edge-

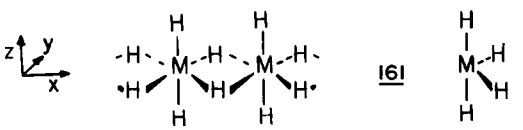

161

162

sharing MH_6 octahedra. First we have to decide on the basis set to use for the problem. As we have seen in Section 3 the same result may be reached in a variety of different ways. Perhaps the easiest route for this example is to first of all set up the valence orbitals of the butterfly MH_4 unit, 162. With HMH angles of 90° and 180° this is very easy and is shown in 163. z^2 is destabilized (by $2.5e_\sigma$ using the angular overlap model[4]) more than xy (by $1.5e_\sigma$)

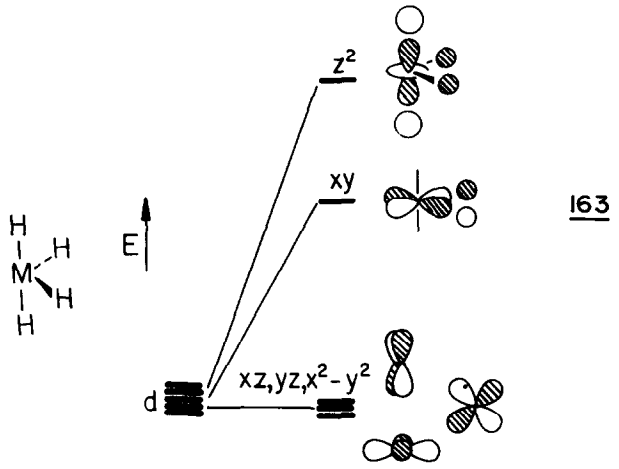

163

and the three other d orbitals remain nonbonding. We know enough about energy bands by now to be able to write down an approximate band structure. This is shown in 164.

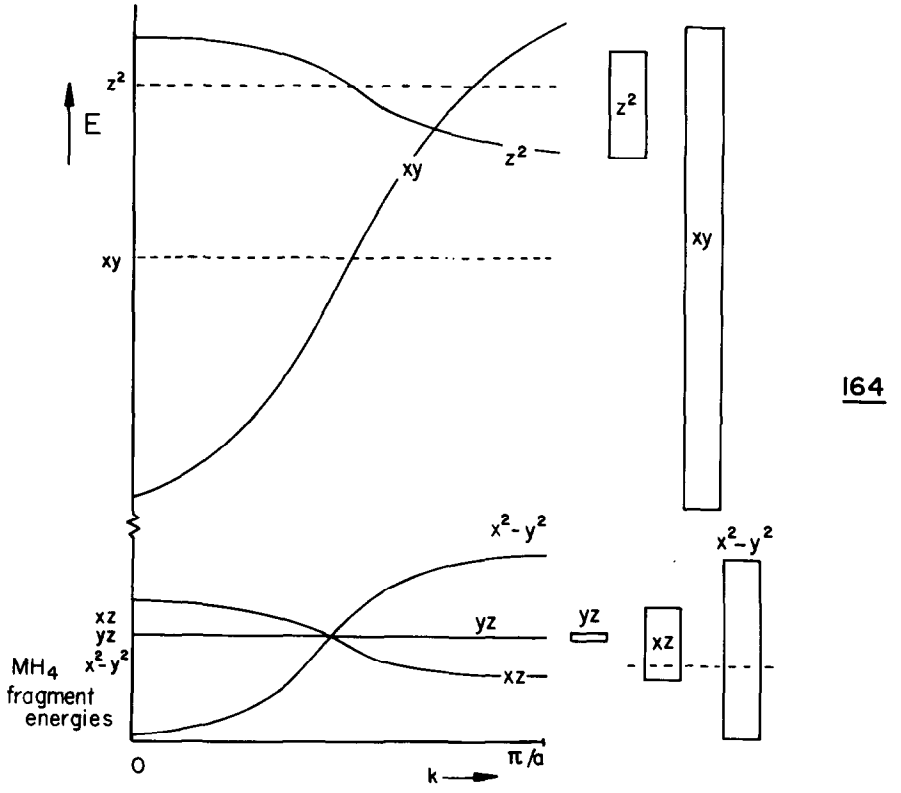

164

The energetic behavior of the levels with respect to k is easily understood. Recall that whether maximum bonding or antibonding is found at the zone center just depends on whether the overlap integral of one basis orbital is positive or negative respectively with its part-

ner in the next unit cell. (The pπ orbitals of the polyacetylene chain is an example of the former, the pσ orbitals of 147 and 148 an example of the latter). The dispersion of the z^2 and xy bands is set by the sign and magnitude of the M—H interactions between cells. From 163 the overlap is negative for z^2 but positive (and larger in magnitude) for xy. Notice the correspondingly larger dispersion of the xy band with the opposite dispersion behavior to that of z^2. If the energetics were dominated by metal-metal interaction, since the z^2 overlap is positive but the x^2-y^2 overlap negative, the dispersion of the two bands would be reversed. The xz, yz and x^2-y^2 orbitals have no hydrogen orbital character and their dispersion is set by the positive overlap for x^2-y^2 and yz and the negative overlap for xz. We show a tiny dispersion for yz since it is unfavorably situated for good M—M interaction compared to the σ and π interactions of x^2-y^2 and xz respectively. The band structure ends up as a two above three pattern typical of octahedral coordination. In 164 we show the Fermi level for a d^1 metal and inquire how the system might distort to lower its energy. The situation is not quite as simple as the one-dimensional Peierls instability of polyacetylene or elemental hydrogen, since there are three accessible energy bands to worry

165

166

about. However a pairing distortion 165 to 166 does stabilize the system considerably as shown in 167 and a semiconductor is generated. This orbital problem is very similar[39] to

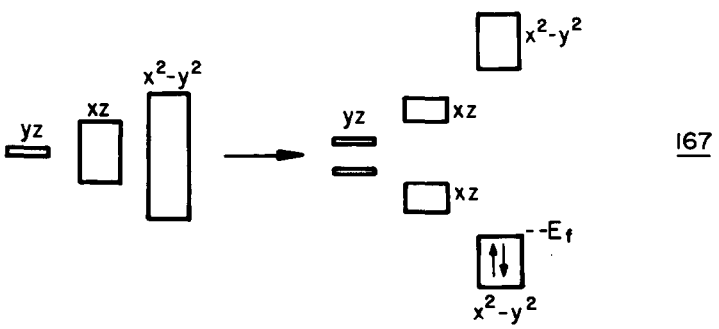

167

that of NbX_4 (X = halogen) which forms chains of the type in 166. NbI_4 under pressure becomes metallic. Just as in the case of elemental hydrogen (135, 136) the Peierls distortion here may be reversed by the application of pressure.

Note that in the distortion shown in 166, and indeed in all of the distortions of the Peierls type we have studied, the bandwidths of each of the components on distortion together are less than the undistorted width. This arises as a simple consequence of the fact that the overlap integrals decrease as the interatomic distance increases. The corresponding interaction matrix elements then become smaller on distortion.

In fact although the band structure of $NbCl_4$ looks very similar to that depicted in 164 the picture which emerges from a quantitative calculation[39] is a little more complex. Our

depiction of the dispersion behavior of the lower set of levels in 164 is perfectly fine for an MH_4 chain, but with π bearing ligands the situation is more involved. The basis set of orbitals now needs to include the effects of π interactions. With donor ligands the 'd' orbitals are metal ligand antibonding and may be written as in 168 – 170. The overlap integral

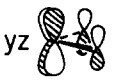

168

169

170

of 168 with its neighbor in the next cell contains a negligible metal-metal component (ignored before) and a negative d–pπ overlap. Maximum bonding is then assured at $k = \pi/a$. 169 is a little problematical. Metal-Metal overlap is negative but d–pπ overlap is positive. Calculations on this system show the two to virtually cancel and a flat band results. Similarly, the overlap integral of 170 with its neighbor is the sum of good positive metal-ligand overlaps. It then receives its maximum bonding at $k = 0$. 171 shows the new result – very similar to that of 164 but with a subtle difference in orbital labeling.

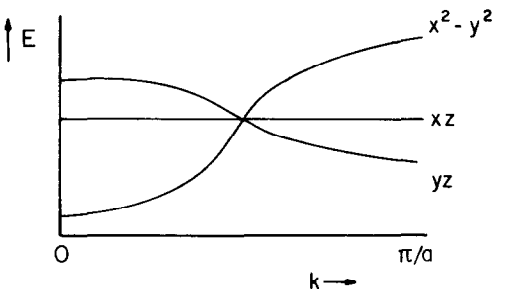

171

A system where there are three bridging atoms occurs 172 in the chains of MX_3 stoichiometry that occur in $BaMS_3$ (M = Ti , V , Ta) for example and also in a series of ternary

172

chlorides $AMCl_3$ (A = Cs , Rb , $N(CH_3)_4$; M = V , Cr , Mn , Fe , Co , Ni , Cu).[40] The orbitals we will use for the MS_3 unit, assuming SMS angles of 90°, are shown in 173. We have shown the situation for an MH_3 unit for simplicity. There are two M–H σ antibonding orbitals (desta-

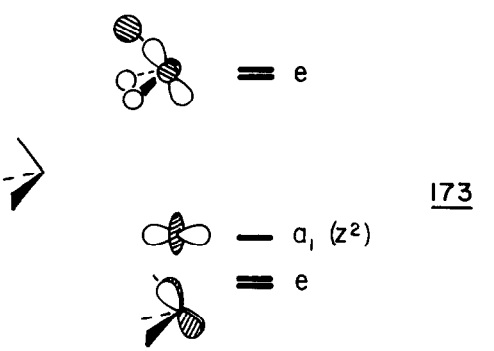

173

bilized by $1.5e_\sigma$ using the angular overlap model) which form a degenerate pair and three nonbonding d orbitals at much lower energy. (Only one component of each e pair is shown.) The a_1, z^2 orbital is nicely set up for good metal-metal interaction across the shared face of the coordination octahedron of 172. Figure 13 shows the calculated band structure for this system. It has similar features to that of the $NbCl_4$ species we have just described.

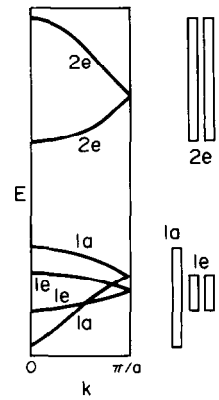

Fig. 13. The d-block bands of a face-sharing octahedral MX_3^{n-} chain. The energy variation with wavevector left and a block diagram right. (Adapted from Ref. 40.)

174 shows how the bands split apart as a result of a pairing distortion 175 of the type described extensively in this article. 174, in fact is the result of a numerical calculation for a VS_3^{2-} chain. The shaded area indicates the bands which are doubly occupied. If the distor-

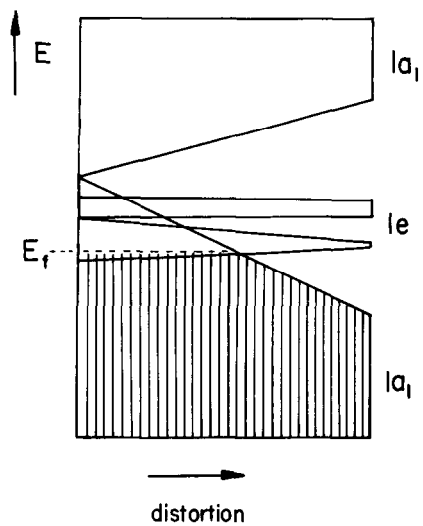

174

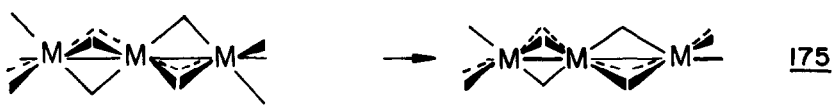

175

tion proceeds far enough then a Peierls insulator results. However $BaVS_3$ is a metal. Just as in the molecular case where dynamic Jahn-Teller processes allow an undistorted structure to be observed, so too with its solid state equivalent. Although the theory of the distortion indicates when it will occur, it is difficult to predict the size of the effect in general, especially if, as in the present case, several bands overlap to complicate the picture. (See also Table 4).

A slightly more complex problem lies in understanding the electronic structure of the mixed valence $Pt^{II}(L)_4 \cdot Pt^{IV}(L)_4X_2^{4+}$ (X = halide) chains[39] 177 which, with $L = NH_3$ or $NEtH_2$, are present in Wolfram's red salt and Reihlen's green salt. These are obvious distortions of the symmetric 'Pt^{III}' structure 176. Let us start with the unit cell of 176 shown

176 177

in 178. We saw the energy levels of the square planar ML_4 unit in 138. The only orbital that we need to consider is z^2 since this is the only one with appreciable overlap with the X orbitals. On X we need to include valence s and pσ orbitals. The secular determinant

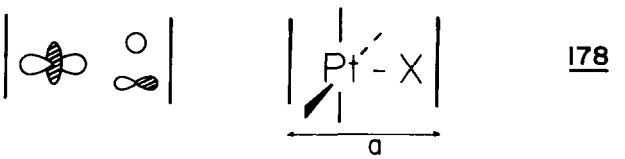

178

for this three orbital problem is simply constructed as in equation (111). Obviously we will not try to solve this in closed form as it stands. First we will study the result obtained by setting

$$\begin{vmatrix} \alpha_s - E & 0 & 2\beta_{sd}\cos ka/2 \\ 0 & \alpha_p - E & -2\beta_{pd}\, i \sin ka/2 \\ 2\beta_{sd}\cos ka/2 & 2\beta_{pd}\, i \sin ka/2 & \alpha_d - E \end{vmatrix} = 0 \qquad (111)$$

$\alpha_p = \alpha_s$, and equate both interaction integrals ($\beta_{sd} = \beta_{pd} = \beta$). The solutions are easily written down

$$\begin{aligned} E &= \alpha_p \qquad (= \alpha_s) \\ E &= \frac{(\alpha_p + \alpha_d) \pm \sqrt{(\alpha_p - \alpha_d)^2 + 16\beta^2}}{2} \end{aligned} \qquad (112)$$

and show dramatically that none of the energy bands have any dispersion at all, i.e., there is no k dependence. Second we put $\alpha_s = \alpha_p$ but allow $\beta_{sd} \neq \beta_{pd}$. The roots now become

$$\begin{aligned} E &= \alpha_p \qquad (= \alpha_s) \\ E &= \frac{(\alpha_p + \alpha_d) \pm \sqrt{(\alpha_p - \alpha_d)^2 + 16[\beta_{pd}^2 - \cos^2(ka/2)(\beta_{pd} - \beta_{sd})^2]}}{2} \end{aligned} \qquad (113)$$

Now, arbitrarily assuming that $|\beta_{pd}| > |\beta_{sd}|$, we may draw out the band structure as in 179. By expansion of equation (113) as a power series the roots are

$$E = \alpha_p - \frac{4(\beta_{pd}^2 - \cos^2(ka/2)(\beta_{pd}^2 - \beta_{sd}^2))}{\alpha_p - \alpha_d} \qquad (114)$$

and

$$E = \alpha_p + \frac{4(\beta_{pd}^2 - \cos^2(ka/2)(\beta_{pd}^2 - \beta_{sd}^2))}{\alpha_p - \alpha_d} . \qquad (115)$$

The result is actually reminiscent of the behavior we have just noted for $NbCl_4$. Interaction of z^2 with the s orbital on X leads to a dispersion with a $\cos^2(ka/2)$ dependence with maximum bonding at $k = 0$, but interaction of z^2 with the p orbital on X leads to a $\sin^2(ka/2)$ dependence with maximum bonding at $k = \pi/a$. The result, if the two interactions

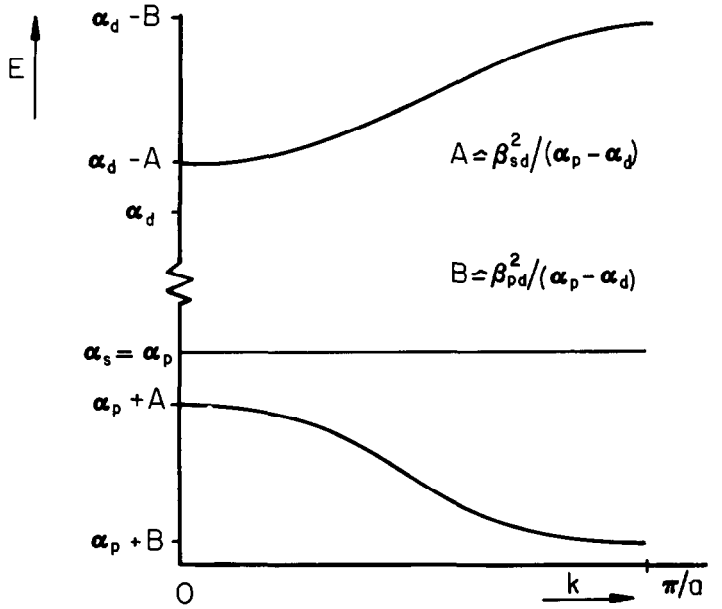

179

are equal, is a dispersion-free band as we found above. The form of the wavefunctions at the top and bottom of the 'z^2' band are shown in 180 and 181 respectively. The oxidation

180

181

state of the platinum in 176 is Pt^{III} and thus this 'z^2' band is half full of electrons. Figure 14 shows the result of an extended Hückel calculation as the symmetric system 176 is distorted to 177. The initially metallic state has become insulating and an energetic stabilization has occurred. As in the case of NbI_4 the conductivity of these salts increases markedly on the application of pressure.

Let us look in a little more detail at the form of the orbitals since it will give clues as to how these systems distort. 182 shows the z^2 band for a doubled PtL_4X cell. At the

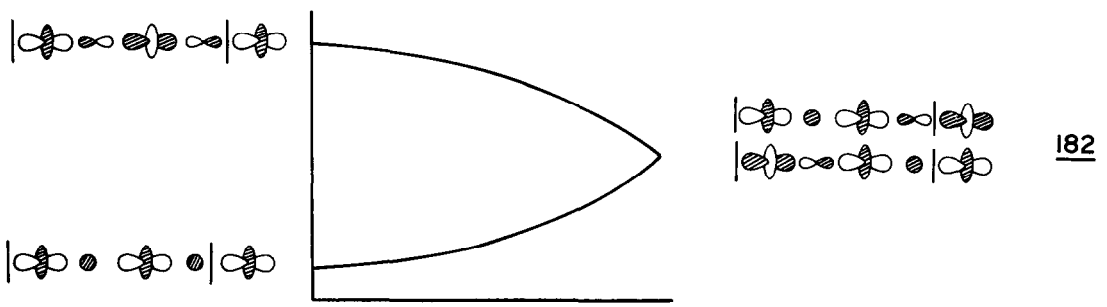

182

zone edge the obvious choice of wavefunctions, intermediate in character between those at the top and bottom of the band, has been made. As in all of the degenerate orbital problems we have looked at so far, a linear combination of these two orbitals as in 183 and 184 leads to another perfectly good pair. Now if the system is distorted slightly (176 → 177) then a band gap opens up at the zone edge. 183 goes up in energy since the Pt—X distances decrease around this metal atom and the antibonding interactions become stronger. 184 goes down in

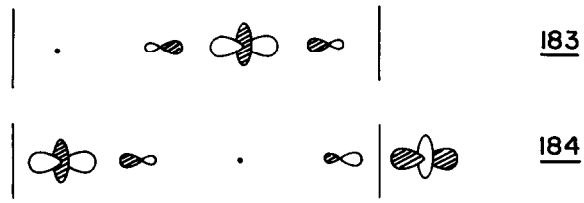

energy since the Pt-X distances around this metal atom increases with a concurrent weakening of the Pt-X antibonding interactions. This is shown in 185 in an exaggerated way. As the

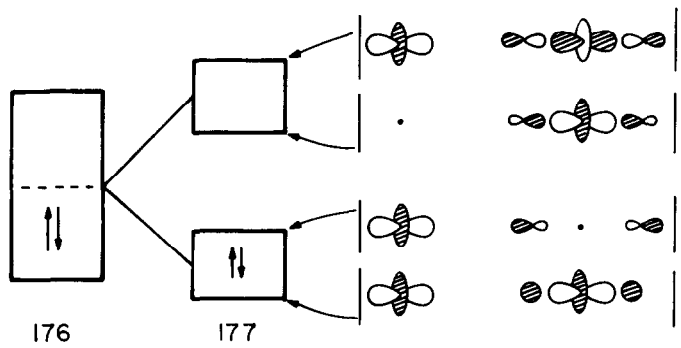

185

distortion proceeds the interaction of the z^2 orbital on the now planar Pt atom with the halogen orbitals of the bridge becomes small and the bandwidths of both the upper and lower parts of this band become very narrow, as in Fig. 14. The lower band (now full) then corresponds largely to a z^2 orbital on the square planar Pt atom 186 which is now Pt^{II}. The upper band (now empty) corresponds to a strongly antibonding orbital on the octahedral Pt^{IV} center 187. The result is a classical mixed valence compound, $Pt^{II}L_4 \cdot Pt^{IV}L_4X_2$.

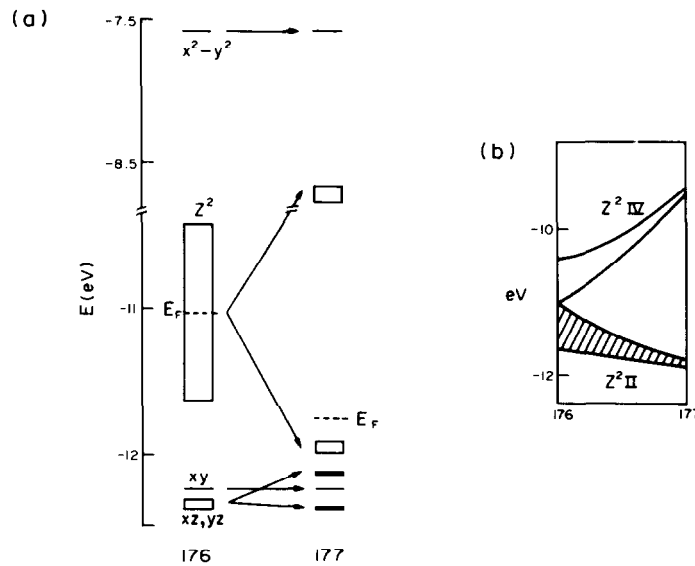

Fig. 14. (a) d-block bands of $[Pt(NH_3)_4 \cdot Pt(NH_3)_4Cl_2]$ chains (176 left and 177 right). (b) The widths of the split z^2 band as a function of the distortion 176 → 177. (Adapted from Ref. 40.)

4.2 Three Dimensions

In three dimensions things get quite complicated but there are places where we may make some simplifications to help us out. Firstly we will consider the simple cubic structure of 188. In many ways we may regard this as a simple sum of three one-dimensional chain problems,

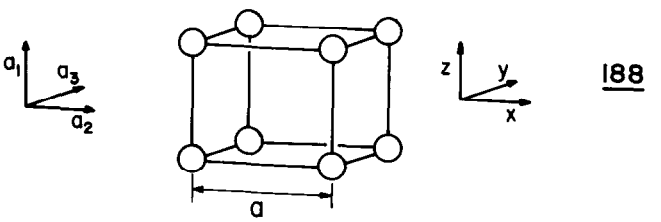

one lying along each Cartesian direction. For a solid composed of s orbitals (cubium) the energy dependence on $\underline{k}$ is, from equation (65) for a one atom cell,

$$E(\underline{k}) = 2\beta(\cos k_x a + \cos k_y a + \cos k_z a) \tag{116}$$

This leads to the dispersion curve in 189 where Γ, M, K and X represent the points $(k_x, k_y, k_z) = (0,0,0)\,2\pi/a$, $(\frac{1}{2},\frac{1}{2},\frac{1}{2})\,2\pi/a$, $(\frac{1}{2},\frac{1}{2},0)2\pi/a$ and $(0,0,\frac{1}{2})2\pi/a$, respectively.

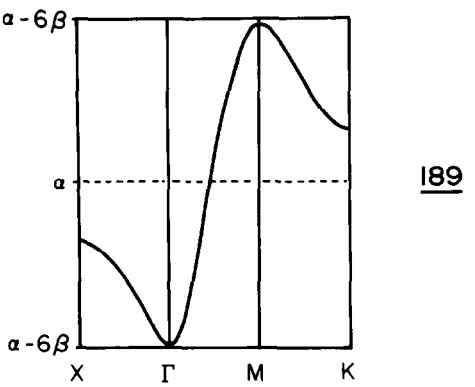

For three p orbitals located on a single atom another simple result applies. If we neglect pπ–pπ interaction 190 between orbitals on adjacent atoms and only consider σ over-

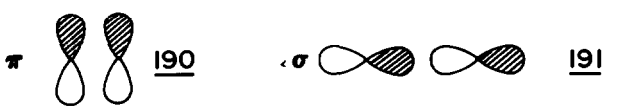

lap, 191 then the energy dependence on $\underline{k}$ for the three p orbitals is, from 148 simply

$$\begin{aligned} p_x \quad & E(\underline{k}) = \alpha - 2\beta\cos k_x a \\ p_y \quad & E(\underline{k}) = \alpha - 2\beta\cos k_y a \\ p_z \quad & E(\underline{k}) = \alpha - 2\beta\cos k_z a\ . \end{aligned} \tag{117}$$

A picture similar to that for the s orbital problem of 189 is shown in 192. Just as the

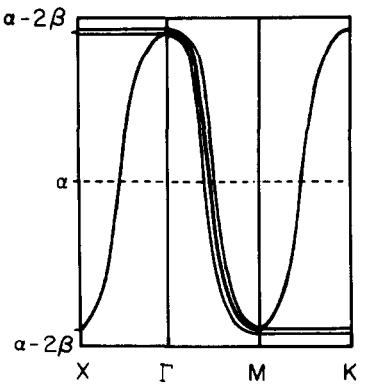

192

half-filled one-dimensional chain of Section 3 underwent a Peierls distortion, so we expect that the simple cubic lattice with three p electrons would similarly be unstable. The structures of elemental arsenic and black phosphorus may be viewed in this way. Let us assume for simplicity that two electrons per atom reside in a deep lying valence s orbital. For these Group V elements, this leaves three electrons to half occupy the three p orbitals. 193 shows how the energy bands change on a distortion which involves pairing up all the atoms along the x, y and z directions. There are several ways in which the pairing up may be

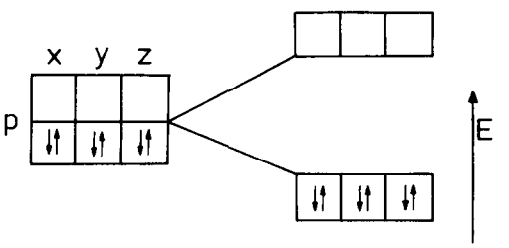

193

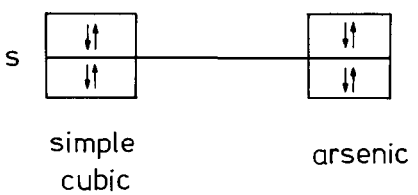

done. It may be shown[41] that there are a total of 36 different possibilities for a simple cubic cell containing eight atoms. Two of these correspond to the black phosphorus 194 and arsenic 195 structures, which we show schematically. On application of pressure to black phosphorus the metallic simple cubic structure is regenerated.[42] So, as in several examples we have seen earlier, the Peierls distortion is reversed by the application of pressure.

For the Group IV elements these ideas lead[43] to the prediction of a structure where the bonds have broken along two Cartesian directions only. The band description is shown in 196 We have artificially half-filled two p orbitals at the simple cubic structure and left the third vacant. One way of executing the distortion leads to the (metallic) white tin structure shown in 197, structurally related to diamond 198.

Can we stabilize the simple cubic structure against a Peierls distortion by substitution, in an exactly analogous way described above for molecules and simpler solids? The answer is

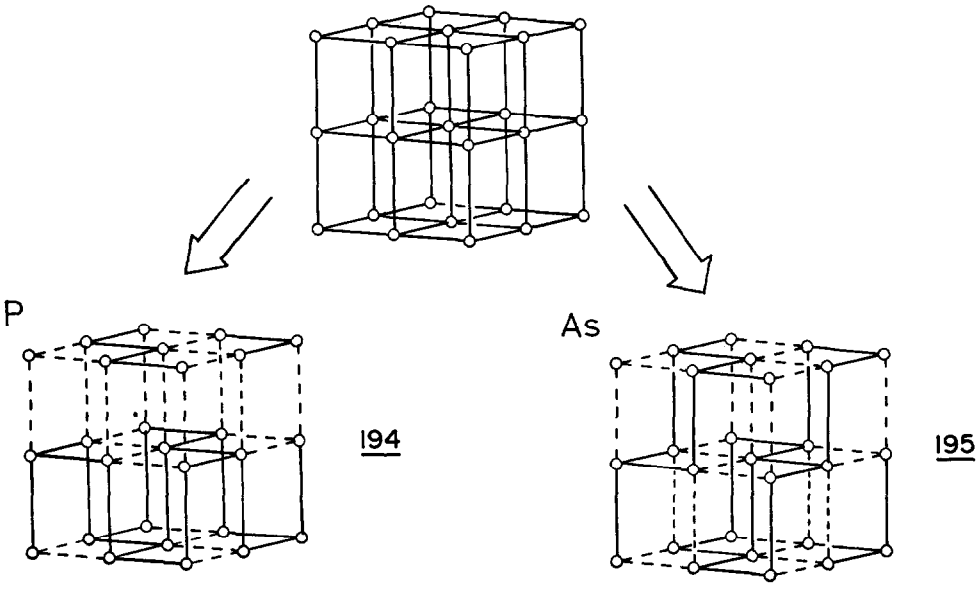

194 195

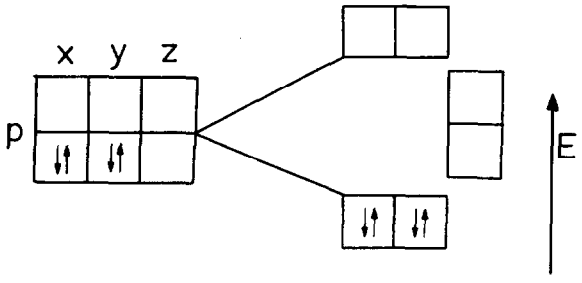

196

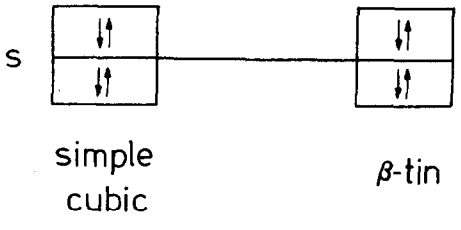

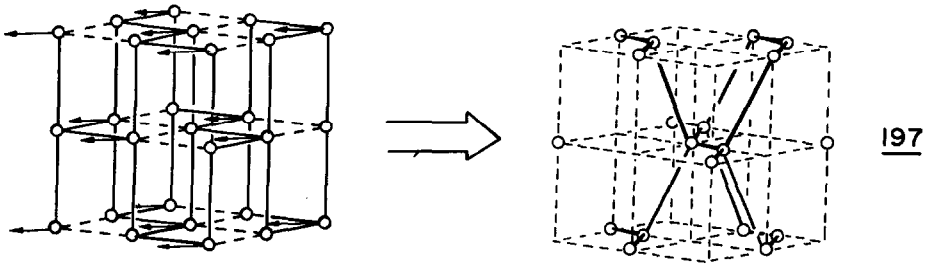

197

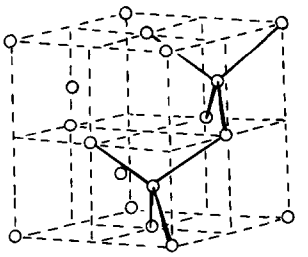

198

yes but in practice there is a twist. 199 shows what happens to the energy bands of the simple cubic structure when we make ...XYXY... substitutions in all three perpendicular chains. Geometrically the result is production of the rocksalt structure. Eventually if the

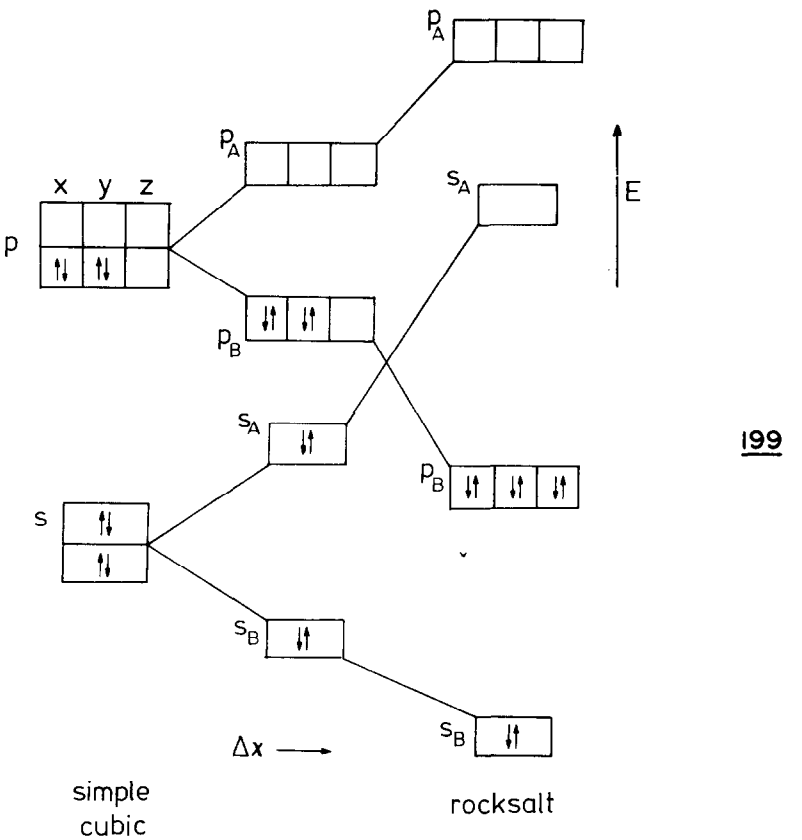

199

electronegativity difference is large enough then both the s and p orbitals of X, the least electronegative atoms rise above the orbitals of Y. Using these ideas we can see that solids with four electrons per atom (or eight electrons per XY atom pair, the so-called octets), unstable at the left-hand side of 199 are stabilized with respect to distortion by increasing the XY electronegativity difference. It is interesting to note that all octets with the NaCl structure have[44] the atomic orbital arrangement shown at the right-hand side of the diagram (i.e., one where both s, p on X lie higher than s, p on Y). Octets with other orbital patterns, and therefore with the s, p orbitals on X close to those on Y, invariably have either the sphalerite or wurtzite structure. Recall that the diamond structure (degenerate sphalerite) is geometrically close to that of white tin as we described above (187 and 198). Clearly we are not in a position to discuss the energetic stability of one geometry out of white tin, diamond (hexagonal or cubic), Si(III), or graphite over another for these systems but it is interesting to be able to cast some light on their electronic structure.

From the simple cubic structure we move to the body-centered cubic (bcc) and face-centered cubic structures. For these we will derive[45] the energy band for a single s orbital

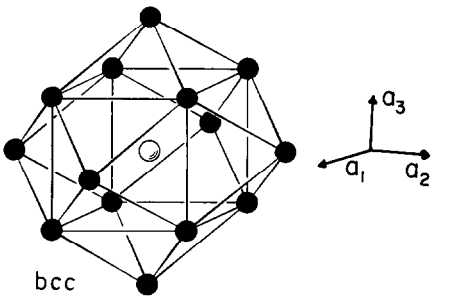

200

located at each center. The bcc structure 200 has a coordination environment around each center which consists of a cube of eight neighbors plus an octahedron of six neighbors some 14% further away. Since this is a one orbital problem we may immediately write down the energy dependence on $\underline{k}$. For the cubal neighbors

$$E(\underline{k}) = \alpha + 2\beta[\cos(\underline{k}\cdot\underline{r}_1) + \cos(\underline{k}\cdot\underline{r}_2) + \cos(\underline{k}\cdot\underline{r}_3) + \cos(\underline{k}\cdot\underline{r}_4)] \tag{118}$$

where

$$\begin{aligned} \underline{r}_1 &= [a_1 + a_2 + a_3]\,; \qquad r_2 = [a_1 - a_2 + a_3]\,; \\ r_3 &= [-a_1 + a_2 + a_3]\,; \qquad r_4 = [-a_1 - a_2 + a_3]\,. \end{aligned} \tag{119}$$

A little trigonometry reduces this to

$$E(\underline{k}) = \alpha + 8\beta[\cos(k_x a) \times \cos(k_y a) \times \cos(k_z a)] \tag{121}$$

For the octahedral neighbors the problem is identical to that of the simple cubic lattice and we may write

$$E(\underline{k}) = \alpha + 2\beta'[\cos(k_x a) + \cos(k_y a) + \cos(k_z a)]\,. \tag{121}$$

For the fcc structure the local coordination is a cuboctahedron with therefore 12 neighbors

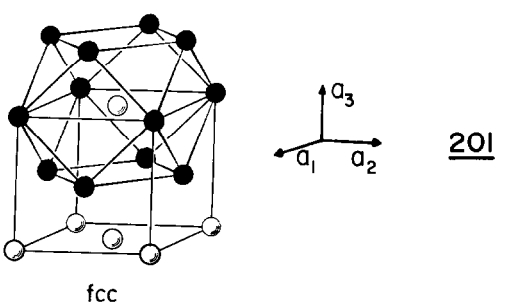

201

201. Now we may write down the energy dependence on $\underline{k}$ for an s band as

$$E(\underline{k}) = \alpha + 2\beta[\cos(\underline{k}\cdot\underline{r}_1) + \cos(\underline{k}\cdot\underline{r}_2) + \cos(\underline{k}\cdot\underline{r}_3) + \cos(\underline{k}\cdot\underline{r}_4) + \cos(\underline{k}\cdot\underline{r}_5) + \cos(\underline{k}\cdot\underline{r}_6)] \tag{122}$$

where

$$\begin{aligned} \underline{r}_1 &= (\underline{a}_1 + \underline{a}_2)/2\,; \quad \underline{r}_2 = (\underline{a}_1 - \underline{a}_2)/2\,; \quad \underline{r}_3 = (\underline{a}_2 + \underline{a}_3)/2\,; \\ \underline{r}_4 &= (\underline{a}_2 - \underline{a}_3)/2\,; \quad \underline{r}_5 = (\underline{a}_1 - \underline{a}_3)/2\,; \quad \underline{r}_6 = (\underline{a}_1 - \underline{a}_3)/2\,. \end{aligned} \tag{123}$$

Again a little trigonometry reduces this to

$$E(\underline{k}) = \alpha + 4\beta[\cos(k_x a)\cos(k_y a) + \cos(k_x a)\cos(k_z a) + \cos(k_y a)\cos(k_z a)] \tag{124}$$

For illustrative purposes we will use the special points method, discussed in Section 3.1, to generate a set of representative energy levels from these bands. If we want to do the job properly we would use a larger number of $\underline{k}$ points but here we will use the $\frac{1}{8}$ points namely $(\frac{1}{8}, \frac{1}{8}, \frac{1}{8})$, $(\frac{3}{8}, \frac{3}{8}, \frac{3}{8})$, $(\frac{1}{8}, \frac{3}{8}, \frac{3}{8})$ and $(\frac{3}{8}, \frac{1}{8}, \frac{1}{8})$. By symmetry we need to weight the last

two points three times as heavily as the first two. (In fact the choice of special points actually depends upon the nature of the lattice. This occurs because the shape of the Brillouin zones for the simple cubic, body-centered cubic and face-centered cubic lattices are different. They are shown in Ref. 29. As it turns out, because of our choice of a single band based on an s orbital, we can use the same set of values for all three structures.) The levels which result are shown in 202. Notice that the levels for the simple cubic structure

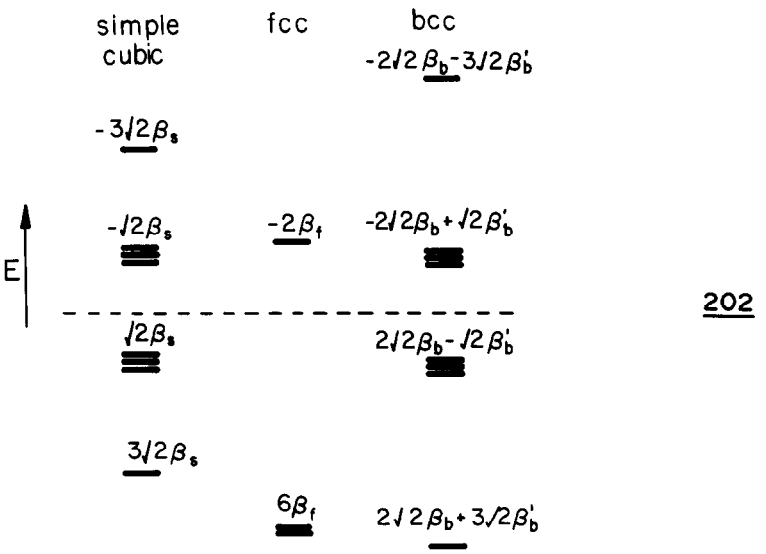

202

and the bcc structure (if either β_b or $\beta_b' = 0$) lie symmetrically disposed about $E = \alpha$, but that those for the fcc structure show no such symmetry. Similar situations were found in molecules in Section 3 and the explanation behind these observations is the same as for them. The simple cubic lattice is bipartite as is the network produced by connecting the central atom in the bcc structure to its first nearest neighbors. The fcc lattice (and the hcp analog too) is not bipartite and so the level structure lacks this mirror symmetry. However for each of the three structures equation (58) holds nicely after we divide out the left-hand side by 8. (There are eight sets of levels included by the special points.) For the simple cubic structure $M = 6\beta_s^2$ and for the fcc structures $M = 12\beta_f^2$. For the cubal neighbors of the bcc structure $M = 8\beta_b^2$ and for the octahedral neighbors $M = 6\beta_b'^2$.

In estimating the relative stabilities of the three structures as a function of band filling we first need an estimate of the four parameters β_s, β_f, β_b and β_b'. These will vary from system to system. Assuming that all three structures have the same density, then the interatomic distance is much smaller in the simple cubic structure and so we know that $\beta_s > \beta_f, \beta_b$. Similar distance arguments lead to $\beta_b > \beta_b'$. 203 shows an energy difference curve between the three structures using the parameters shown (arbitrary units). A very interesting result is the domination of this picture by the stability of the fcc structure at the quarter filled band and the emergence of the simple cubic structure for the almost full band. Unfortunately, as is often the case with such ultra-simple examples, there is no series of structures we can tie in with these results. But the indications both here, and above, are quite clear. The most stable structure at one band filling may not always be the lowest energy structure at another filling. Of course molecular chemists are very familiar with structural changes occurring as a result of a change in electron count. For example, the geometries of the AF_2 molecules are linear for A = Be, Xe (two and five valence electron pairs, respectively) but nonlinear for A = Si, O (three and four valence electron pairs, respectively).

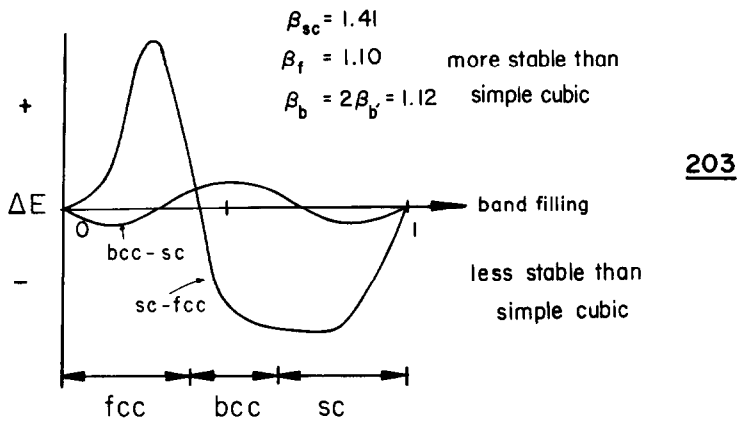

Table 5. The Structures of the Transition Metals

Period	N	3	4	5	6	7	8	9	10	11
3d , 4s		Sc	Ti	V	Cr	(Mn)	(Fe)	(Co)	Ni	Cu
4d , 5s		Y	Zr	Nb	Mo	Tc	Ru	Rh	Pd	Ag
5d , 6s		(La)	Hf	Ta	W	Re	Os	Ir	Pt	Au
Structure		hcp	hcp	bcc	bcc	hcp	hcp	fcc	fcc	fcc

As a final series of examples which show how an extension of the ideas presented in this article lead to some very dramatic results, we very briefly describe the problem of the crystal structures of the transition elements. Table 5 shows how the most stable structure varies across the Periodic Table. Note that, with the exception of the magnetic elements, Mn, Fe and Co, the structure is determined by the column of the Periodic Table. The sequence that is found is hcp → bcc → hcp → fcc as the number of electrons increases, or in the languange used here, as the d band is filled with electrons. The detailed discussion of this problem, although fascinating, is beyond the scope of this review. However, in Fig. 15 we show the results[46] of simple Hückel calculations for the bcc, fcc and hcp structures.

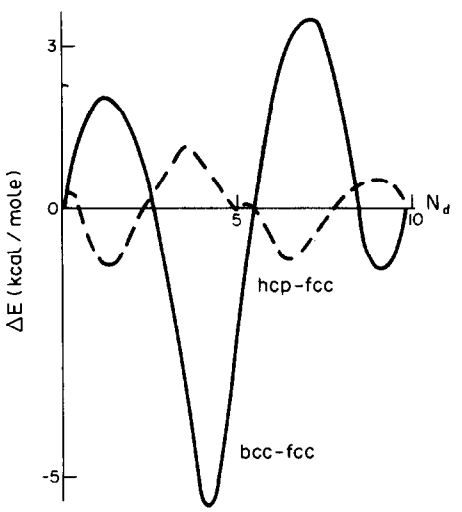

Fig. 15. Calculated variation in lowest energy crystal structure of the transition metals with band filling using a Hückel model.

The computation is more difficult than in the examples we have used before. Here there are five d orbitals per metal atom instead of the single s or pπ orbital. In addition the overlap integrals between the d orbitals on one atom and those on its neighbors are dependent upon the d orbitals concerned, and the geometrical location of the central atom with respect to its neighbors. For example the overlap integral between the two orbitals in 204 is different to that between those in 205. But, taking this into account, and writing the

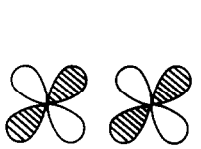

204

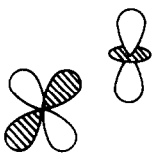

205

interaction integrals, $\beta\alpha$ overlap integral leads to the plot of Fig. 15 for the energy differences between the three structures. Now, the current view[46] of the electronic configuration of the solid metals is one where ~1 electron resides in an s orbital and the other valence electrons occupy d orbitals. So the electronic configuration of elemental chromium is represented as $s^1 d^5$. Ignoring the effect of the lone s electron on the structure we can see from Fig. 15 that the bcc structure is indeed predicted for chromium with this configuration. This is the structure actually found (Table 5). In general the agreement between the observed and calculated structures is quite good. There are some problems with such a d-orbital-only-model at the right-hand side of the series where the bcc rather than the fcc structure is calculated to be more stable.

Iron is found under ambient conditions as a magnetic metal with the bcc structure. As shown in 206 the top group of occupied levels contain unpaired electrons. Under pressure the

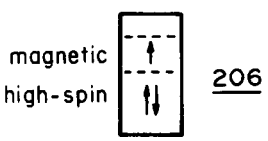

206

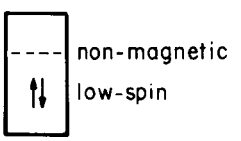

207

hcp structure, predicted in Fig. 15, is found. It is nonmagnetic 207. By knowing how many unpaired electrons to include in 206 for iron we can recalculate the set of curves of Fig. 15. at d^7 the bcc structure is found,[46,47] in nice agreement with experiment. The behavior in 206 and 207 is similar to the stereochemical observations associated with high and low spin molecular complexes. In 208 and 209 we show the relevant orbital patterns and occupancy of four coordinate d^8 systems. One is high spin and distorted tetrahedral and the other low

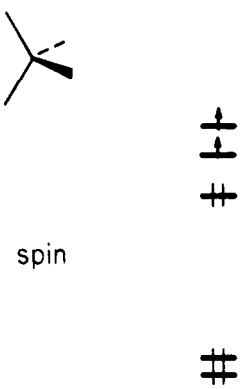

high spin

208

low spin 209

spin and square planar. Notice the similarity between the electron occupancy patterns in 206 and 208 and also in 207 and 209. Associated with the spin change in both cases is a geometrical change.

Finally we show in Fig. 16 the energy difference curve calculated[48] for two AB alloys derived from the bcc structure as a function of band filling. The CsCl structure may be regarded as arising via the stacking of square nets in an XYXY sequence and the CuTi structure as a result of an analogous XXYY stacking. Notice that the shape of the energy difference curve is very similar to that of 74 and arises for similar reasons. Figure 16 also shows the regions where CsCl and CuTi examples are actually found. The agreement is excellent.

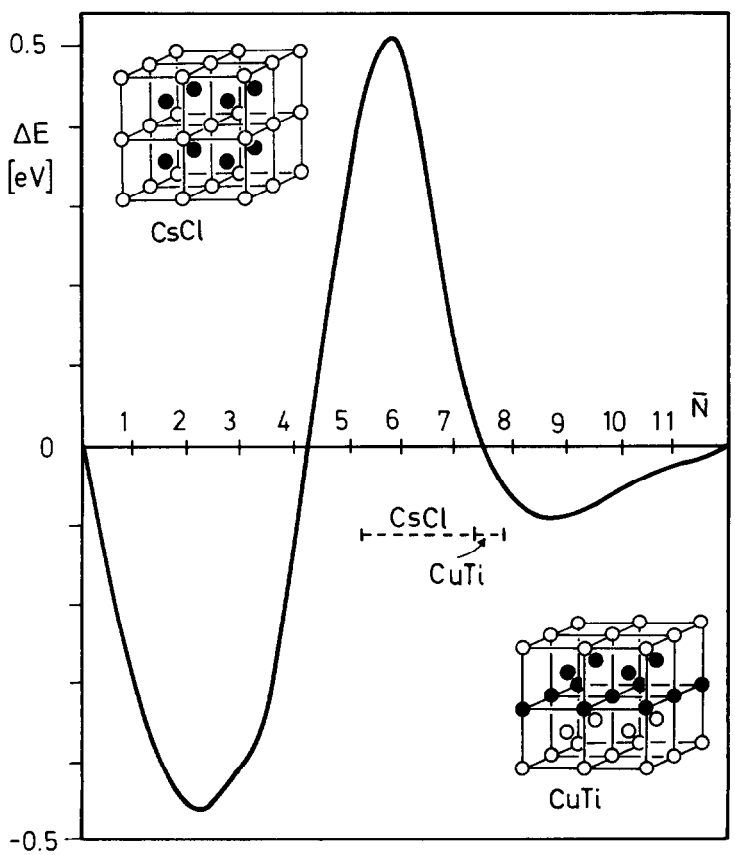

Fig. 16. Energy difference curve[48] ΔE between CsCl and CuTi for transition metal-transition metal alloys as a function of the average number of d + s electrons per atom ($\bar{N}$). In the top part of the diagram the CsCl structure is more stable and at the bottom the CuTi structure

5. CONCLUSION

In this article the emphasis has lain very much with very simple theoretical ideas, based largely on the Hückel simplification of the orbital problem. We have used this approach because it has provided a vehicle with which to stress the strong underlying symmetry and connectivity aspects of the level structures we have studied. So we have not just reported numbers and left the concepts buried in a machine. The cost of such a treatment has of course been virtually a complete lack of numerology of any type. The most obvious absence from our discussion of the planar hydrocarbons has been detailed discussion of the role of the σ manifold of orbitals, both in polyacetylene and in the ladders and sheets derived from it. How do they come into the picture energetically ? Do they influence the relative energies of these structures ? In general, the mixing together of s and p or even s, p and d orbitals requires numerical solution of the electronic problem. The natural extension of the ideas described in this article is use of the extended Hückel method, where the determinant of equation (71) is solved for a basis set containing all the valence orbitals of the unit cell. All of the band structures we have shown as Figures have been obtained using this method. In recent years this method, and variation on it, has been a popular one for theorists of varying persuasions. Symmetry considerations, however, transcend the calculational method. The band touching at the point K in the Brillouin zone found in 119 is reproduced in Fig. 10. Degeneracies appear in the σ manifold too at the point Γ which also have an underlying symmetry explanation.

We need to go beyond the one-electron model to look at systems with different spin configurations. The simple ideas presented here will not allow the reader to decide which out of 206 or 207 will be the more stable arrangement for elemental iron under ambient conditions. Another problem to be answered is the prediction of the pressure for the onset of metallic behavior in any of the one-dimensional Peierls distorted solids we have discussed. All of these questions require the use of high quality numerical calculations where the one- and two-electron terms in the energy are properly taken into account. Such methods are not generally available at present for systems of any complexity. However pseudopotential-based calculations appear quite promising and recently have been very successfully applied to the coordination number problem in the octets.[49,50] However the size of the problem that may be tackled is still quite small as a direct result of computational demands. There is another problem with such calculations however, a philosophical one. While the agreement with experiment is spectacular in numerical terms the understanding of why the results come out the way they do is lacking. They have been described[50] as complex ideas for simple systems and this is one big problem which besets numerical calculations in general How does one dig out of the numerology concepts and pictures which the nonspecialist can appreciate ? The ideas of symmetry and connectivity which we have stressed in this article, may be a useful starting point.[51]

ACKNOWLEDGEMENTS

This research has been supported by the National Science Foundation (NSF DMR 8019741) by the donors of the Petroleum Research Fund administered by the American Chemical Society and by a grant from the Exxon Foundation. Some of the material in this article has been assembled from informal discussions within our research group and thanks are due to all of the participants. Special thanks are due to E. Canadell, T. Hughbanks, G.J. Miller, and M-H Whangbo who read the manuscript.

REFERENCES

1. F.A. Cotton, *Chemical Applications of Group Theory*, 2nd Edn, Wiley (1971).

2. E. Heilbronner and H. Bock, *The HMO Method and its Application*, Wiley (1976).

3. G.A. Segal, ed., *Semi-Empirical Methods of Electronic Structure Calculation*, Plenum (1977).

4. J.K. Burdett, *Molecular Shapes*, Wiley (1980).

5. T.A. Albright, J.K. Burdett, and M-H Whangbo, *Orbital Interactions in Chemistry*, Wiley (1985).

6. A. Streitweiser, *Molecular Orbital Theory for Organic Chemists*, Wiley (1961).

7. A. Streitweiser, J.I. Brauman, and C.A. Coulson, *Supplemental Tables of Molecular Orbital Calculations*, Pergamon (1965).

8. R. Hoffmann, *Accts. Chem. Res.* 4, 1 (1971).

9. M.M.L. Chen and R. Hoffmann, *J. Amer. Chem. Soc.* 98, 1647 (1976).

10. J.K. Burdett, N.J. Lawrence, and J.J. Turner, *Inorg. Chem.* 23, 2419 (1984).

11. For example, A.J. Hoffman in *Studies in Graph Theory*, Vol. 12, Part II, D.R. Fulkerson, ed., Math. Assoc. America (1975).

12. I. Gutman and N. Trinajstić, *Chem. Phys. Lett.* 20, 257 (1973).

13. H.A. Jahn and E. Teller, *Proc. Roy. Soc.* A161, 220 (1937).

14. J.K. Burdett, *Inorg. Chem.* 20, 1959 (1981).

15. J.A. Jafri and M.D. Newton, *J. Am. Chem. Soc.* 100, 5012 (1978).

16. R. Hoffmann, *Chem. Commun.* 240 (1969).

17. R. Gomper and G. Seybold, *Angew. Chem.* 80, 804 (1968).

18. A.F. Wells, *Structural Inorganic Chemistry*, Oxford University Press (1984).

19. B.C. Gerstein, *J. Chem. Educ.* 50, 316 (1973).

20. N.W. Ashcroft and N.D. Mermin, *Solid State Physics*, Saunders (1976).

21. D.J. Chadi and M.L. Cohen, *Phys. Rev.* B 8, 5747 (1973).

22. A. Baldareschi, *Phys. Rev.* B 7, 5212 (1973).

23. R.E. Peierls, *Quantum Theory of Solids*, Oxford University Press (1955).

24. For a review see M. Kertesz, *Adv. Quantum Chem.* 15, 161 (1982).

25. J.K. Burdett, unpublished calculations.

26. See, for example, B.M. Hoffmann, J. Martinsen, L.J. Pace, and J.A. Ibers in Ref. 27, Vol. III.

27. J.S. Miller, ed., *Extended Linear Chain Compounds*, Plenum (1982).

28. M-H. Whangbo, R. Hoffmann and R.B. Woodward. *Proc. R. Soc.* A366, 23 (1979).

29. C.J. Bradley and A.P. Cracknell, *The Mathematical Theory of Symmetry in Solids*, Oxford University Press (1972).

30. See, for example, B.G. Hyde and M. O'Keeffe, *Phil. Trans. R. Soc.* 295, 553 (1980).

31. M. Kertesz, F. Vonderviszt and R. Hoffmann in *Intercalated Graphites*, M. Dresselhaus, ed., Elsevier (1983).

32. There is no conclusive evidence that the Sc atoms are effectively Sc(III). In fact some recent results (E. Canadell) suggest that the B_2C_2 sheet is isoelectronic with graphite (i.e., the scandium is present as Sc(II).)

33. J.K. Burdett and S. Lee (in press).

34. M. Kertesz and R. Hoffmann, *Solid St. Commun.* 47, 97 (1983).

35. P.S. Hawke, T.J. Burgess, D.E. Duerre, J.G. Heubel, R.N. Keeler, H. Klapper, and W.C. Wallace, *Phys. Rev. Lett.* 41, 994 (1978).

36. See, for example, J.M. Williams, A.J. Schultz, A.E. Underhill and K. Carneiro in Ref. 27, Vol. 1.

37. See, for example, L. Alcacer and H. Novais in Ref. 27, Vol. III.

38. See, for example, T.J. Marks and D.W. Kalina in Ref. 27, Vol. I.

39. M-H. Whangbo and M.J. Foshee, *Inorg. Chem.* 20, 113 (1981).

40. M-H. Whangbo, M.J. Foshee, and R. Hoffmann, *Inorg. Chem.* 19, 1723 (1980).

41. J.K. Burdett, T.J. McLarnan, and P. Haaland, *J. Chem. Phys.* 75, 5764 (1981).

42. J.C. Jamieson, *Science*, 139, 1291 (1963).

43. J.K. Burdett and S. Lee, *J. Am. Chem. Soc.* 105, 1079 (1983).

44. J.K. Burdett and S.L. Price, *J. Phys. Chem. Solids*, 43, 521 (1982).

45. J.R. Reitz, *Adv. Sol. State Phys.* 1, 2 (1955).

46. D.G. Pettifor, *Calphad*, 1, 305 (1977).

47. D.G. Pettifor in *Physical Metallurgy*, 3rd edn. P.W. Kahn and P. Haasen, eds, North-Holland (1984).

48. J.K. Burdett and T.J. McLarnan, *J. Solid State Chem.* 53, 382 (1984).

49. M.T. Yin and M.L. Cohen, *Phys. Rev.* B 26, 5668 (1982).

50. M.L. Cohen in *Structures of Complex Solids* M. O'Keeffe and A. Navrotsky, eds, Academic Press (1981).

51. J.K. Burdett, *J. Phys. Chem.* 87. 4368 (1983).

52. D.E. Nixon and G.S. Parry, *J. Phys.* C 2, 1732 (1962).